Analytical method developments of antibody drug conjugates and disease biomarkers in microdialysis samples

By

Yunan Wang

Submitted to the graduate degree program in Chemistry and the Graduate Faculty of the University of Kansas in partial fulfillment of the requirements for the degree of Doctor of Philosophy.

_____

Chairperson Dr. Susan Lunte

_____

Dr. Heather Desaire

_____

Dr. Julie Stenken

_____

Dr. Robert Dunn

_____

Dr. Zhuo Wang

Date Defended: January 27th, 2016

The Dissertation Committee for Yunan Wang

certifies that this is the approved version of the following

dissertation:

Analytical method developments of antibody drug conjugates and disease biomarkers in microdialysis samples

_____

Chairperson Dr. Susan Lunte

Date approved: February 1st, 2016

Abstract

This dissertation focuses on developing analytical methods to study biomarkers in different pharmaceutical samples. Three different analytical methods were developed for microdialysis samples and antibody drug conjugates as anti-tumor drug.

The first part of this dissertation is to develop a capillary electrophoresis with laser induced fluorescence (CE-LIF) method to monitor the change of amino acids in rat brain microdialysate as biomarkers of oxidative stress in epileptic seizures. Ornithine and citrulline was successfully separated and quantified. 3-Mercaptopropionic acid (3-MPA) was administrated to rat brain hippocampus region as a convulsant to induce epileptic seizures to free-moving rats. An increase of citrulline and ornithine level was observed after the seizure, and this confirmed nitric oxide were produced in epileptic seizures.

In the second project, a high-performance liquid chromatography with mass spectrometry (HPLC-MS) method is developed to simultaneously monitor the change of 13 eicosanoids as biomarkers in rat colon microdialysate to study the enzymatic pathways of inflammatory bowel disease. Moreover, cyclodextrin were added into microdialysis perfusate to improve the microdialysis recovery and solubility of the

hydrophobic eicosanoids.

The last part is to utilize enzyme deconjugation and HPLC-UV-Vis to study the stability and compatibility of antibody drug conjugates (ADCs). Bromelain was utilized as an enzyme to fully cleave off the small molecule cytotoxic drug from the ADCs. This allows a direct analysis of the small molecule cytotoxic drug on the ADCs. The stability of antibody drug conjugates was studied with LC-UV-Vis after mixing with other conjugation reagents and formulation excipients.

This dissertation is dedicated to my parents, Mingxin and Xiaohui, for supporting me all the way.

To the memory of my mentor, Dr. Craig Lunte

Acknowledgement

I must first thank my parents, Mingxin and Xiaohui for being so supportive while I'm chasing my Ph.D. on the other side of the ocean. Thank you for being such great parents and making me who I am. Whatever path I took, you just supported me and told me to go for it. My mom is also my high school chemistry teacher, so I think my interest in chemistry runs in my blood. I also want to thank my aunts, Yan and Ping, and my big warm family for helping and taking care of my parents when we went through the family hard time. I won't make it here without all of your support.

Craig, I wish you could be here and see all of these. I still feel you are around. In my final defense, I felt like you were sitting down there and smiling at me. You were an amazing advisor. Thank you for giving me the freedom to do whatever I'm interested in and good for my future. I remember you said your goal is to cultivate successful graduate students. This has become my motivation and your guidance will be a life fortune to me.

I would like to thank my committee members, Dr. Sue Lunte, Dr. Julie Stenken, Dr. Heather Desaire, Dr. Michael Wang, Dr. Bob Dunn and Dr. Yong Zeng, especially to Dr. Sue Lunte. English is not my native language; it was a lot of work to edit my dissertation. I greatly appreciate it.

Dr. Julie Stenken, thank you for reading through my dissertation so carefully and giving me great comments.

I also want to thank all the current and past Lunte group members and collaborators. I want to thank Dr. Sara Thomas for doing my rat surgeries, and Amanda, Kavisha for taking care of my rats time to time. Dr. Mike Ducey helped with my CE-LIF project and taught me a lot about CE separation. It was a very productive summer. Thank you, Dr. Alex Brewer, Dr. Carl Cooley and Ryan for your help with LC-MS. And of course, all the other Lunte group members, Nhan, Michael, Hasitha. At last, I would like to thank my manger Dr. Colin Medley at Genentech for giving me the opportunity to work in such a great company.

At last, I want to thank all of my best friends, Yan, Tianran, Shengkai and all the other great friends. Thank you for listening to me and giving me advise, when I doubt myself and need to vent my frustration. Though we live in different time zone now, I miss all the great time we spent together.

Table of Contents

Table of Figures

1 Introduction of Microdialysis

1.1 Microdialysis

Microdialysis is a commonly practiced *in vivo* sampling method that can be used to recover small molecules from or administer a drug to a target tissue. A 100-500 μm diameter probe containing a dialysis membrane is used to effectively recover analytes from the extracellular fluid (ECF) of tissue or deliver exogenous drugs to tissues of interest. This is accomplished by perfusing a liquid through a probe implanted into the tissue using a solution similar in composition and ionic strength to extracellular fluid. Sampling and delivery of substances in the tissue can both be accomplished due to the differential concentration gradient between the perfusate and the ECF, thus a diffusion-based sampling technique. (Figure 1.1)

Plasma concentrations are commonly used for pharmacokinetic/pharmacodynamic (PK/PD) studies in the drug development. Drug doses are usually determined on the basis of their PK behavior that is determined from plasma concentrations. This is based on the assumption that the tissue-to-plasma drug concentration is in equilibrium. This assumption is reasonable for those drugs that exert their effects in the bloodstream. However, since most drugs act in peripheral compartments, this supposition is oversimplified. Also tissue and plasma

PK values can vary from person to person. There is nothing simple about the human body and the complexities associated with understanding and modeling different tissues and the effects of blood flow, protein binding, and pH. Other techniques have been developed to solve the oversimplified PK activity issue, for example, skin blister fluid, tissue biopsy or mathematical modeling. Another approach is to determine the concentration of the drug in the ECF most closely related to the site of concern to monitor real drug activity. Microdialysis is an effective sampling method that makes it possible to directly measure drugs in the ECF in a variety of tissues.[1,2] Another advantage of microdialysis sampling for PK studies is that the ECF concentrations can be continuously monitored from a single animal. This greatly reduces the number of animals needed for a drug disposition experiment.

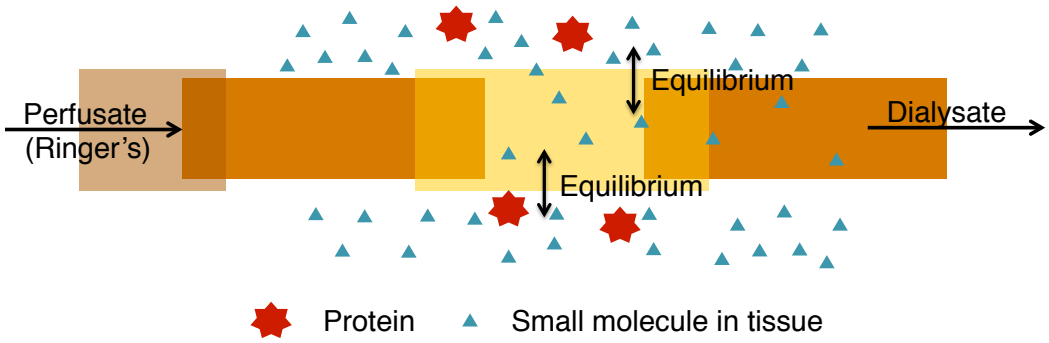

Figure 1.1 A scheme of general microdialysis sampling mechanism. Perfusate similar with extracellular fluid composition is perfused through the probe. Small molecules in the tissue diffuse through the semipermeable membrane driven by concentration gradient. Molecules larger than the molecular weight cutoff are excluded outside the membrane.

The concept of microdialysis was initially used by Kalant in 1958 to measure steroid concentration in the blood.[3] Bito et al. used this dialysis based technique to sample amino acids in cerebrospinal fluid (CSF) from dogs in 1966.[4] In 1974, Ungerstedt and Pycock developed the microdialysis technique as we know it today. They used a hollow fiber microdialysis probe to monitor amphetamine induced dopamine release in the rat brains.[5] Now microdialysis has become a standard sampling technique that is widely used in neuroscience and pharmacological research. The U.S. Food and Drug Administration (FDA) has approved microdialysis catheter use for human brain studies.[2]

The microdialysis sampling process is similar to that of a small blood vessel. It is accomplished by implanting a short hollow semipermeable dialysis fiber into the tissue of interest. Similar with the exchange of nutrients and waste products in a blood vessel, small molecules in the extracellular fluid diffuse through the probe into the perfusate and elute as dialysate. Conversely, small analytes in the perfusate can be delivered to the tissue in a manner analogous to nutrient delivery by blood vessels to tissues.

The simplest probe design is the linear probe, which is produced by affixing a piece of dialysis membrane to two pieces of narrow bore tubing on each side as inlet and outlet. (Fig 1.1) Small molecules diffuse across the semipermeable membrane, while macromolecules, such as proteins

and DNA, are excluded.[2, 6-8] Another probe design, the concentric probe, can be implanted into the brain using a guide cannula.[9,10] A flexible version of this concentric probe can be used to monitor compounds in the blood. Linear probes can be used to sample the ECF of many other soft tissues including colon,[11] heart,[12] and muscle.[13] More details of the probe design are described in the next section.

The perfusate used in microdialysis sampling is a physiologically compatible solution similar in composition and ionic strength to the ECF and is pumped through the probe slowly, generally with a flow rate of 0.1 to 5.0 μl/min. Examples of perfusates include saline, Ringer's solution, and artificial cerebrospinal fluid (aCSF).[7]

Mass transport of compounds across the membrane is driven by the concentration gradient between the ECF and the perfusate. Theoretically, if the perfusate is perfectly matched to ECF, there should be no net fluid loss. The solute exchange direction depends on the concentration gradient orientation. When the concentration of a solute in ECF is higher than the concentration in perfusate, the solute diffuses into the probe. This process is called recovery. On the other hand, if the concentration in ECF is lower than that of perfusate, the solute diffuse into the tissue, making delivery possible.[6]

1.2 Microdialysis Probe Design

Different tissues have different requirements for microdialysis

sampling. For example, the brain is a very heterogeneous tissue and generally requires site-specific probes to sample specific brain regions. On the other hand, other tissues, such as the colon, are more homogeneous, so site-specificity is not as critical as that of the brain. There are different probe designs developed for specific tissues; these include the concentric, linear, flexible and shunt probe.[8,14] (Figure 1.2)

1.2.1 Concentric Probe

A concentric probe is commonly used for brain microdialysis sampling. It consists of two tubes—one placed inside the other. The semipermeable membrane is located at the end of the inner tube. The probe is approximately 15 mm long, and the semipermeable membrane is between 1-4 mm. In the brain sampling experiment, a pin-style cannula is first implanted into the brain to guide the microdialysis probe into the tissue. (Figure 1.2A)

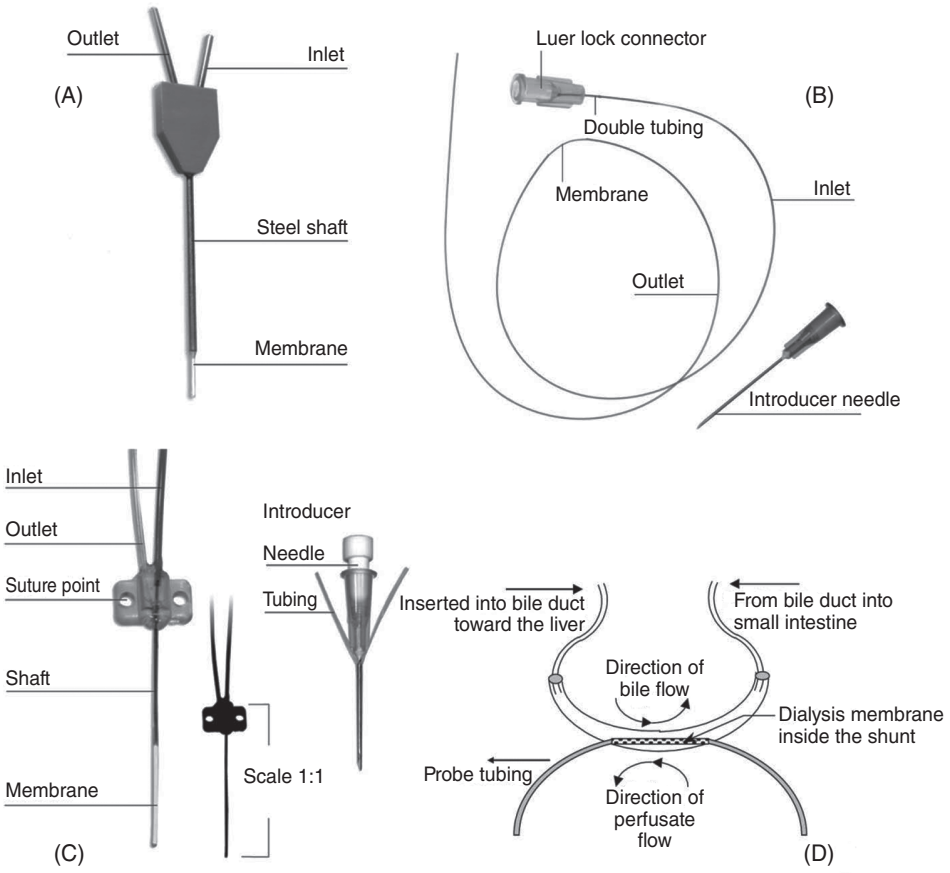

Figure 1.2 Microdialysis probe design: (A) concentric cannula (B) linear probe (C) flexible probe (from CMA product catalog) (D) shunt probe.[14]

1.2.2 Linear Probe

A linear probe is commonly used in tissues where the spatial resolution is not critical, such as the liver, heart and colon. The semipermeable membrane has a length of 4–10 mm and a diameter of 100-500 μm, connected by two pieces of flexible tubing.

The probe is commonly guided through the tissue by a needle acting as the guide cannula. Since the spatial resolution is not critical here, the membrane length can be larger than that used in concentric probe designs. Therefore, the recovery achieved with a linear probe can be better than the concentric probe. It is also widely used for *in vitro* experiments, such as drug dissolution studies. (Figure 1.2B)

1.2.3 Other Probe Designs

Telting-Diaz et al.[15] designed a flexible probe to sample blood in freely moving rats. This probe had a similar design with that of a cannula style brain probe. The only difference is that, instead of the rigid tubing required by brain experiments, flexible probes use capillary tubing that can bend in the blood vessel when the animal moves. Scott and Lunte designed the shunt probe to sample moving fluids.[16] The primary application of shunt probe is bile analysis. A piece of plastic tubing is implanted in the bile duct and a linear microdialysis probe is placed inside of the tubing. Another interesting application of the shunt probe is to desalt protein samples in electrospray ionization-mass spectrometry (ESI-MS).[17]

1.3 Microdialysis Recovery

1.3.1 Extraction Efficiency and Relative Recovery

Since microdialysis sampling is a dynamic sampling technique, the perfusate is continuously pumped through the probe and, even at low flow rates, concentration equilibrium is not usually established between inside and outside of the membrane. We assume the microdialysis is under steady state when the concentration equilibrium is reached. The concentration of the analyte in the dialysate is usually a fraction of that presents in the external tissue. The term extraction efficiency (EE) is introduced here to describe this fraction. Extraction efficiency is defined by the following equation:

$$\mathrm{EE} = \frac{\mathrm{C_p} - \mathrm{C_d}}{\mathrm{C_p} - \mathrm{C_s}} \qquad \text{(Equation 1.1)}$$

where C_p is the concentration in the perfusate, C_d is the concentration in the dialysate and C_s is the concentration in the ECF. In an *in vivo* microdialysis recovery study, C_p is usually zero. In this particular case, the extraction efficiency is also called relative recovery (RR)[2.7]:

$$\mathrm{RR} = \frac{\mathrm{C_d}}{\mathrm{C_s}} \qquad \text{(Equation 1.2)}$$

1.3.2 Improvement of Recovery

Relative recovery is also defined as:

$$\mathrm{RR} = 1 - \exp\left[-\frac{1}{\mathrm{Q_d}(\mathrm{R_d} + \mathrm{R_m} + \mathrm{R_e})}\right] \qquad \text{(Equation 1.3)}$$

where Q_d is flow rate of perfusate, R_d is the mass transport resistance of dialysate, R_m is the mass transport resistance of the membrane, and R_e is the mass transport resistance of extracellular space. The membrane refers to the semipermeable membrane of the microdialysis probe. The dialysate is the solution carrying small molecules out of the probe. Therefore, microdialysis recovery can be improved by changing these parameters as discussed below.[14,18]

1.3.2.1 Flow Rate

From the Equation 1.3, it can be seen how decreasing the flow rate can improve analyte recovery. However, in real practice, this is not suggested because it will reduce the dialysate sample volume per unit time. For the *in vivo* rat experiments in this dissertation, the sampling time interval was 10-15 min and the common flow rate was 1 μL/min, so the sample volume collected was 10-15 μL. For example, if we reduce the flow rate to 0.5 μL/min, the sample volume would be 5-7.5 μL. In our *in vivo* studies, the samples were usually divided for analysis by at least three different analytical systems to monitor the change of different biomarkers. In order to accurately pipet and inject the samples, the sample volume needed for each analytical system had to be larger than 2 μL. Therefore, lower sample volumes (5-7.5 μL) can result in bad reproducibility or accuracy. To achieve both larger sample volumes and higher recoveries using lower flow rates, we also can simply collect

samples for longer time; however, this will compromise the temporal resolution in PK studies.

1.3.2.2 Diffusion

According to the Stokes–Einstein equation, the diffusion coefficient can be expressed as:

$$D = \frac{k_b T}{6\pi\eta\sigma} \qquad \text{(Equation 1.4)}$$

where k_b is the Boltzmann constant, T is temperature, η is the viscosity of the medium, and σ is the particle radius. Therefore, temperature and molecule size will influence diffusion of the analyte and influence recovery.

R_d is related to the diffusion of the analytes in the dialysate, which includes dialysate composition. R_e takes into the consideration of the extracellular environment of tissues, including tissue tortuosity and other metabolic processes such as enzyme digestion.[19] R_e also can be affected by the tissue damage during probe implantation.[14]

1.3.2.3 Membrane Material

R_m is related to the membrane material. Commonly used membrane materials include polyacrylonitrile (PAN) polyethersulfone (PES), polyarylethersulfone (PAES), cuprophan (CUP), and cellulose acetate.[14] The hydrophobicity or charge of the membrane influences the recovery. Different molecular weight cutoffs of different membrane materials also influences analyte recovery. Common molecular weight cutoffs of the

semipermeable membranes used in microdialysis studies range from 20 to 100 kDa. Moreover, physical parameters, such as membrane length and probe geometry, also influence the recovery of different compounds.[20]

1.3.2.4 Affinity Trapping Reagents

Affinity trapping reagents have been added to the perfusate to improve analyte recovery. They can attract the analytes of interest to the microdialysis probe through a concentration gradient and bind with them after diffusing into the probe. This decreases the concentration of target analytes near the membrane to almost zero. According to Fick's law, the diffusion of a molecule is dependent on the concentration gradient across the probe.[18] Affinity reagents will increase the concentration gradient and improve relative recovery. (Figure 1.3)

Stenken's group has performed extensive research on improving recovery by adding cyclodextrin and antibodies to the perfusate.[21] The cone shaped cyclodextrin molecule can react with low solubility analytes to form an inclusion complex and improve the recovery.[22] In another application, Stenken's group improved cytokines recovery by adding antibody-immobilized beads into perfusate.[23-25]

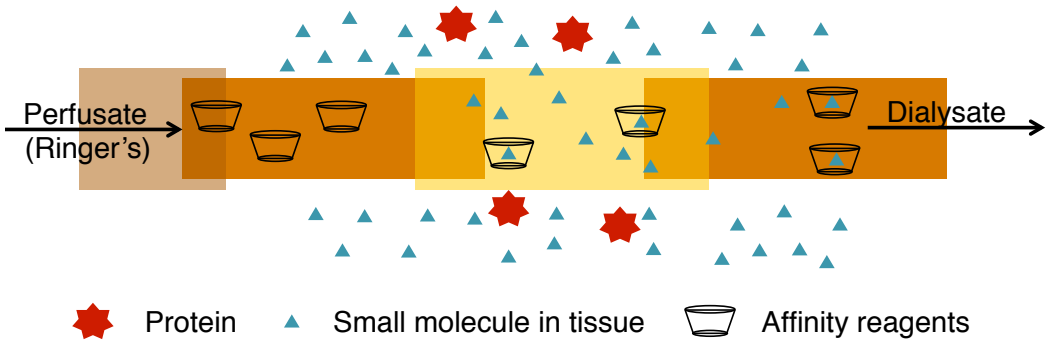

Figure 1.3 A scheme of improving microdialysis recovery by adding affinity-based trapping agents in microdialysis perfusate. The affinity agents trap analytes diffused in the probe. The concentration gradient is increased and the recovery is improved.

1.4 Calibration Methods

Under normal flow rate (1 μL/min) conditions, concentration equilibrium between the ECF and dialysate is not always achieved, especially in more tortuous tissues, such as brain, liver or muscle; therefore, the recovery is usually not 100%. When the exact ECF concentrations are needed, the microdialysis probe needs to be calibrated first.

1.4.1 No Net Flux Method

The no net flux (NNF) method is used to determine steady state concentrations of analytes in the tissue. To perform NNF, several different concentrations of a known analyte are added into perfusate. The microdialysis probe is implanted into target tissue, and a series of perfusates with known concentrations are perfused through the probe, and the dialysate is collected. When choosing the concentrations of the known analyte to use in the experiment, the concentration range should include the expected ECF concentration. Figure 1.4 is an example of the NNF plot. C_p stands for the known concentration in the perfusate, C_d refers to the concentration in the collected dialysate. A graph of C_p-C_d vs. C_p is plotted. When C_p-C_d equals to zero, there is no net flux, and C_p is the concentration in the tissue. The x-intercept is the extracellular concentration.[2,14]

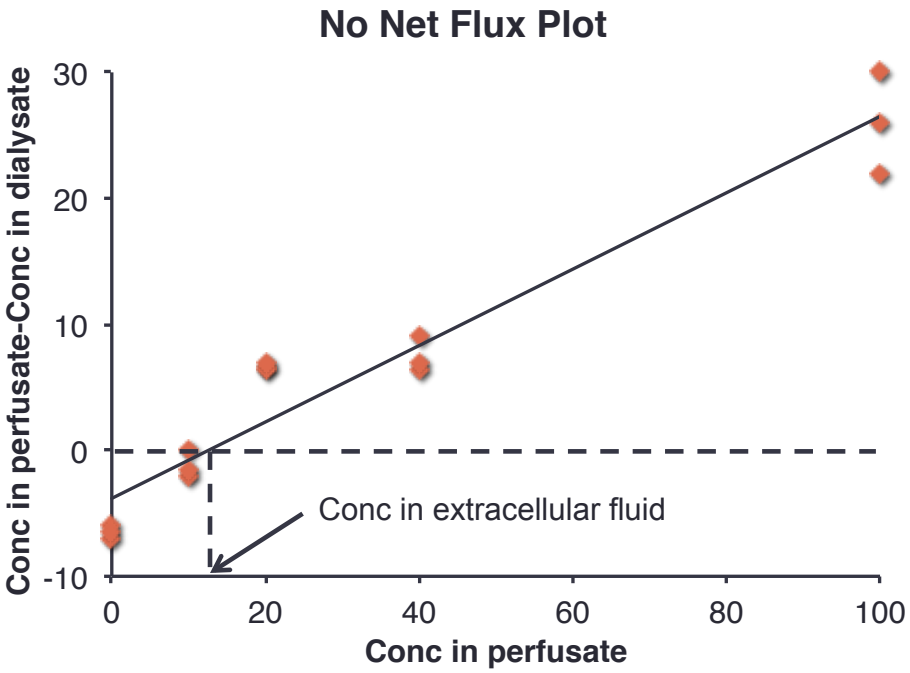

Figure 1.4 An example of a no net flux plot. The x-intercept is the no net flux point, and the concentration equals to the concentration in extracellular fluid.

1.4.2 Dynamic No Net Flux Method

In more complicated cases, when drugs are administrated or endogenous compounds concentrations change over time, the steady-state no net flux method is not applicable. The dynamic no net flux method requires groups of animals instead of a single animal; so the concentration change over time can be monitored. In the dynamic no net flux method, different concentrations of a known analyte are perfused into different animals and C_d at each time point is measured while the corresponding no net flux graph is plotted so the extracellular concentration change can be obtained.[26]

1.4.3 Retrodialysis

Retrodialysis, also called reverse dialysis, is an easier method to measure the concentration of exogenous analytes. It is based on the assumption that the diffusion of a compound is the same for both directions across the semipermeable membrane. A known concentration of a calibrator that has similar diffusion and metabolism properties as the target exogenous analyte is added into the perfusate. Another assumption is that the concentration of the target exogenous analyte in the extracellular fluid is zero.

$$\text{Recovery}\ (\%) = 100 - (100 \times \frac{C_d}{C_p}) \qquad \text{(Equation 1.5)}$$

The limitation of retrodialysis is that it is only applicable to the

exogenous analytes that are not present in the extracellular fluid such as administered drugs, and it cannot be used to monitor concentration and recovery changes over time.[2,14,27]

1.5 Advantages and Disadvantages of Microdialysis

1.5.1 Advantages

The microdialysis sampling process is driven by a concentration gradient; therefore, there is no net fluid loss across the membrane. It allows continuous sampling from the same animal, so the animal can serve as its own control. This can greatly reduce the number of animals used. Long-term studies in awake animals can also be achieved by microdialysis.

The semipermeable membrane on the microdialysis probe excludes large molecules such as proteins. Therefore, the microdialysis sample can normally be injected directly into the analytical system without sample preparation. Biochemical degradation of analytes is also inhibited because enzymes are excluded by the dialysis membrane.

Microdialysis is a site-specific sampling technique. It samples the drug or endogenous species at the site of action, making it a very powerful tool for PK/PD studies. It also can locally deliver the exogenous drug to the site of interest, reducing systemic adverse events.[7,8,18]

1.5.2 Disadvantages

The microdialysis probe/cannula implantation usually requires

surgery and will result in local tissue damage. Studies have shown that biomarkers such as thromboxane B_2, K^+, and lymphocytes are elevated,[28] and inflammation responses are observed following probe implantation.[2,18,29] In addition, microdialysis samples are usually small volumes (1-20μL) and high salt concentration; this can make analytical method development challenging. Analytical considerations of microdialysis sampling are discussed in the following section.[2]

1.6 Analytical Methods for Microdialysis Sampling

1.6.1 Liquid Chromatography

1.6.1.1 LC theory

Liquid chromatography (LC) is one of the most commonly used separation methods. The separation is based on the interaction of analytes between a mobile phase and stationary phase. There are several types of chromatography such as normal phase liquid chromatography, reverse phase, size exclusion chromatography, ion pairing chromatography. For microdialysis samples, reverse phase LC is more commonly used, since the dialysate are aqueous-based solutions.

Isocratic separations is a simple method to begin with, where only one constant solvent composition is used as the mobile phase. However, if the polarity difference between different analytes is too large, the analysis time can be very long. Gradient elution, that changes the mobile phase composition as a function of time, is designed for this situation.

There are several factors that are used to describe LC performance. The capacity factor (k') is used to describe the retention of an analyte on the column.

$$k' = \frac{t_{an} - t_0}{t_0} \qquad \text{(Equation 1.6)}$$

where t_{an} is the retention time of the analyte, t_0 is the void volume of the column that is defined as the time required for an unretained analyte to elute from the column.

The separation of two analytes, A and B, is described by the selectivity or separation factor (α) and resolution (R),

$$\alpha = \frac{k'_B}{k'_A} = \frac{t_B - t_0}{t_A - t_0} \qquad \text{(Equation 1.7)}$$

$$R = \frac{t_B - t_A}{0.5(w_A + w_B)} \qquad \text{(Equation 1.8)}$$

where w_A and w_B are the peak widths, t_A and t_B are the retention time of A and B.

The column efficiency is described by plate height (H). The column efficiency per unit length is described by plate number (N)

$$N = 16\left(\frac{t_A}{w_A}\right)^2 = 5.54\left(\frac{t_A}{w_{0.5}}\right)^2 \qquad \text{(Equation 1.9)}$$

$$H = \frac{L}{N} \qquad \text{(Equation 1.10)}$$

where $w_{0.5}$ is peak width at half-height, L is the column length, w_A is the

peak width of the analyte. Resolution can also be described as follows.

$$R = 0.25\left(\frac{\alpha-1}{\alpha}\right)\left(\frac{k'_B}{1+k'_B}\right)\sqrt{N} \qquad \text{(Equation 1.11)}$$

1.6.1.2 LC in Microdialysis

The limitation of LC for the analysis of microdialysis samples comes from the low sample volumes obtained. A typical flow rate used in microdialysis is ~1 µL/min, resulting in a sample volume at each time point of 5 to 10 µL and a temporal resolution between 5 and 10 min. Increasing the flow rate will increase the sample volume collected; however, it will decrease the recovery, which produces another analytical challenge due to the limits of detection. Another way to solve the sample volume issue is to compromise the temporal resolution, though this is not ideal.[14]

In order to minimize zone dispersion and improve the limits of detection, while maintaining temporal resolution, microbore columns and capillary liquid chromatography (cLC) have been used. The common inner diameters of microbore columns range from 0.3 to 1.0 mm. The smaller column diameter leads to less peak dispersion, so the limit of detection can be improved with the same detector. The temporal resolution of microbore LC can be 3-5 min with 3-5 µL injection.[30]

In recent years, cLC has become a good solution for the LOD issue. The inner diameter of cLC is 25 to 150 µm, which allows for LOD as low as 20 to 80 amol for 16 derivatized amino acids with a laser induced

fluorescence detection.[31] The off-line temporal resolution achieved with this method was as fast as 10 seconds.[30] However, the smaller diameter column requires a slower flow rate, so the separation times are relatively long, such as ~30 min, so cLC is not a good option for on-line microdialysis analysis.[14,30,32]

1.6.2 Capillary Electrophoresis

1.6.2.1 CE Theory

Capillary electrophoresis (CE) is a more microdialysis compatible separation method than LC; since it only requires pL to nL injection volumes and can perform faster separations. In capillary electrophoresis, the analytes are separated based on difference in electrophoretic mobility. A fused silica capillary is filled with background electrolytes (BGE), and high voltage is applied across the capillary. In conventional capillary zone electrophoresis, the migration of analytes is determined by two factors, electroosmotic flow (EOF) and size to charge ratio (electrophoretic mobility).

EOF is the result of an electrical double layer, and serves as bulk flow in CE separation. Typically, the BGE has a pH > 3 so that the silanol groups at the inner wall of the fused silica capillary are ionized. The negatively charged capillary wall attracts cations in BGE and builds an electrical double layer, referred to as an inner Helmholtz layer at the capillary wall. The outer Helmholtz layer is the diffusion region that

migrates towards the outlet (normal polarity) and creates EOF. The magnitude of EOF (v_{eof}) is defined as:

$$v_{eof} = \varepsilon\zeta E/\eta \qquad \text{(Equation 1.12)}$$

where ε is the dielectric constant of the buffer, ζ is zeta potential of the electrical double layer, E is electric field and η is the viscosity of BGE.

The analyte velocity due to electrical field v is described as

$$v_{ep} = \mu E = \frac{\mu V}{L} \qquad \text{(Equation 1.13)}$$

where V is the applied voltage, L is total capillary length, and μ is the electrophoretic mobility that is determined as:

$$\mu = \frac{q}{6\pi\eta R} \qquad \text{(Equation 1.14)}$$

where q is the charge of analytes, R is the hydrodynamic radius of analytes. Therefore, the actual electrophoresis velocity is the combination of EOF and electrophoretic velocity of the analytes.

$$v_{app} = v_{ep} + v_{eof} \qquad \text{(Equation 1.15)}$$

Stacking methods are used in capillary electrophoresis to improve the LOD. Stacking is a sample preconcentration method based on the different electrophoretic mobility of ions on the boundary of different solution plugs in the capillary. The stacking is based on different electric field strength. According to Ohm's Law, the solution with lower conductivity has higher electric field, so the ions migrate faster in the lower conductivity

solution. When the ions migrate to the boundary of higher conductivity solution, their velocities are decreased leading to stacking.[33]

1.6.2.2 CE in Microdialysis

Capillary electrophoresis (CE) is a common separation method for the analysis of microdialysis samples. The injection volume is usually in the nano liter range, which allows multiple injections of the same sample. The sample can also be split for analysis using different analytical systems. The separation efficiency of CE is better than LC. The theoretical plate number from CE separation can be as high as 300,000 to 500,000.[34] Moreover, microchip CE (MCE) is gaining favor since it can achieve even faster separation, and smaller volume for on-animal sensing.

One disadvantage of CE and MCE is that the perfusate, such as Ringer's solution, saline, or aCSF, normally has a much higher salt concentration than BGE. This leads to a conductivity difference between the sample plug and BGE. When a constant voltage is applied across the capillary, destacking will happen due to the electrical field drop across the sample/BGE boundary. Destacking will cause band broadening and result in a loss of sensitivity and resolution. Joule heating caused from solution resistance is another reason for band broadening. The separation voltage needs to be carefully optimized to achieve best separation while avoiding band broadening.

1.6.3 Mass Spectrometry

1.6.3.1 Mass Spectrometry Theory

Mass spectrometry (MS) is a standard detector for pharmacokinetic studies, since in addition to good sensitivity; the MS/MS mode can also be regarded as secondary separation step. MS can be coupled with either LC or CE, although LC is more commonly used. MS detection and identification analysis is based on ions mass to charge ratio (*m/z*).

The first step in MS is ionization, analytes are converted into gaseous phase ions in the ionization source. The most commonly used ionization source for the analysis of microdialysis sample is electrospray (ESI). ESI is a soft ionization method with very high sensitivity, and it can be easily connected to a liquid chromatography or capillary electrophoresis.

The positive ionization mode is used as an example to explain the electrospray ionization mechanism here. The LC eluent continuously flows through a capillary tube. A high positive voltage (3–6 kV) is applied across the capillary and counter-electrodes, and an inert gas coaxially flows along the capillary and liquid. An excess positive charge accumulates on the liquid surface and charged droplets are formed. As the inert gas sprays, the liquid evaporates and droplets shrink, resulting in an electrical field increase. When the electrical field force gets larger than surface tension force, the droplet forms a Taylor cone shape and explodes into small

droplets on the tip, producing an electrospray.[35,26]

The ionized analytes then go into a high vacuum mass analyzer, which detects the *m/z*. Common mass analyzers include ion trap, triple quadrapole and time-of-flight (TOF). An ion trap is used as an example to illustrate how to detect *m/z*. A traditional 3D ion trap consists of three electrodes: one top ellipsoid electrode, one bottom ellipsoid electrode and one circular electrode in the middle. These three electrodes form a box in the middle. The ions are trapped in the middle box and are expelled based on their *m/z*. The linear ion trap, also know as a 2D ion trap, has a 10 fold higher ion trapping capacity. (Figure 1.5) It replaces the middle circular electrode with quadrupoles. In the linear ion trap, the mass analyzer is able to not only analyze the parent ions, but it can also conduct tandem MS analysis. In tandem MS, inert gas molecules are introduced into the high vacuum chamber and collide with the parent ions. This causes parent ions to break up into different fragments; hence, tandem MS can greatly improve selectivity and sensitivity, as well as provide structural information of the analytes.[37]

1.6.3.2 MS Analysis of Microdialysis Samples

One issue with MS analysis of microdialysis samples comes from the high salt concentrations of the perfusate. With ESI ionization, the high salt can result in ion suppression that will reduce ionization efficiency. Also, when the dialysate passes through the heated capillary, the salt can

clog the capillary. To solve this problem, a divert valve can be used that allows the first several minutes of eluent flow to directly go into the waste reservoir instead of LC-MS system. Salts usually exhibits low retention on reverse phase columns and the valve reduces the amount of salt that goes into the ESI source. Sample pre-treatment, such as solid phase extraction (SPE), can also be a solution. However, for very small volume samples, SPE might not be practical.

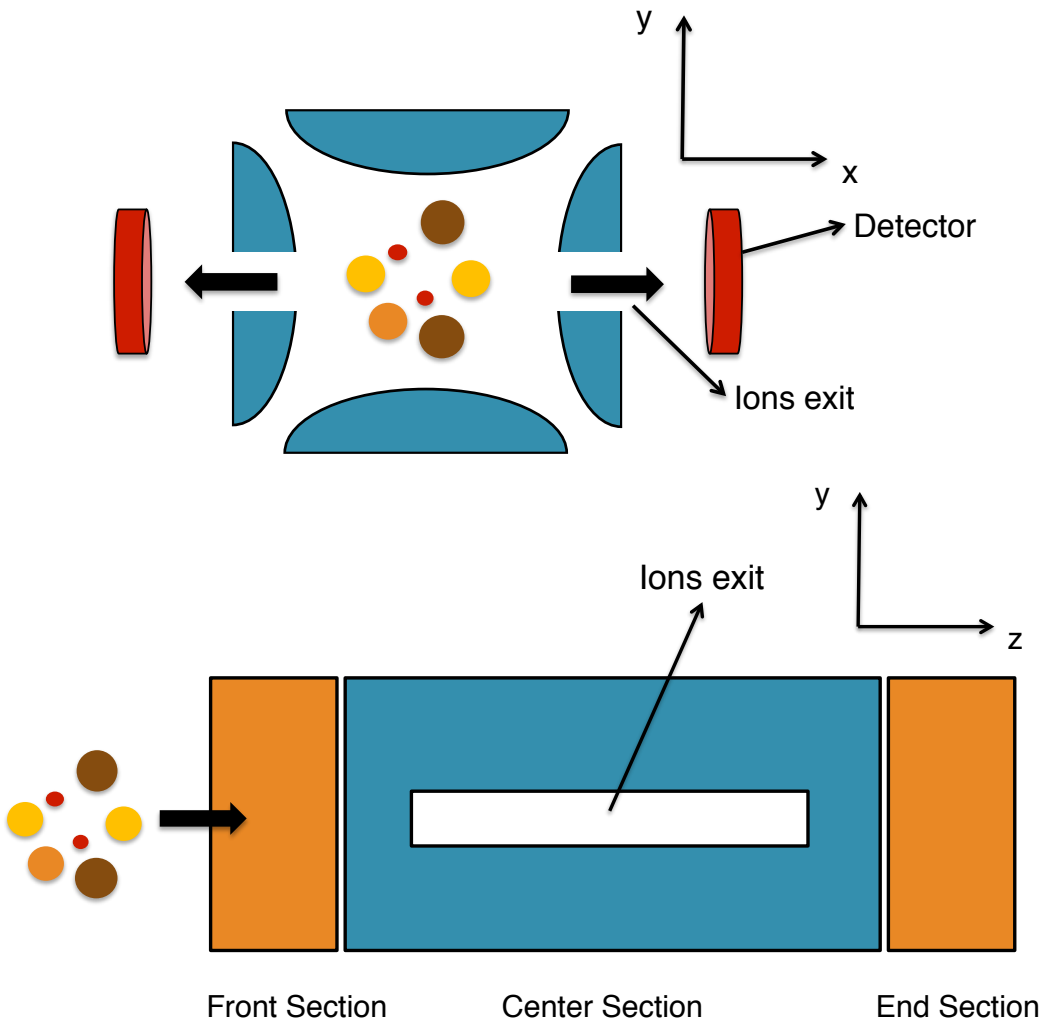

Figure 1.5 An illustration of linear ion trap mass spectrometry. The top figure is a front view of the center section. The bottom figure is a side view of the LTQ MS.

1.7 Objective

In this dissertation, three different analytical methods were developed and used to study biomarkers in microdialysis samples and the stability of antibody drug conjugates. Chapter two describes the development of a CE-LIF method to study changes in amino acids in rat brain microdialysates during epileptic seizures. Chapter three and four describe the development of an LC-MS method to detect eicosanoids in rat colon microdialysate samples to study inflammatory bowel disease. Chapter five describes the development of an enzymatic digestion and LC-UV method to study the compatibility of antibody drug conjugates.

1.8 Reference

(1) Joukhadar, C.; Müller, M. Microdialysis: Current applications in clinical pharmacokinetic studies and its potential role in the future. *Clinical Pharmacokinetics* **2005**, *44*, 895-913.

(2) Chaurasia, C.; Müller, M.; Bashaw, E.; Benfeldt, E.; Bolinder, J.; Bullock, R.; Bungay, P.; DeLange, E. M.; Derendorf, H.; Elmquist, W.; Hammarlund-Udenaes, M.; Joukhadar, C.; Kellogg, D., Jr.; Lunte, C.; Nordstrom, C.; Rollema, H.; Sawchuk, R.; Cheung, B. Y.; Shah, V.; Stahle, L.; Ungerstedt, U.; Welty, D.; Yeo, H. AAPS-FDA workshop white paper: microdialysis principles, application and regulatory perspectives. *Pharmaceutical Research* **2007**, *24*, 1014-1025.

(3) Kalant, H. A microdialysis procedure for extraction and isolation of corticosteroids from peripheral blood plasma. *Biochemical Journal* **1958** *69*, 99–103.

(4) Bito, L.; Davson, H.; Levin, E.; Murray, M.; Snider, N. The concentrations of free amino acids and other electrolytes in cerebrospinal fluid, *in vivo* dialysate of brain, and blood plasma of the dog. *Journal of Neurochemistry* **1966**, *13*, 1057-1067.

(5) Ungerstedt, U.; Pycock, C. Functional correlates of dopamine neurotransmission. *Bull Schweiz Akad Med Wiss*. **1974**, *30*, 44-55.

(6) Song, Y.; Lunte, C. E. Calibration methods for microdialysis sampling *in vivo*: muscle and adipose tissue. *Analytica Chimica Acta* **1999**, *400*, 143-152.

(7) Davies, M. I. A review of microdialysis sampling for pharmacokinetic applications. *Analytica Chimica Acta* **1999**, *379*, 227-249.

(8) Davies, M. I.; Cooper, J. D.; Desmond, S. S.; Lunte, C. E.;

Lunte, S. M. Analytical considerations for microdialysis sampling. *Advanced Drug Delivery Reviews* **2000**, *45*, 169-188.

(9) Umbrain, V.; Shi, L.; Poelaert, J.; Smolders, I. Application of spinal microdialysis in freely moving rats. In *Microdialysis Techniques in Neuroscience*; Di Giovanni, G., Di Matteo, V., Eds.; Neuromethods; Humana Press, **2013**, 75; 157-174.

(10) Anderzhanova, E.; Wotjak, C. Brain microdialysis and its applications in experimental neurochemistry. *Cell and Tissue Research* **2013**, *354*, 27-39.

(11) Högberg, N.; Carlsson, P. O.; Hillered, L.; Meurling, S.; Stenbäck, A. Intestinal ischemia measured by intraluminal microdialysis. *Scandinavian Journal of Clinical and Laboratory Investigation* **2011**, *72*, 59-66.

(12) Yu, B.; Cao, Y.; Xiong, Y. Pharmacokinetics of aconitine-type alkaloids after oral administration of Fuzi (Aconiti Lateralis Radix Praeparata) in rats with chronic heart failure by microdialysis and ultra-high performance liquid chromatography–tandem mass spectrometry. *Journal of Ethnopharmacology* **2015**, *165*, 173-179.

(13) Bilgin-Freiert, A.; Dusick, J.; Stein, N.; Etchepare, M.; Vespa, P.; Gonzalez, N. Muscle microdialysis to confirm sublethal ischemia in the induction of remote ischemic preconditioning. *Translational Stroke Research* **2012**, *3*, 266-272.

(14) Nandi, P.; Kuhnline, C. D.; Lunte, S. M. Analytical considerations for microdialysis sampling. In *Applications of Microdialysis in Pharmaceutical Science*; John Wiley & Sons, Inc., **2011**, 39-92.

(15) Telting-Diaz, M.; Scott, D. O.; Lunte, C. E. Intravenous microdialysis sampling in awake, freely-moving rats. *Analytical Chemistry*

1992, *64*, 806-810.

(16) Scott, D.; Lunte, C. *In Vivo* microdialysis sampling in the bile, blood, and liver of rats to study the disposition of phenol. *Pharmaceutical Research* **1993**, *10*, 335-342.

(17) Wu, Q.; Liu, C.; Smith, R. D. On-line microdialysis desalting for electrospray ionization-mass spectrometry of proteins and peptides. *Rapid Communications in Mass Spectrometry* **1996**, *10*, 835-838.

(18) Plock, N.; Kloft, C. Microdialysis—theoretical background and recent implementation in applied life-sciences. *European Journal of Pharmaceutical Sciences* **2005**, *25*, 1-24.

(19) Kehr, J. A survey on quantitative microdialysis: theoretical models and practical implications. *Journal of Neuroscience Methods* **1993**, *48*, 251-26.

(20) Zhao, Y.; Liang, X.; Lunte, C. E. Comparison of recovery and delivery *in vitro* for calibration of microdialysis probes. *Analytica Chimica Acta* **1995**, *316*, 403-410.

(21) Duo, J.; Fletcher, H.; Stenken, J. A. Natural and synthetic affinity agents as microdialysis sampling mass transport enhancers: Current progress and future perspectives. *Biosensors and Bioelectronics* **2006**, *22*, 449-457.

(22) Khramov, A. N.; Stenken, J. A. Enhanced microdialysis extraction efficiency of ibuprofen *in vitro* by facilitated transport with β-cyclodextrin. *Analytical Chemistry* **1999**, *71*, 1257-1264.

(23) Ao, X.; Sellati, T. J.; Stenken, J. A. Enhanced microdialysis relative recovery of inflammatory cytokines using antibody-coated microspheres analyzed by flow cytometry. *Analytical Chemistry* **2004**, *76*, 3777-3784.

(24) Wang, Y.; Stenken, J. A. Affinity-based microdialysis sampling using heparin for *in vitro* collection of human cytokines. *Analytica Chimica Acta* **2009**, *651*, 105-111.

(25) Fletcher, H. J.; Stenken, J. A. An *in vitro* comparison of microdialysis relative recovery of Met- and Leu-enkephalin using cyclodextrins and antibodies as affinity agents. *Analytica Chimica Acta* **2008**, *620*, 170-175.

(26) Invernizzi, R. W.; Sacchetti, G.; Parini, S.; Acconcia, S.; Samanin, R. Flibanserin, a potential antidepressant drug, lowers 5-HT and raises dopamine and noradrenaline in the rat prefrontal cortex dialysate: role of 5-HT1A receptors. *British Journal of Pharmacology* **2003**, *139*, 1281-1288.

(27) Song, Y.; Lunte, C. E. Comparison of calibration by delivery versus no net flux for quantitative *in vivo* microdialysis sampling. *Analytica Chimica Acta* **1999**, *379*, 251-262.

(28) Desai, P. R.; Shah, P. P.; Patlolla, R. R.; Singh, M. Dermal microdialysis technique to evaluate the trafficking of surface modified lipid nanoparticles upon topical application. *Pharmaceutical research* **2012**, *29*, 2587-2600.

(29) Hascup, E. R.; Bjerkén, S. a.; Hascup, K. N.; Pomerleau, F.; Huettl, P.; Strömberg, I.; Gerhardt, G. A histological studies of the effects of chronic implantation of ceramic-based microelectrode arrays and microdialysis probes in rat prefrontal cortex. *Brain research* **2009**, *1291*, 12-20.

(30) Schultz, K. N.; Kennedy, R. T. Time-resolved microdialysis for *in vivo* neurochemical measurements and other applications. *Annual Review of Analytical Chemistry* **2008**, *1*, 627-661.

(31) Boyd, B. W.; Witowski, S. R.; Kennedy, R. T. Trace-Level Amino Acid Analysis by Capillary Liquid Chromatography and Application to *in Vivo* Microdialysis Sampling with 10-s Temporal Resolution. *Analytical Chemistry* **2000**, *72*, 865-871.

(32) MacNair, J. E.; Patel, K. D.; Jorgenson, J. W. Ultrahigh-Pressure Reversed-Phase Capillary Liquid Chromatography: Isocratic and Gradient Elution Using Columns Packed with 1.0-µm Particles. *Analytical Chemistry* **1999**, *71*, 700-708.

(33) Osbourn, D. M.; Weiss, J. D.; Lunte, C. E. On-line preconcentration methods for capillary electrophoresis. *Electrophoresis* **2000** *21* 2768–2779.

(34) Bowser, M. T.; Kennedy, R. T. *In vivo* monitoring of amine neurotransmitters using microdialysis with on-line capillary electrophoresis. *Electrophoresis* **2001**, *22*, 3668-3676.

(35) Mann, M.; Meng, C. K.; Fenn, J. B. Interpreting mass spectra of multiply charged ions. *Analytical Chemistry*, **1989**, *61*, 1702-1708.

(36) Ho, C.; Lam, C.; Chan, M.; Cheung, R.; Law, L.; Lit, L.; Ng, K, Suen, M; Tai, H. Electrospray Ionisation Mass Spectrometry: Principles and Clinical Applications. *The Clinical Biochemist Reviews* **2003** *24*, 3–12.

(37) Douglas, D. J.; Frank, A. J.; Mao, D Linear ion traps in mass spectrometry. *Mass Spectrometry Reviews* **2005**, *24*, 1-29.

2 A CE-LIF Method Development for the Determination of Amino Acids in Rat Brain Microdialysate to Study Epileptic Seizure

2.1 Introduction

2.1.1 Epileptic Seizures

Epilepsy is one of the most common neurological disorders in the world. Epileptic seizures are caused by an abnormal neuronal imbalance in the brain. The brain disorder that generates multiple epileptic seizures is defined as epilepsy. It affects 3 million people in the United States and 70 million people worldwide.[1] Nearly 40 different anti-seizure drugs were developed between the year of 1850 and 2010, however, 32% of patients remain incurable.[2,3] There are many causes of epilepsy, including trauma, tumors, genetic, however, the causes of over 50% cases of epilepsy are still unclear.

2.1.2 Seizure and Oxidative Stress

Seizure activity increases intracellular calcium concentrations and induces the production of reactive oxygen species (ROS) and reactive nitrogen species (RNS). This leads to oxidative stress, which is an important secondary effect of seizure activity. Common ROSs and RNSs include free radicals, such as hydroxyl (•OH), superoxide ($O_2^{\bullet -}$) and nitric oxide (NO), and other pro-oxidants, such as hydrogen peroxide and lipid

peroxides. Low concentrations of ROS and RNS are beneficial in biological processes, however, when endogenous antioxidants are unable to scavenge excessive amounts of ROS and RNS, oxidative stress happens.[4] Epilepsy induced oxidative stress can lead to neurotoxicity and affect many other biological pathways. ROS and RNS can attack nucleotides, lipids, and proteins causing irreversible cellular damage and cell death. The central nervous system (CNS) is particularly vulnerable to the detrimental effects of ROS and RNS because it consumes a high amount of oxygen and has weaker antioxidant enzymes.[5] Oxidative stress has been proposed to be a secondary effect and a cause of epilepsy, as well as other neurodegenerative disease, including Alzheimer's disease and Parkinson's disease.[6]

2.1.3 Nitric Oxide

This chapter focuses on one particular RNS, nitric oxide. NO is an abundant molecule in the brain and exhibits important physiological effects in vascular, immune and central and peripheral nervous systems. However, it reacts with other free radicals; for example, superoxide ($O_2^{-\bullet}$), to produce peroxynitrite ($ONOO^-$).[7] Peroxynitrite is a more reactive oxidant than NO and it reacts with various biomolecules and eventually cause cell death.[8] Both nitric oxide and peroxynitrite are unstable under physiological conditions and have short life spans, they usually degrade or react within a

few seconds.[8,9] Therefore, to monitor the production of NO, alternative stable biomarkers are necessary.

Nitric oxide is produced through the nitric oxide synthase (NOS) pathway. There are three common types of NOS in the brain, including neuronal NOS (nNOS), endothelial NOS (eNOS), and inducible NOS (iNOS).[7] nNOS and eNOS are Ca^{2+} dependent, and constitutively express low amount of NO in the cells[10], while iNOS is Ca^{2+} independent and express high amount of NO after being induced.

2.1.4 NO Production and Arginine Cycle

NO is one of the products from arginine cycle (Figure 2.1). On the left side of the arginine cycle, NOS catalyzes the production of NO and *L*-citrulline from *L*-arginine and with the present of NADPH and O_2.[11,12] NO is degraded into nitrate and nitrite within a few seconds and hard to be directly detected, so citrulline is chosen as a stable biomarker of NOS pathway. On the right side, arginine is also metabolized to *L*-ornithine and urea via the arginase pathway. These two pathways might compete each other.[13,14] Ornithine is chosen as a biomarker of arginase pathway. In this chapter, the purpose was to develop a method that can be used monitor the production of nitric oxide *in vivo*. This will then be used to monitor the mechanism, damage, and treatment of oxidative stress in epileptic seizure. Therefore, a method that simultaneously detects citrulline and ornithine as biomarkers of arginine metabolism and NO production and

regulation would be useful for these studies.

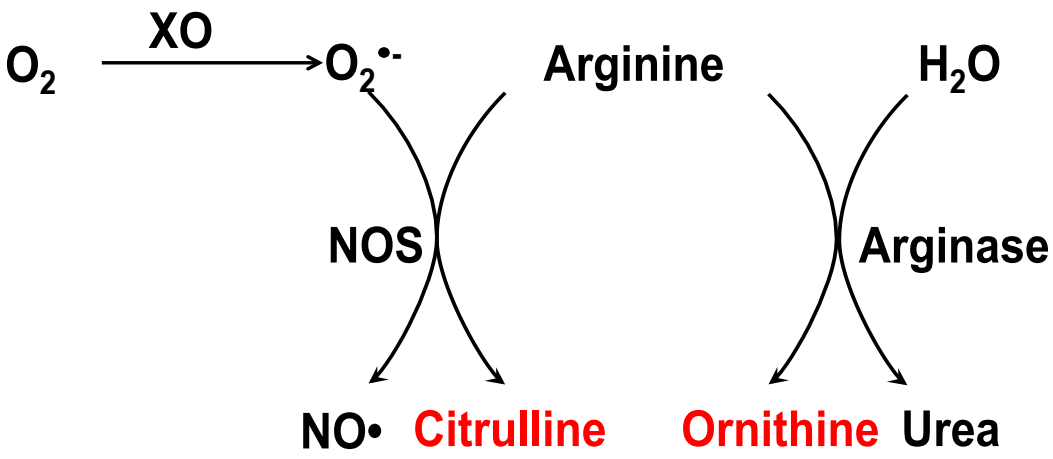

Figure 2.1 Arginine goes through NOS and arginase pathways simultaneously. Arginine is converted into citrulline and nitric oxide through NOS pathway, and it is also converted into ornithine and urea through arginase pathway.

2.1.5 Analytical Methods

The *in vivo* sampling technique used in these studies was microdialysis. As introduced in Chapter 1, microdialysis is a powerful *in vivo* sampling technique. It is able to sample from awake free-moving animals with good temporal resolution, thus it greatly reduce the number of animals utilized. The common microdialysis flow rate is 0.1-5 μL/min, and lower flow rates are preferred to achieve higher recovery. If one assumes a constant flow rate, smaller microdialysate volumes must be collected and analyzed to achieve better temporal resolution. In most cases the volume collected is typically 1-20 μL.[15,16] The small sample volumes characteristic of microdialysis sampling makes capillary electrophoresis (CE) an ideal method for the analysis of these samples. The injection volume of CE is usually in nanoliter range as compared to several microliters for liquid chromatography. Therefore, we utilized CE as the separation method in this project. Moreover, in order to enhance the separation, (2-hydroxypropyl)-β-cyclodextrin (HP-β-CD) was added to the background electrolyte in these studies, because cyclodextrins can form inclusion complexes with small molecules.

Laser induced fluorescence (LIF) was employed as a detection method due to its high sensitivity and low detection limits. Since neither citrulline nor ornithine is natively fluorescent, pre-column derivatization with a fluorophore is needed. 4-(N,N-dimethylaminosulfonyl)-7-fluoro-

2,1,3-benzoxadiazole (DBD-F) was chosen as the derivatization reagent here. DBD-F reacts with both primary and secondary amines and the corresponding derivatives exhibit fluorescence at excitation and emission wavelengths of 450 and 490 nm, respectively.[17-19]

2.2 Experimental

2.2.1 Chemicals and Reagents

L-Citrulline (Cit), *L*-ornithine monohydrochloride (Orn), lithium tetraborate (LTB), (2-hydroxypropyl)-β-cyclodextrin (HP-β-CD), 3-mercaptopropinoic acid (3-MPA), and the internal standard 6-aminocaproic acid (6-ACA) were purchased from Sigma-Aldrich (St. Louis, MO, USA). Methanol, hydrochloric acid (HCl), sodium hydroxide (NaOH), glacial acetic acid (HAc), sodium acetate trihydrate ($NaAc{\cdot}3H_2O$), acetonitrile (MeCN), calcium chloride dihydrate ($CaCl_2{\cdot}2H_2O$), magnesium chloride ($MgCl_2$), potassium chloride (KCl), and sodium chloride (NaCl) were purchased from Fisher (Fair Lawn, NJ, USA). The derivatization reagent 4-(N,N-dimethylaminosulfonyl)-7-fluoro-2,1,3-benzoxadiazole (DBD-F) were purchased from TCI America (Portland, OR, USA). Ethanol was purchased from Decon Labs, Inc (King of Prussia, PA, USA). Ultrapure water was prepared with a Milli-Q system (Millipore, Bedford, MA, USA)

2.2.2 Solutions Preparation

The Ringer's solution used in these studies was composed of 145

mM NaCl, 2.7 mM KCl, 1.2 mM $CaCl_2$ and 1.0 mM $MgCl_2$. Amino acids standard stock solutions and the internal standard stock solution were prepared in 0.1 M perchloric acid and stored at 4 °C and diluted with Ringer's solution prior to use. A 40 mM DBD-F solution was prepared by dissolving the solid in 1 mL MeCN and stored at 4 °C. Optimization of the separation conditions were carried out using 10 µM standard solutions.

2.2.3 Derivatization Procedure

The derivatization reagent DBD-F reacts with primary and secondary amines groups of the amino acids and internal standard. The derivatization reaction is shown in Figure 2.2. For derivatization of the samples and standard 5 µL 40 mM DBD-F in MeCN was mixed with 5 μL amino acids standards/microdialysate sample and 2 µL 80 mM LTB. The reaction was allowed to proceed at 60 °C in dark for 90 minutes. The reaction was stopped by placing the mixture in a freezer at -20 °C.

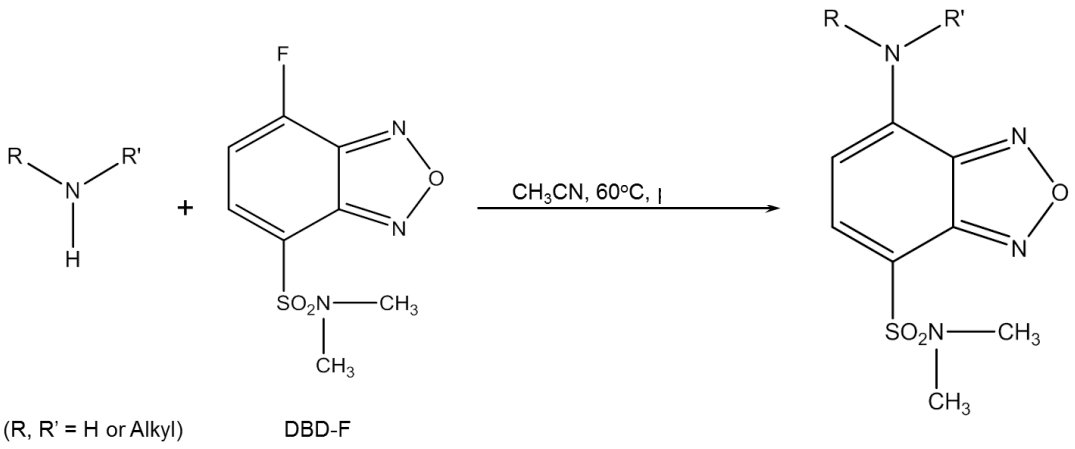

Figure 2.2 The DBD-F derivatization reaction. The reaction conditions consisted of 5 µL 40 mM DBD-F in MeCN mixed with 5 µL amino acids standards/microdialysis sample and 2 µL 80 mM LTB in dark at 60 °C for 90 minutes.

2.2.4 CE-LIF System

A laboratory-built CE separation system was used in these studies. The fused-silica capillary was purchased from Polymicro Technology (Phoenix, AZ, USA). The internal diameter was 50 μm, the total length was 70 cm and the effective length was 55 cm. The capillary was conditioned with methanol for 5 min, 1 M HCl for 3 min, ultrapure water for 3 min, 1 M NaOH for 20 min, millipore water for 3 min, and background electrolyte (BGE) for 20 min at 15 psi every day prior to performing analyses. Between each run, the capillary was flushed with 1 M NaOH for 3 min, millipore water for 3 min and BGE for 3 min. An external ZETALIF detector from Picometrics (Toulouse, France) coupled with a laser (444.6 nm) from CrystaLaser (Reno, NV, USA) was used. A Spellman CZE 1000R high voltage power supply was used and data was acquired using a Chrom&Spec Chromatography Data System (version 1.52y).

2.2.5 CE Separation Conditions

To separate the NO metabolites, a BGE consisting of 20 mM LTB, 20 mM HP-β-CD, and 25% ethanol was employed. Prior to the separation, 6 μL derivatized sample was mixed with 2 μL buffer, which consisted of 135 mM HAc, 15 mM NaAc and 25% MeCN to obtain better resolution. This formed a stacking environment that reduced band broadening and improved the resolution. The sample was introduced by hydrodynamic injection at 5 psi for 3 seconds. A separation voltage of 24 kV was

employed.

2.2.6 Animal Procedures

All animal experiments were performed in accordance with the local Institutional Animal Care and Use Committee. CMA 12 Elite 4 mm brain probes with a 20 kDa cutoff were purchased from CMA Microdialysis (North Chelmsford, MA, USA).

Male Wistar rats (Charles River) weighing from 250-450 g were used for these studies. Aseptic techniques were utilized to minimize contamination and infections. The rats were initially anesthetized in an isoflurane chamber to effect, followed by intraperitoneal injection of an anesthetic cocktail: ketamine (67.5 mg/kg), xylazine (3.4 mg/kg), acepromazine (0.67 mg/kg). The rat body temperature was regulated at 37 ^{o}C by PhysioSuite temperature probe and heating pad (Kent Scientific Cooperation, Torrington, Connecticut, USA). The rat was shaved once it was fully under anesthesia. The brain cannula incision coordinates were determined by placing the rat in a stereotaxic apparatus. The skull was exposed and bregma line was identified. The CMA 12 microdialysis guide cannula (CMA, N. Chelmsford, MA) was implanted into the rat's hippocampus CA3 region (-5.6 A/P, +4.8 L/M, and -5.0 D/V, relative to the bregma line).

After surgery, the rat was placed into a Culex with Raturn System (Bioanalytical Systems Inc., West Lafayette, IN, USA) and food and water

were provided. The microdialysis probe was inserted through the guide cannula into rat brain after it was put in the Raturn. The rat was allowed to recover from anesthetic immediately following surgery.

2.2.7 Microdialysis Sample Collection

Microdialysis sample collection was started 24 hours after recovery from the surgery. Perfusate with and without added convulsant were perfused through the probe using a BASi syringe pump (Bioanalytical Systems Inc., West Lafayette, IN, USA). The convulsant used to induce the seizures was 10 mM 3-mercaptopropinoic acid (3-MPA) dissolved in Ringer's solution. Microdialysis samples were collected over 10 min intervals using a HoneyComb fraction collector (Bioanalytical Systems Inc., West Lafayette, IN, USA). Basal samples were collected for 2 hours by perfusing Ringer's solution at a flow rate of 1.0 µL/min. Then, 10 mM 3-MPA in Ringer's solution was perfused through the probe for 50 minutes at 1.0 µL/min flow rate. Following 3-MPA administration, the perfusate was changed back to Ringer's solution. Sample collection was then continued for another 230 minutes. The control experiments followed the exact same procedures except that Ringer's solution was perfused instead of 3-MPA during the 50 min dosing period. All microdialysis samples were stored at -80 ^{o}C until analysis, typically less than 3 days.

2.3 Method Development

2.3.1 Internal Standard

In order to improve the accuracy and reproducibility of the CE-LIF method, 6-aminocaproic acid (6-ACA), a derivative of lysine, was used as an internal standard. (Figure 2.3) 6-aminocaproic acid can be derivatized and separated from the other amino acids with the DBD-F derivatization method and has similar fluorescence properties to that of citrulline and ornithine. With 6-ACA, the reproducibility of the method was improved as shown in Table 2.1. The peak area %RSD of citrulline was improved from 13% to 10%, and %RSD of ornithine was improved from 18% to 6%.

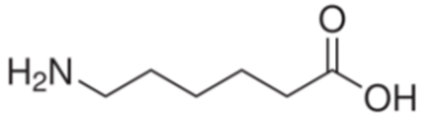

Figure 2.3 Structure of internal standard, 6-aminocaproic acid.

Table 2.1 Reproducibility study results for citrulline and ornithine. (N=5)

	Migration Time		Peak Height		Peak Area	
	Citrulline	Ornithine	Citrulline	Ornithine	Citrulline	Ornithine
%RSD	2	2	25	18	13	18
%RSD IS	NA	NA	21	19	10	6

2.3.2 Optimization of Separation Conditions

The separation conditions were optimized to obtain the best resolution between adjacent peaks including ornithine and the internal standard, the internal standard and citrulline, citrulline and the DBD-F byproduct, and other peaks in the brain microdialysate sample. 20 μM lithium tetraborate (LTB) was used to provide steady electroosmotic flow (EOF). The lithium ion has larger hydrated radii compared to sodium ion. When anions are the same, lithium has lower electrokinetic mobility and provided more stable and slower EOF. Micellar electrokinetic chromatography (MEKC) was also evaluated by adding lithium dodecyl sulfate (LDS); however, it was not able to separate the complicated microdialysis samples.

In order to improve resolution, (2-hydroxypropyl)-β-cyclodextrin (HP-β-CD) was added to the background electrolyte. HP-β-CD can form inclusion complexes with analytes through hydrogen bonding. The electrophoretic migration velocities of different analytes changed due to the different interaction with HP-β-CD.[20] The resolution between the internal standard and citrulline peak, the two least resolved peaks in the electropherogram, was greatly improved with high HP-β-CD concentration as shown in Figure 2.4 (A). When the concentration of HP-β-CD was higher than 20 μM, no significant increase in resolution was observed. However, the total analysis time was longer. Therefore, the optimized

concentration of HP-β-CD was determined to be 20 μM.

To further improve the resolution, ethanol was evaluated as an organic modifier. Ethanol increases the hydrophobicity of the surrounding solvent thereby modifying the interaction between the analyte and the cyclodextrin.[20] Figure 2.4 (B) shows the relationship between ethanol percentage and the resolution between three adjacent peaks: ornithine and internal standard, internal standard and citrulline, citrulline and DBD-F byproduct. Although the resolution between the internal standard and citrulline peaks decreased with increasing ethanol, the resolution between the other peaks were greatly improved. Therefore, the optimized percentage of ethanol was determined to be 25%. An electropherogram of citrulline, ornithine, and the internal standards is shown in Figure 2.5. A basal rat brain microdialysis sample was also analyzed under the optimized separation conditions. The electropherogram is shown in Figure 2.6. Ornithine and citrulline peaks were identified by spiking the microdialysis sample with authentic standards.

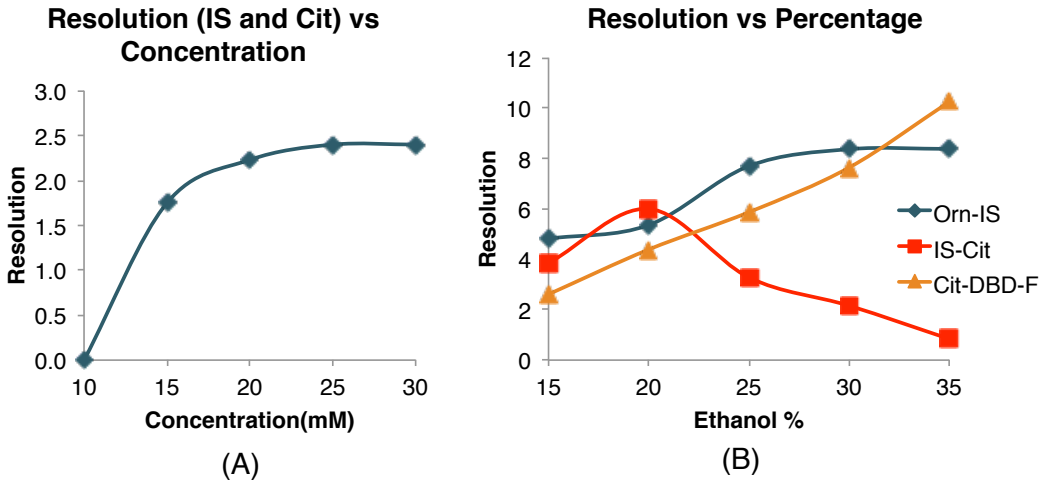

Figure 2.4 Optimization of background electrolyte composition. (A) HP-β-CD concentration optimization. X-axis is HP-β-CD concentration, and y-axls is the resolution between citrulline and the internal standard peak. (B) Ethanol percentage optimization. X-axis is ethanol percentage, and y-axis is the resolution of peaks compared to the internal standard.

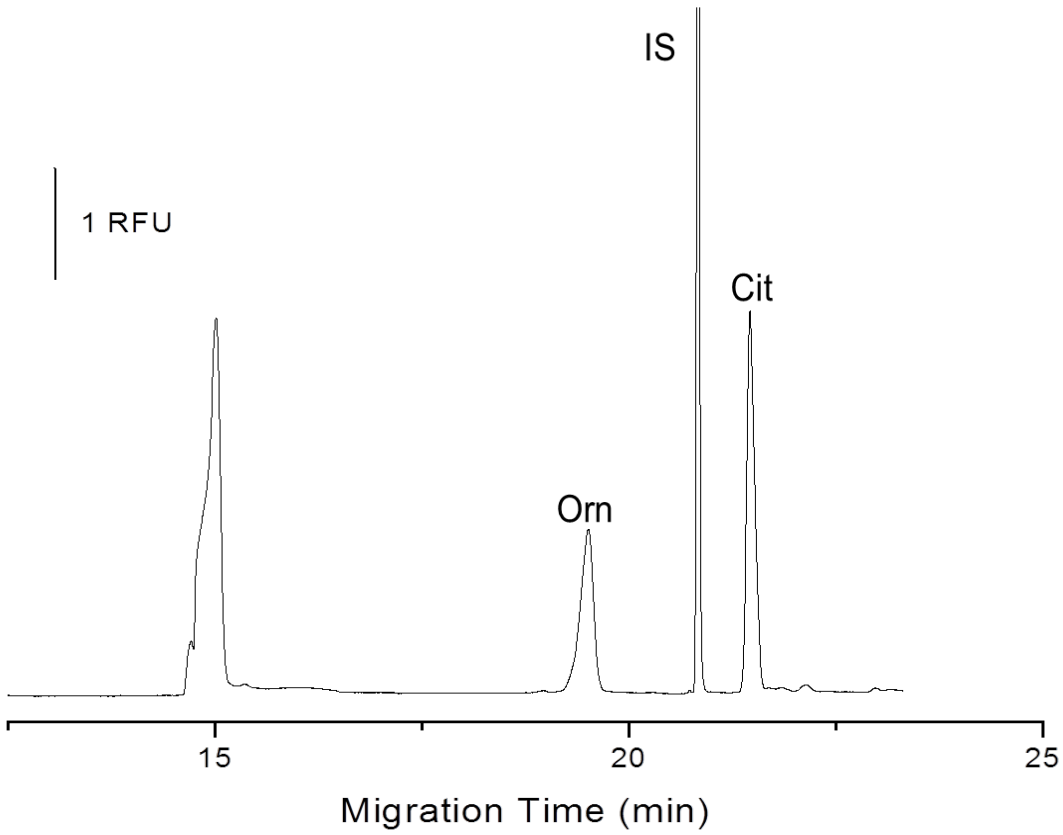

Figure 2.5 Electropherogram of 10 μM citrulline, ornithine, and the internal standard. Separation condition: 20 mM LTB, 25 mM HP-beta-CD, 25% EtOH, pH adjusted to 10.35.

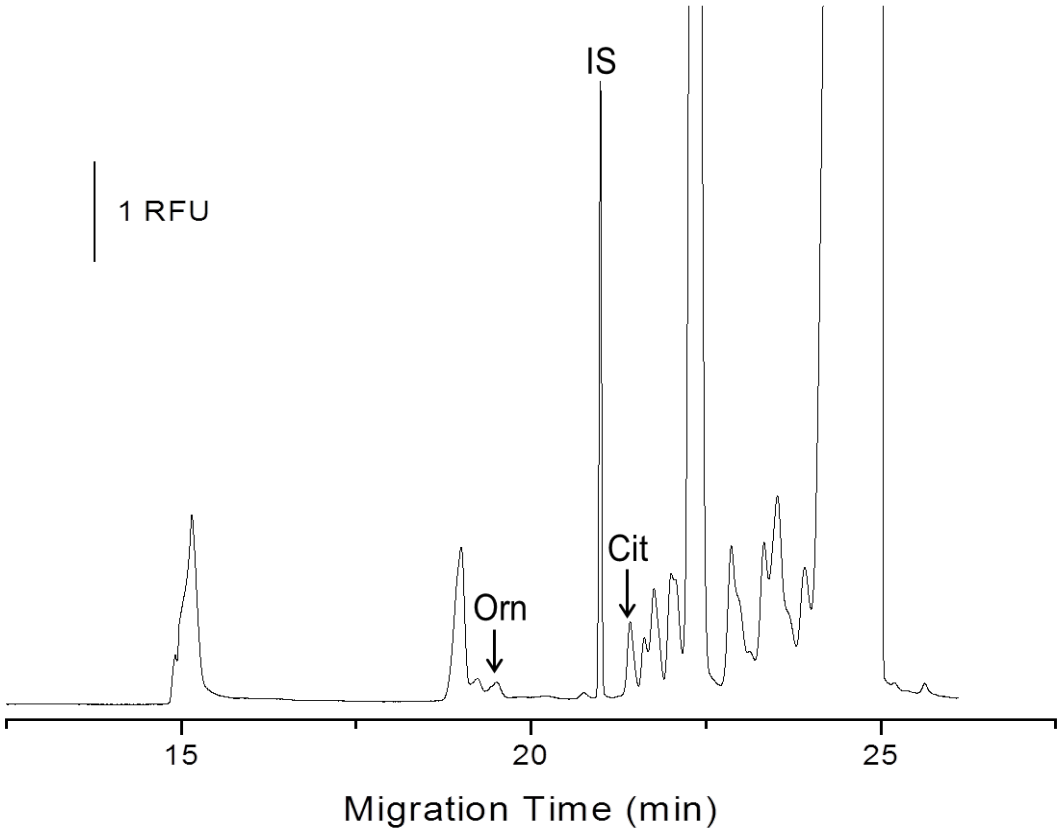

Figure 2.6 Electropherogram of a basal rat brain microdialysis sample. Separation conditions: 20 mM LTB, 25 mM HP-beta-CD, 25% EtOH, pH adjusted to 10.35. The ornithine and citrulline peaks were determined by spiking the microdialysis sample with standards and comparing migration times with internal standard peak.

2.4 Method Validation

Reproducibility of the method was evaluated with and without the use of an internal standard. The standard sample with internal standard is derivatized with the method described in Section 2.2.3. Then the derivatized sample was injected five times and separated using the same batch of BGE. The results are shown in Table 2.1. The normalized result refers to the peak height (peak area) ratio of amino acids to internal standard. It indicates that reproducibility is improved by adding the internal standard. The peak area %RSD of citrulline was improved from 13% to 10%, and %RSD of ornithine was improved from 18% to 6%.

A calibration curve was obtained by using standard solutions of ornithine, citrulline and the internal standard over the concentration range of 0.2 to 10 μM. The measurement at each concentration was repeated three times. The calibration curve was plotted as the peak area ratio of the amino acid to the internal standard versus concentration. The linear regression equation for ornithine peak area was y=0.2300x+0.0144 with R^2=0.9976, and citrulline's linear regression equation from is y=0.3068x+0.0091 with R^2=0.971, where y is peak area ratio of citrulline to internal standard, x is concentration in μM, slope unit is μM^{-1}.The limit of detection was measured as the lowest concentration that gave a signal-to-noise ratio of 3. The LOD of citrulline was 9 nM and the LOD of ornithine was 23 nM.

2.5 *In vivo* Microdialysis Study

The most commonly used seizure model to study epilepsy is the chemically induced seizure model. Our group has applied a 3-mercaptopropinoic acid (3-MPA) induced seizure model, in which 3-MPA is administrated as chemical convulsant to induce seizures.[21-25] Glutamate (Glu) is the major excitatory neurotransmitter in the brain, while γ-aminobutyric acid (GABA) is the major inhibitory neurotransimitter. GAD (glutamic acid decarboxylase) is the enzyme that converts Glu to GABA. 3-MPA is a competitive inhibitor of GAD. When 3-MPA is administrated, it decreases the GABA concentration in the brain and increases Glu concentration. This results an imbalance between GABA and Glu leading to seizures.[26] In this project, 3-MPA was delivered through the microdialysis probe to induce the seizure, and the concentration change of citrulline and ornithine was monitored.

In these studies, the animal was awake and freely moving. In contrast to studies using anesthetized animals, an awake animal study can better mimic the real biomarker changes in the brain, especially since the supplemental anesthesia can affect the concentrations of neurotransmitters in the brain.

Figure 2.7 shows the concentration change of extracellular citrulline and ornithine in the brain during 10 mM 3-MPA dosing. The results show that, after 3-MPA dosing, the concentration of citrulline increased by ~50%

and the concentration of ornithine increased by ~100%, and both of them stay relatively leveled for ~3 hours. T-test was performed with the area under the curve (AUC) at each time point. This provides evidence that both the NOS pathway and arginase pathways are activated as a function of seizure activity. Even though arginase competes with NOS, NO is still produced during epileptic seizure.

This data can be compared with that obtained in future studies investigating the role of oxidative stress in seizures, for example, electrocochleography (ECoG) seizure activity studies. It also can be correlated with the oxidative damage biomarkers such as malondialdehyde (MDA) to determine the damage due to oxidative stress in epileptic seizure, or correlated with how antioxidants such as glutathione and coenzyme Q10 modulate oxidative damage.

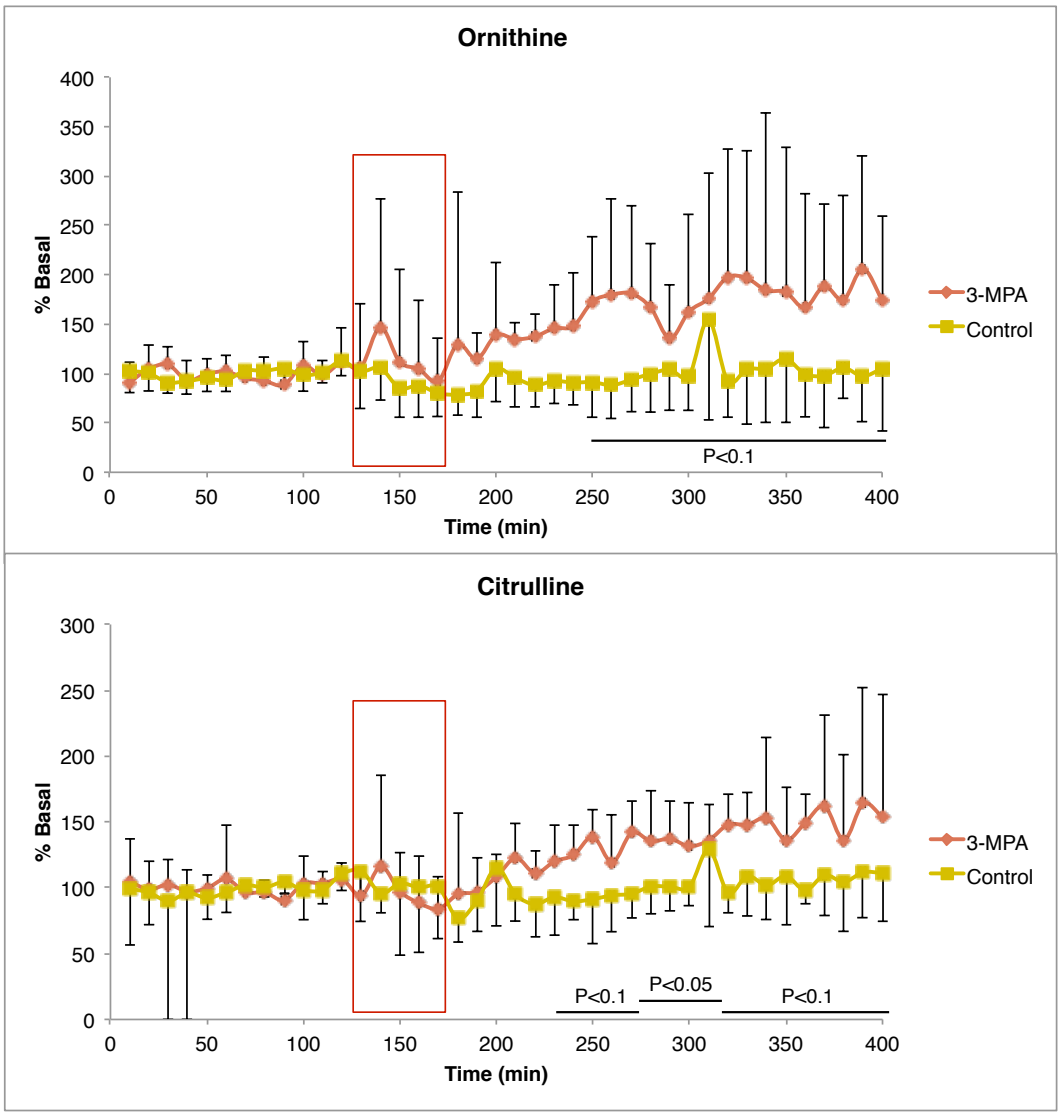

Figure 2.7 Concentration changes of ornithine and citrulline during an epileptic seizure induced by 3-MPA. Red boxes indicate the administration period of 10 mM 3-MPA.

2.6 Conclusion

A cyclodextrin-modified CE-LIF separation method with DBD-F derivatization was developed for citrulline and ornithine that exhibited good linearity, reproducibility and low detection limits. The microdialysis experiments described in this chapter prove that the seizure induced oxidative stress and that this results in an increase in the concentration of both citrulline and ornithine.. From the mechanism shown in Figure 2.1, this indicates that arginine participates in both the NOS and arginase pathways and the production of nitric oxide in the brain is also confirmed.

The method and results described here will be compared with other studies of oxidative stress during seizures in the future, to elucidate the mechanism, damage and methods of treatment. Moreover, although this chapter is focused on citrulline and ornithine, the DBD-F derivatization and cyclodextrin modified CE separation can also be applied to the determination of other amino acids in rat brain microdialysis samples.

2.7 References

(1) Ngugi, A. K.; Kariuki, S. M.; Bottomley, C.; Kleinschmidt, I.; Sander, J. W.; Newton, C. R. Incidence of epilepsy: A systematic review and meta-analysis. *Neurology* **2011**, *77*, 1005-1012.

(2) Brodie, M. J. Meta-analyses of antiepileptic drugs for refractory partial (focal) epilepsy: an observation. *British Journal of Clinical Pharmacology* **2013**, *76*, 630-631.

(3) Löscher, W.; Schmidt, D. Modern antiepileptic drug development has failed to deliver: Ways out of the current dilemma. *Epilepsia* **2011**, *52*, 657-678.

(4) Aguiar, C. C. T.; Almeida, A. B.; I.; Araújo, P. V. P.; Abreu, R. N. D. C. d.; Chaves, E. M. C.; Vale, O. C. d.; Macêdo, D. S.; Woods, D. J.; Fonteles, M. M. d. F; Vasconcelos, S. M. M. Oxidative stress and epilepsy: literature review. *Oxidative Medicine and Cellular Longevity* **2012**, Article ID 795259, 12 pages.

(5) Li, J.; O, W.; Li, W.; Jiang, Z. G.; Ghanbari, H. A. Oxidative stress and neurodegenerative disorders. *International Journal of Molecular Sciences* **2013**, *14*, 24438-24475.

(6) Chang, S. J.; Yu, B. C. Mitochondrial matters of the brain: mitochondrial dysfunction and oxidative status in epilepsy. *Journal of Bioenergetics and Biomembranes* **2010**, *42*, 457-459.

(7) Guix, F. X.; Uribesalgo, I.; Coma, M.; Muñoz, F. J. The physiology and pathophysiology of nitric oxide in the brain. *Progress in Neurobiology* **2005**, *76*, 126-152.

(8) Szabo, C.; Ischiropoulos, H.; Radi, R. Peroxynitrite: biochemistry, pathophysiology and development of therapeutics. *Nature Reviews Drug Discovery* **2007**, *6*, 662-680.

(9) Valko, M.; Rhodes, C. J.; Moncol, J.; Izakovic, M.; Mazur, M. Free radicals, metals and antioxidants in oxidative stress-induced cancer. *Chemico-Biological Interactions* **2006**, *160*, 1-40.

(10) Mungrue, I. N.; Bredt, D. S.; Stewart, D. J.; Husain, M. From molecules to mammals: what's NOS got to do with it? *Acta Physiologica Scandinavica* **2003**, *179*, 123-135.

(11) Ebadi, M.; Sharma, S. K. Peroxynitrite and mitochondrial dysfunction in the pathogenesis of Parkinson's disease. *Antioxidants & Redox Signaling* **2003**, *5*, 319-335.

(12) Iadecola, C.; Zhang, F.; Xu, S.; Casey, R.; Ross, E. M. Inducible nitric oxide synthase gene expression in brain following cerebral ischemia. *Journal of Cerebral Blood Flow & Metabolism* **1995**, *15*, 378-384.

(13) Lai, Y.; Aoyama, S.; Nagai, R.; Miyoshi, N.; Ohshima, H. Inhibition of L-arginine metabolizing enzymes by L-arginine-derived advanced glycation end products. *Journal of Clinical Biochemistry and Nutrition* **2010**, *46*, 177-185.

(14) Xia, Y.; Zweier, J. L. Superoxide and peroxynitrite generation from inducible nitric oxide synthase in macrophages. *Proceedings of the National Academy of Sciences of the United States of America* **1997**, *94*, 6954-6958.

(15) Chaurasia, C.; Müller, M.; Bashaw, E.; Benfeldt, E.; Bolinder, J.; Bullock, R.; Bungay, P.; DeLange, E. M.; Derendorf, H.; Elmquist, W.; Hammarlund-Udenaes, M.; Joukhadar, C.; Kellogg, D., Jr.; Lunte, C.; Nordstrom, C.; Rollema, H.; Sawchuk, R.; Cheung, B. Y.; Shah, V.; Stahle, L.; Ungerstedt, U.; Welty, D.; Yeo, H. AAPS-FDA workshop white paper: Microdialysis principles, application and regulatory perspectives.

Pharmaceutical Research **2007**, *24*, 1014-1025.

(16) Nandi, P.; Kuhnline, C. D.; Lunte, S. M.: Analytical considerations for microdialysis sampling. In *Applications of Microdialysis in Pharmaceutical Science*; John Wiley & Sons, Inc., **2011**, 39-92.

(17) Sugiura, K.; Min, J. Z.; Toyo'oka, T.; Inagaki, S. Rapid, sensitive and simultaneous determination of fluorescence-labeled polyamines in human hair by high-pressure liquid chromatography coupled with electrospray-ionization time-of-flight mass spectrometry. *Journal of Chromatography A* **2008**, *1205*, 94-102.

(18) Tsutsui, H.; Mochizuki, T.; Inoue, K.; Toyama, T.; Yoshimoto, N.; Endo, Y.; Todoroki, K.; Min, J. Z.; Toyo'oka, T. High-throughput LC–MS/MS based simultaneous determination of polyamines including N-acetylated forms in human saliva and the diagnostic approach to breast cancer patients. *Analytical Chemistry* **2013**, *85*, 11835-11842.

(19) Uchiyama, S.; Santa, T.; Okiyama, N.; Fukushima, T.; Imai, K. Fluorogenic and fluorescent labeling reagents with a benzofurazan skeleton. *Biomedical Chromatography* **2001**, *15*, 295-318.

(20) Tang, W.; Ng, S. C. Monosubstituted positively charged cyclodextrins: Synthesis and applications in chiral separation. *Journal of Separation Science* **2008**, *31*, 3246-3256.

(21) Crick, E. W.; Osorio, I.; Frei, M.; Mayer, A. P.; Lunte, C. E. Correlation of 3-mercaptopropionic acid induced seizures and changes in striatal neurotransmitters monitored by microdialysis. *European Journal of Pharmaceutical Sciences* **2014**, *57*, 25-33.

(22) Mayer, A. P.; Osorio, I.; Lunte, C. E. Microperfusion of 3-MPA into the brain augments GABA. *Epilepsy & behavior: E&B* **2013**, *29*, 478-484.

(23) Mayer, A. P. Local dosing in a 3-Mercaptopropionic acid chemically-induced epileptic seizure model with microdialysis sampling. Ph.D., University of Kansas, 2010.

(24) Crick, E. W.; Osorio, I.; Bhavaraju, N. C.; Linz, T. H.; Lunte, C. E. An investigation into the pharmacokinetics of 3-mercaptopropionic acid and development of a steady-state chemical seizure model using *in vivo* microdialysis and electrophysiological monitoring. *Epilepsy research* **2007**, *74*, 116-125.

(25) Crick, E. W. *In vivo* microdialysis coupled with electrophysiology for the neurochemical analysis of epileptic seizures. Ph.D., University of Kansas, 2007.

(26) Netopilová, M.; Dršata, J.; Haugvicová, R.; Kubová, H.; Mareš, P. Inhibition of glutamate decarboxylase activity by 3-mercaptopropionic acid has different time course in the immature and adult rat brains. *Neuroscience Letters* **1997**, *226*, 68-70.

3 LC-MS Method Development of Eicosanoids in Rat Colon Microdialysate to Study Inflammatory Bowel Disease

3.1 Background

3.1.1 Inflammatory Bowel Disease

Inflammatory bowel disease (IBD) is a chronic relapsing inflammatory gastrointestinal (GI) tract disorder. It is one of the most prevalent GI tract diseases in the world and affects 1.4 million people in the US and 2.2 million people in Europe in total currently. [1-2] IBD has a peak incidence in 15-30 years old adults.[3] It has two important subtypes, Crohn's disease (CD) and ulcerative colitis (UC). They are mostly distinguished from each other by the inflammation tissue sites. In CD, inflammation spreads throughout the entire GI tract, while in UC, the inflammation is confined to the colon. Moreover, in CD, the inflammation infects all the GI tract layers, while in UC, the inflammation only involves mucosa and submucosa layers. The clinical symptoms of IBD, including bloody diarrhea, abdominal pain during bowel movement, fever, loss of appetite, and sequential weight loss, are mostly due to inflammation.[4] Chronic inflammation increases the risk of IBD developing into colorectal cancer approximately 18 fold.[5] CD and UC have similar treatment plans including 5-aminosalicylic acid[6,7], anti-tumor necrosis factor-α (TNF-α)

therapies[8] and enzyme modulators[9,10].

The pathogenesis of IBD involves three factors: genetic predisposition, environmental triggers, and inappropriate mucosal immune response. Nod2 gene mutations are the gene predisposition primarily responsible for IBD.[4] IBD is more prevalent among Caucasians and Ashkenazi Jews. It has its highest incidence rate in northern Europe and North America. It is also clustered within families, with a reported 50%–60% concordance of Crohn's disease in identical twins.[3] Environmental triggers include viral/bacterial infection and smoking. Interestingly, cigarette smoking shows different influences with regard to UC and CD. In CD patients, smoking exacerbates inflammation; however, non-smokers have a higher risk of getting UC.[2,11] In healthy people, the gut can tolerate some amount of the nonpathologic antigens such as viral or bacterial; however, for those who have a genetic susceptibility toward IBD, the antigens induce an inappropriate mucosal immune response and cause IBD.[3,12,13]

3.1.2 Enzyme Pathways

In this section, we introduce the third factor—inappropriate mucosal immune response—in detail. The inflammatory response begins with CD4+ T-lymphocytes being recognized as nonpathologic antigens. These T-lymphocytes are called T-helper (Th) cells and are important in mediating and regulating the immune response. The antigen presenting

cells interact with Th cells, activating the Th cells that differentiate into Th1 cells that secrete interleukin-2 (IL-2) and interferon gamma (IFN-γ). Similarly in patients with UC, Th cells differentiate into Th2 cells producing IL-5 and the transforming growth factor β (TGF-β).[14] These cytokines induce the gene expression of several enzymatic pathways, such as cyclooxygenase (COX), lipoxygenase (LOX) and inducible nitric oxide synthase (iNOS). In healthy people, the inflammation is self-limiting, but in those with genetic susceptibility, it develops into the chronic inflammation of IBD. The exact mechanism of IBD is still not fully understood. The objective of the studies in this chapter is to investigate two of the enzymatic pathways, COX and LOX using *in vivo* microdialysis sampling. We chose 13 prostaglandins, thromboxane, hydroxyeicosatetraenoic acids and leukotrienes as the biomarkers for COX and LOX pathways. This chapter focuses on the development of a LC-MS/MS method to study the biomarkers in rat colon microdialysate.

3.1.2.1 Cyclooxygenase

Cyclooxygenases (COXs) are the enzymes involved in the three-step metabolism of arachidonic acid (AA) to prostaglandins (PGs) and thromboxane (TXB). There are two major isoforms of COX, COX-1 and COX-2. COX-1 is known as “housekeeping” enzyme that is constitutively expressed in prostanoid-producing cells under normal physiological conditions. It is responsible for the normal physiological production of PGs.

COX-2 is an inducible enzyme present that exists in inflamed tissues. The gene expression of COX-2 is very low in the healthy tissue. However, it is secreted by inflamed tissues and mediates the inflammation response. Studies have shown the messenger ribonucleic acid (mRNA) expression of COX-1 remains normal while mRNA expression of COX-2 greatly increases during the acute inflammatory response.[15]

COX first catalyzes AA oxidation to prostaglandin G_2 (PGG_2s). PGG_2 are sequentially reduced to the prostaglandin H_2 (PGH_2). PGH_2 are converted into various prostaglandins and thromboxanes, including prostaglandin D_2 (PGD_2), prostaglandin E_2 (PGE_2), prostaglandin $F_{2\alpha}$ ($PGF_{2\alpha}$), TXB_2, 8-isoprostaglandin $F_{2\alpha}$ (8-iso$PGF_{2\alpha}$) and 6-ketoprostaglandin $F_{2\alpha}$ (6-keto$PGF_{2\alpha}$) via different synthases.[16,17] The detailed pathways are shown in Figure 3.1. The pro-inflammatory prostaglandins including PGD_2, PGE_2, $PGF_{2\alpha}$, TXB_2, 8-iso$PGF_{2\alpha}$ and 6-keto$PGF_{1\alpha}$ were chosen as biomarkers of the COX pathway to monitor the IBD inflammatory response.[18,19]

3.1.2.2 Lipoxygenase

Similar to the behavior noted for COX, lipoxygenases (LOX) mediate the conversion of AA into hydroxyeicosatetraenoic acids (HETE) and leukotrienes (LTs). There are three common isoforms of LOX: 5-LOX, 12-LOX and 15-LOX. LOX first catalyzes AA oxidation to hyperperoxyeicosatetraenoic acids (HPETEs), more specifically, 5-

HPETE, 12-HPETE and 15-HPETE. These HPETEs are unstable intermediates and are subsequently reduced to their corresponding HETEs, 5-HETE, 12-HETE and 15-HETE by glutathione peroxidase or microsomal glutathione S-transferases.

In the 5-LOX pathway, 5-HPETE not only produces 5-HETE, but also produces LTA_4. LTA4 is an unstable epoxide that can be further converted into the more stable products: LTB_4, LTC_4, LTD_4 and LTE_4. LTs are lipid signaling compounds that are important in modulating the inflammatory response.[20] As shown in Figure 3.1, the more stable final products (LTB_4, LTC_4, LTD_4, LTE_4, 5-HETE, 12-HETE and 15-HETE) were chosen as the biomarkers for LOX pathways.

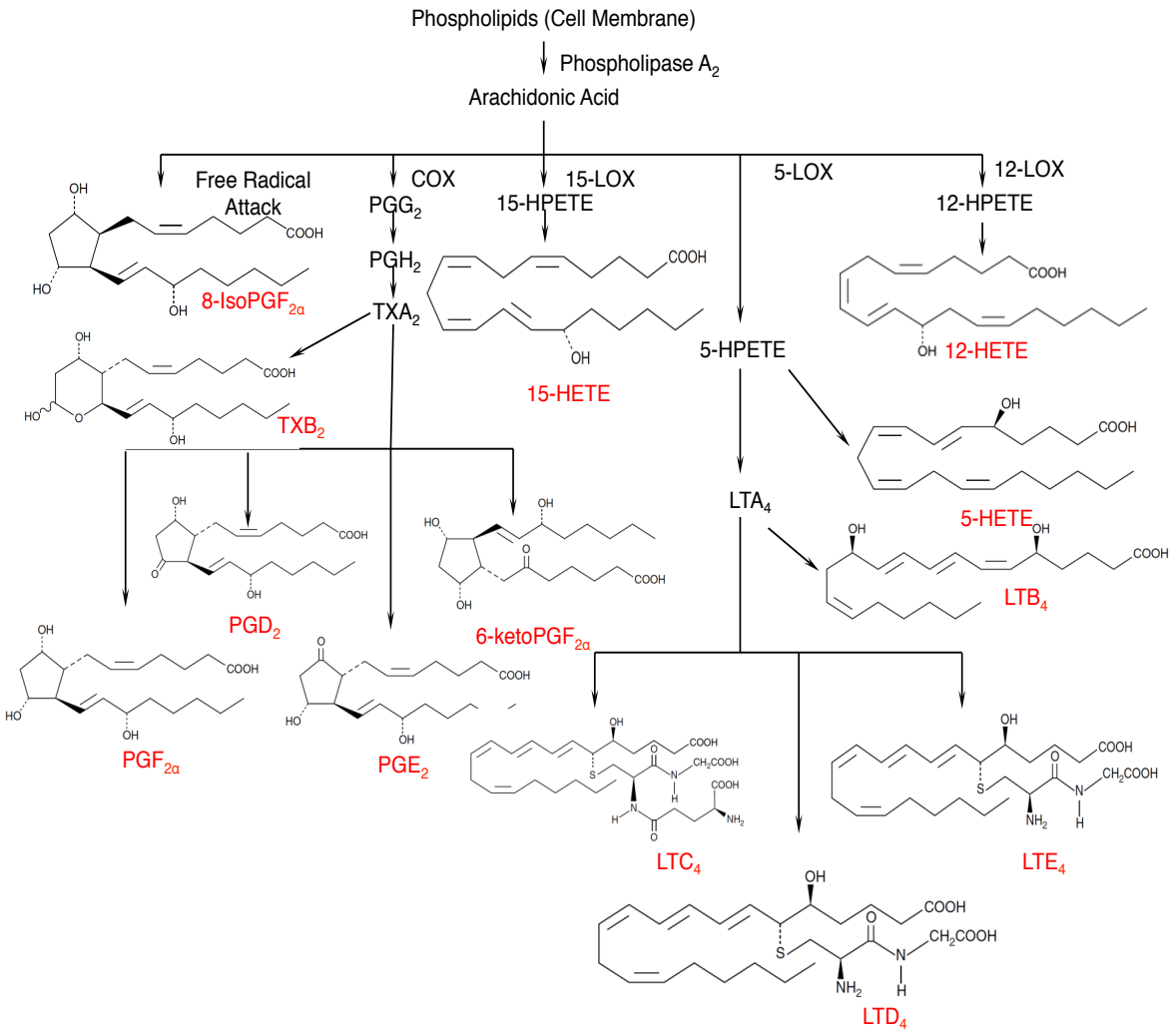

Figure 3.1 Phospholipid degradation pathways catalyzed by COX, LOX enzymes. The analytes shown in red are the target analytes in this project.

3.2 Experimental

3.2.1 Chemicals and Reagents

PGD_2, PGE_2, $PGF_{2\alpha}$, TXB_2, 8-iso$PGF_{2\alpha}$, 6-keto$PGF_{1\alpha}$, TXB_2, LTB_4, LTC_4, LTD_4, LTE_4, 5-HETE, 12-HETE and 15-HETE were purchased from Cayman Chemicals (Ann Arbor, MI, USA). LC-MS grade formic acid and acetic acid were purchased from Sigma-Aldrich (St. Louis, MO, USA). Acetonitrile (MeCN), calcium chloride dihydrate ($CaCl_2 \cdot 2H_2O$), magnesium chloride ($MgCl_2$), potassium chloride (KCl), and sodium chloride (NaCl) were purchased from Fisher (Fair Lawn, NJ, USA). Ethanol was received from Decon Labs, Inc (King of Prussia, PA, USA). Ultrapure water was prepared with a Milli-Q system (Millipore, Bedford, MA, USA)

3.2.2 Solution Preparations

Ringer's solution used for microdialysis studies consisted of 145 mM NaCl, 2.7 mM KCl, 1.2 mM $CaCl_2$ and 1.0 mM $MgCl_2$. PGs and TXB stock solutions were prepared by dissolving them into ethanol at a concentration of 1 mg/mL. The resulting solutions were stored at -80 ^oC . The standard solutions containing 5 µM PGs, LTs, TXB and HETEs were prepared in Ringer's solution. For long-term storage (> 3 days), the standard diluted solutions were stored at –80 ^oC. For short-term storage (≤ 3 days), the standard diluted solutions were stored at –20 ^oC.

3.2.3 LC-MS Condition

3.2.3.1 LC Condition

The LC separation system was a binary gradient system made up of two Shimadzu LC 20 ADxr pumps and a CBM-20A system controller. The LC column was a Phenomenex Kinetex XB-C18 column (100 mm long, 2.1 mm i.d., 1.7 µm particle size). The optimized separation was achieved by gradient elution. Solvent A consisted of 60 mM acetic acid. Solvent B was 100% acetonitrile containing 60 mM acetic acid. A linear gradient profile was employed as follows: 0–18 minutes, solvent B increased from 25 to 55%. Then it was increased to 60% and held there between 18 to 27.5 minutes; finally, the gradient was decreased back to 25% of mobile phase B for 10 minutes to establish equilibrium in the column. (Figure 3.2)

3.2.3.2 MS Detection

Tandem mass spectra were acquired via a Thermo LTQ XL ion-trap mass spectrometer coupled with an ESI interface in the negative ion mode. The ESI source conditions were optimized to achieve the optimal ionization efficiency as follows: spray voltage at 4.5 kV, capillary temp at 225 ^{o}C. For different analytes, the detection was divided into different segments based on the LC retention time to improve sensitivity. In each segment where MS/MS detection was utilized, the collision energy and isolation width were optimized. The optimal isolation width is smallest

window of *m/z* value that gives highest intensity. If the isolation width is too small, the peak height might be small. If the isolation width is too large, the noise can be high. The segments and corresponding optimized conditions are listed in Table 3.1. A diverting valve was utilized to guide the first 6.5 min and the last 7.5 min eluents to waste. MS data were obtained and analyzed by Xcalibur software.

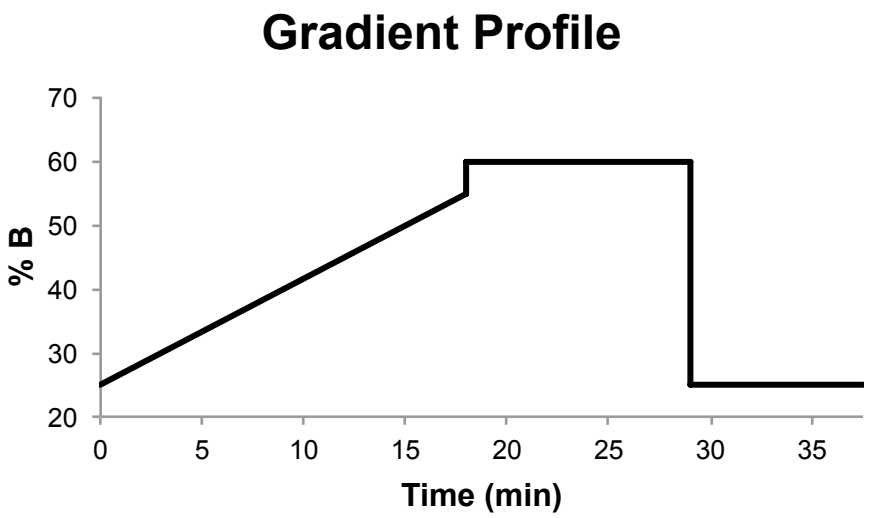

Figure 3.2 LC separation mobile phase gradient. Mobile phase A consists of an aqueous solution of 60 mM acetic acid. Mobile phase B is acetonitrile containing 60 mM acetic acid.

Table 3.1 MS/MS detection conditions. The detection windows are divided into different segments based on elution time. The parent ions are identified by full scan. Isolation width, collision energy and product ions are optimized to achieve best S/N.

Segment	Elution Time (min)	Analytes	Parent Ion (m/z)	Isolation Width (m/z)	Normalized CID Energy (%)	Product Ions (m/z)
1	0-6.50	To Waste				
2	6.50-9.83	6-keto	369.48	3.0	35	315.31, 333.32, 351.34
3	9.83-12.83	PGF, 8-IsoPGF	353.45	1.0	25	335.34
		TXB	369.31	1.5	35	169.17, 195.18
4	12.83-15.33	PGE, PGD	351.43	1.5	35	315.30, 333.31
5	15.33-18.23	LTD	496.50	3.0	35	351.32, 477.39
		LTE	439.50	2.5	35	420.32
		LTC	624.50	3.5	35	354.17, 272.17, 606.46
6	18.23-21.94	LTB	335.47	1.0	25	195.16
7	21.94-30.00	5-HETE, 12-HETE, 15-HETE	319.42	1.0	30	219.3, 257.33, 301.35
9	30.00-37.50	To Waste				

3.3 Method Development

3.3.1 LC Separation Optimization

Thirteen analytes with different properties were separated by reverse phase LC. The total analysis time was greater than one hour using isocratic elution. In order to reduce total analysis time, gradient elution was used. The gradient changed from 25 to 55% mobile phase B within the first 18 minutes to separate the PGs, TXB, LTC, LTD and LTE. The mobile phase B was then increased and held at 60% from 18–27.5 min to separate LTB and HETEs. At last the %B was changed back to 25% to establish equilibrium for the next run, ending at 37.5 min. A detailed gradient profile is shown in Figure 3.2. The LC column was an XB-C18 column (100 mm long, 2.1 mm i.d., 1.7 µm particle size). The column diameter and stationary phase particle size was small leading to column pressures that were too high for the Shimadzu 20 ADxr HPLC pumps. In order to maintain a lower column pressure at faster flow rates, acetonitrile was used as the organic phase instead of methanol because of its lower viscosity. A flow rate of 0.12 mL/min was used in these studies. The injection volume was 10 µL.

The goal of this chapter was to design a LC-MS method for the analysis of eicosanoids in colon microdialysis samples. The endogenous extracellular concentration of the eicosanoids is less than 20 nM, and microdialysis recovery of the eicosanoids is only 5-20%. The sample

volume available for LC injection is also limited (<15 µL). All of these challenges require a high sensitivity LC-MS method.

In order to improve ionization efficiency and sensitivity, LC mobile phase modifiers were evaluated. Common ESI-LC-MS modifiers include volatile weak acids or weak bases. Examples include acetic acid, formic acid, and ammonium acetate. In most circumstances, weak acids are utilized for positive ionization mode. This is a straightforward solution because weak acids add positively charged hydrogen ions to the ESI spray droplets and protonate the analytes.

In initial experiments, positive mode was assessed; however, higher baseline noise was observed in the positive mode as compared to the negative mode, which compromised the LOD. This is because more interfering compounds are ionized and detected in the positive ion mode. After switching to the more selective negative ionization mode, the baseline noise was reduced. The weak acids improved the limits of detection.

Adding a weak acid to the mobile phase while applying a negative voltage is not as common as applying a positive voltage, but this phenomenon was observed before.[21-23] Dalton et al. performed a systematic study using four different carboxylic acids: formic acid, acetic acid, propionic acid, and n-butyric acid as mobile phase modifiers.[24] They added them individually as mobile phase modifiers in a negative ionization

mode ESI. Their results were as follows: Although formic acid diminished ionization, the other three weak carboxylic acids improved negative ionization efficiency. Among those three, acetic acid was the most effective.

They also found that ionization efficiency varies along with different acid concentrations and target analytes. They proposed a "wrong way round" theory to explain this phenomenon. Small droplets are formed in the ESI ion source. The weak acids provided both excessive protons and their corresponding negative ions accumulated on ESI spray tip and droplet surface. In the negative ionization mode, a negative electric field was applied, which reduced H^+ to hydrogen gas that evaporated from the droplets; hence, excessive negative ions were left on the droplet surface. This is how weak acids help improve negative ionization efficiency. Based on this hypothesis, they also investigated the relationship between gas-phase proton affinities of carboxylic anions and their ionization efficiency. Formic acid has a Gibbs free energy of the formation from ions of 1415.0 ± 8.4 kJ/mol; while acetic acid has 1427.0 ± 8.4 kJ/mol. Not surprisingly, acetic acid gave the best ionization efficiency.[24]

We performed similar studies using formic acid and acetic acid. We added the same amount of formic acid or acetic acid in the mobile phase, and the ionization was conducted in the negative mode. As shown in Figure 3.3 and Figure 3.4, the results are consistent with Dalton's work.[24]

With acetic acid, all 13 analytes gave a better response than that with formic acid. We also further optimized the concentration of acetic acid. As stated in Dalton's paper, different analytes also responded differently under different concentrations. For the relatively better ionized analytes, 6-ketoPGF, 8-isoPGF and PGE, the 23.5 mM concentration proved to be the most favorable. However, for the other analytes, 60 mM was better. Since the 6-ketoPGF, 8-isoPGF and PGE give higher response than the other analytes, we chose the high concentration of 60 mM acetic acid as the optimized mobile phase modifier condition.

3.3.2 MS Detection Optimization

For initial experiments, standard analytes were infused into MS, and detected in the full scan mode to identify the parent ions *m/z*. After the parent ions were determined, collision gas was applied to fragment the parent ions, and then the product ions were determined. Collision energy and isolation width were optimized to achieve the best sensitivity. In order to optimize the LODs, the most abundant 1–3 product ions in SRM detection and their different combinations were analyzed. The combinations with best S/N were chosen as the optimized SRM fragmentations. Table 3.1 summarizes the optimized MS conditions.

In the *in vivo* study, the perfusate was Ringer's solution. No matter what the standards were dissolved in, Ringer's solution or *in vivo* microdialysate, the sample matrices all contained a high concentration of

salt. When such a large amount of salt goes into ESI-MS, it will cause ESI source capillary to clog and can also lead to ion suppression. In order to avoid this, we used a divert valve to elute the first 6.5 min and last 7.5 min of the eluent to the waste. The salt is not retained on the C-18 column and exits as waste in the first 6.5 minutes.

In order to improve sensitivity, MS detection was divided into different segments based on LC elution time. Only one analyte was tried to be assigned to one segment; however, for analytes that co-eluted or that elute closely with each other, two or three analytes were assigned to one segment. For example, LTC, LTD, and LTE all eluted around 16-17 min, so they were assigned in a 15.33-18.23 min segment together. More details of the other segments are listed in Table 3.1.

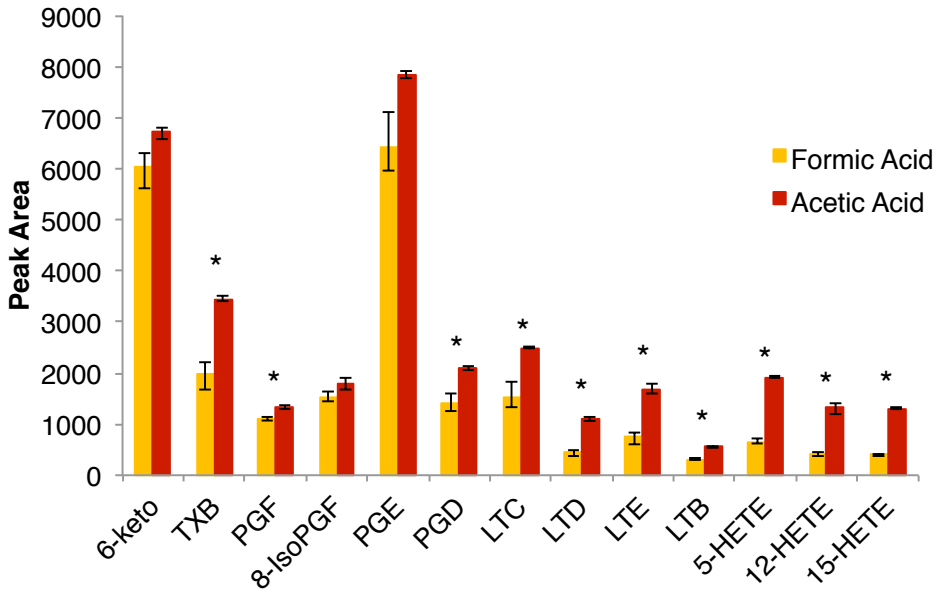

Figure 3.3 Mobile phase modifier optimization-weak acid type comparison. (20nM standards, N=3) * shows the data was statistical significant at p=0.05.

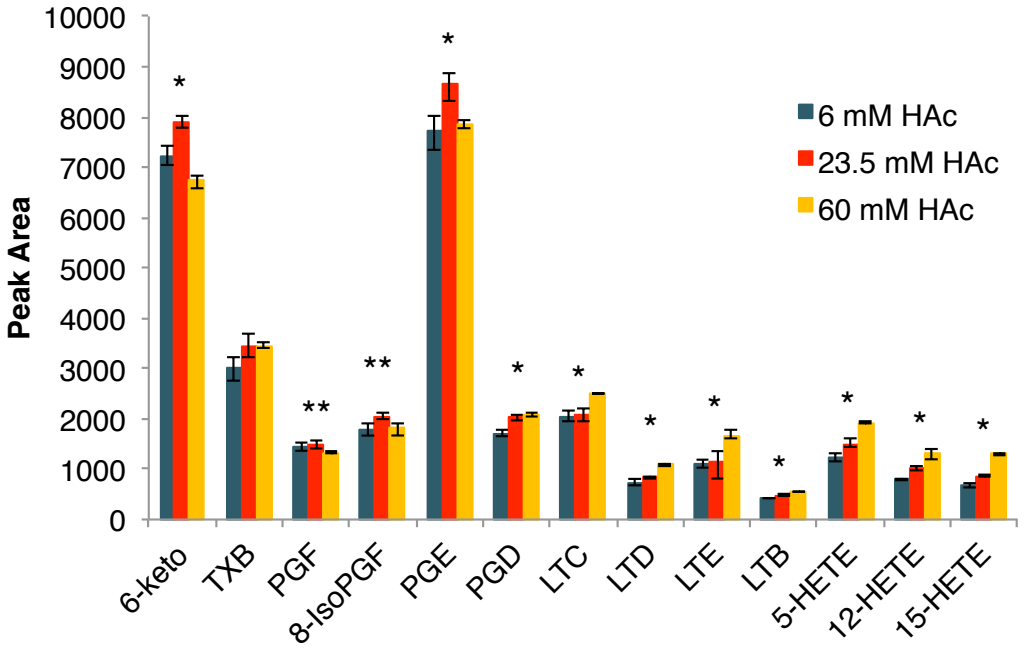

Figure 3.4 Comparison of mobile phase modifier concentration on peak area. (20nM standards, N=3) * shows the result is significant in ANOVA F test at alpha=0.05. ** shows the result is significant in ANOVA F test at alpha=0.1.

3.4 Method Validation

3.4.1 Calibration Curve

Standard solutions with 13 eicosanoids were prepared in Ringer's solution by serial dilution to build calibration curves. The calibration range was 1-100 nM, and the seven calibration points were 1, 2, 5, 10, 20, 50, 100 nM. Since analytes exhibit different degrees of hydrophobicity and different ionization efficiency, the linear range will be different for each compound. The calibration curve of TXB only had four points between 10-100 nM; the calibration curves of PGD, 5-HETE, 12-HETE and 15-HETE had six points between 2-100 nM. All the other analytes used a seven-point calibration from 1-100 nM. The calibration range and linear regression coefficients are listed in Table 3.2.

The linear regression coefficients obtained using this method were not optimal. One of the reasons is that some of the analytes are hydrophobic, so they precipitated out or attached to vial walls during the serial dilution process. The predicted octanol-water partition coefficients (logP) of the 13 eicosanoids are listed in Table 3.3.[25] Only 6-ketoPGF has a log P less than 1 (P=0.93), all the other analytes had a log P larger than 1, which indicates they are hydrophobic. Also, the LTs and HETEs are more hydrophobic compared to PGs, since their log P values are larger than 5 while PGs log P values are around 2. This issue was addressed by adding cyclodextrin, which will be discussed in Chapter 4.

Table 3.2 Calibration curves, their R^2, and the calibration range, where x is the concentration in nM and y is the signal intensity.

Analytes	Calibration Curve	R2	Calibration Range
6-keto	y=352x+477	0.9907	2-100 nM
TXB	y=173x-341	0.9898	10-100 nM
PGF	y=71x+127	0.9879	1-100 nM
8-IsoPGF	y=117x+160	0.9921	1-100 nM
PGE	y=370x+25	0.9896	1-100 nM
PGD	y=106x+112	0.9962	2-100 nM
LTC	y=320x-245	0.9946	1-100 nM
LTD	y=116x+235	0.9963	1-100 nM
LTE	y=206x-199	0.9980	1-100 nM
LTB	y=90x-140	0.9841	1-100 nM
5-HETE	y=153x-658	0.9577	2-100 nM
12-HETE	y=90x-306	0.9920	2-100 nM
15-HETE	y=99x-259	0.9934	2-100 nM

Table 3.3 Predicted octanol-water partitioning coefficients.[25]

Analyte	log P
6-keto	0.93
TXB	2.09
PGF	2.14
8-IsoPGF	2.6
PGE	1.88
PGD	2.02
LTC	5.99
LTD	5.78
LTE	5.65
LTB	4.06
5-HETE	5.56
12-HETE	5.45
15-HETE	5.22

3.4.2 Reproducibility

A mixture containing10 nM standard solutions of the 13 analytes in Ringer's solution was injected five times into the LC-MS to test reproducibility. The percent relative standard deviation (%RSD) results are shown in Table 3.4. The reproducibility of the peak area was better than that of peak height, so all further quantification was based on peak area.

3.4.3 Chromatography

A chromatogram of the 10 nM 13 standards is shown in Figure 3.5 under the optimized separation and MS detection conditions discussed above. The LC system successfully separated most of the analytes. Only the LTC_4, LTD_4 and LTE_4 peaks coeluted, but they have different molecular masses, so they are easily distinguished with MS.

Table 3.4 Reproducibility results from 10 nM standard solutions. (N=5)

Analytes	Peak Height % RSD	Peak Area % RSD
6-keto	35	2
TXB	21	6
PGF	18	10
8-IsoPGF	11	4
PGE	7	1
PGD	6	3
LTC	13	3
LTD	13	5
LTE	8	6
LTB	6	4
5-HETE	7	12
12-HETE	12	5
15-HETE	3	5

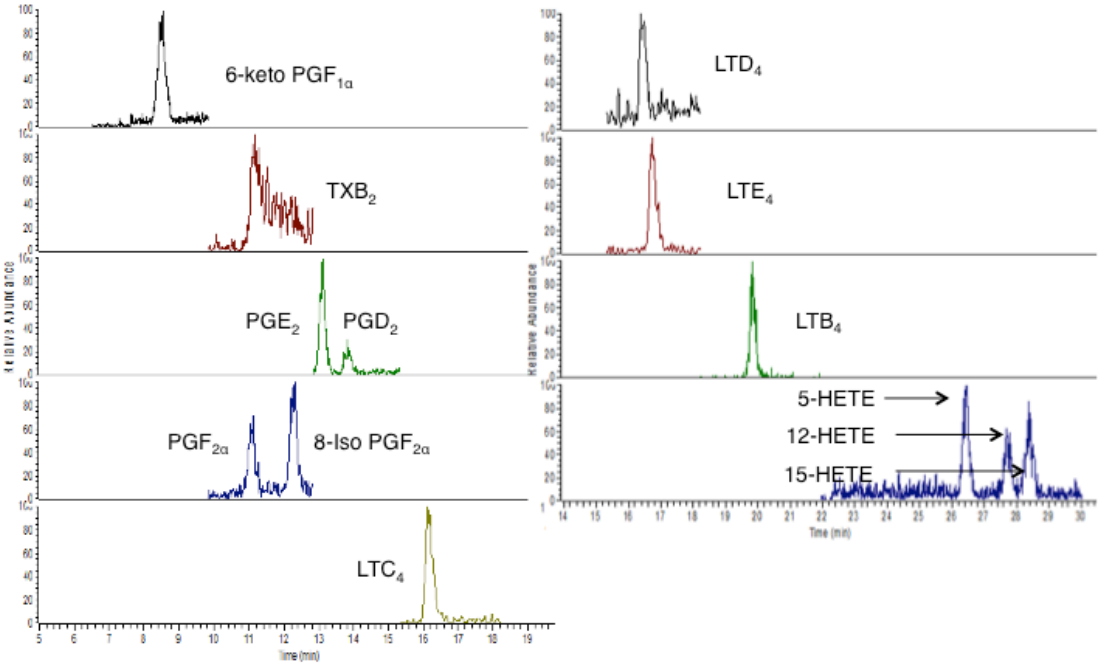

Figure 3.5 Extracted ion chromatograms of thirteen analytes (10 nM) dissolved in Ringer's solution. Data acquired with Thermo Xcalibur software, peak identification used Genesis mode, and peak smoothing used Gaussian and seven data points.

3.5 Conclusion

In this chapter, we describe the successful development of an LC-MS/MS method to separate and detect 13 PGs, LTs and HETEs. The conditions were optimized to achieve the best sensitivity and LODs. However, the sensitivity and LOD of some analytes still was not adequate for the needs of current microdialysis studies. Further optimization of the analytical method was needed and this is described in Chapter 4.

3.6 References

(1) Loftus Jr, E. V. Clinical epidemiology of inflammatory bowel disease: incidence, prevalence, and environmental influences. *Gastroenterology* **2004**, *126*, 1504-1517.

(2) Neuman, M. G. Immune dysfunction in inflammatory bowel disease. *Translational Research* **2007**, *149*, 173-186.

(3) Abraham, C. M. D.; Cho, J. H. M. D. Inflammatory bowel disease mechanisms of disease. *The New England Journal of Medicine* **2009**, *361*, 2066-2078.

(4) Cho, J. H.; Abraham, C. Inflammatory bowel disease genetics: Nod2. *Annual Review of Medicine* **2007**, *58*, 401-416.

(5) Azer, S. A. Overview of molecular pathways in inflammatory bowel disease associated with colorectal cancer development. *European Journal of Gastroenterology & Hepatology* **2013**, *25*, 271-281.

(6) Frieri, G.; Giacomelli, R.; Pimpo, M.; Palumbo, G.; Passacantando, A.; Pantaleoni, G.; Caprilli, R. Mucosal 5-aminosalicylic acid concentration inversely correlates with severity of colonic inflammation in patients with ulcerative colitis. *Gut* **2000**, *47*, 410-414.

(7) Li, J.; Chen, C.; Cao, XN.; Wang, GH.; Hu, JB.; Wang, J. Efficacy of topical versus oral 5-aminosalicylate for treatment of 2,4,6-trinitrobenzene sulfonic acid-induced ulcerative colitis in rats. *Journal of Huazhong University of Science and Technology [Medical Sciences]* **2014**, *34*, 59-65.

(8) Kooloos, W. M.; de Jong, D. J.; Huizinga, T. W. J.; Guchelaar, H. J. Potential role of pharmacogenetics in anti-TNF treatment of rheumatoid arthritis and Crohn's disease. *Drug Discovery Today* **2007**, *12*, 125-131.

(9) Rossi, A.; Pergola, C.; Koeberle, A.; Hoffmann, M.; Dehm, F.; Bramanti, P.; Cuzzocrea, S.; Werz, O.; Sautebin, L. The 5-lipoxygenase inhibitor, zileuton, suppresses prostaglandin biosynthesis by inhibition of arachidonic acid release in macrophages. *British Journal of Pharmacology* **2010**, *161*, 555-570.

(10) Lee, Y.; Kim, W.; Hong, S.; Park, H.; Yum, S.; Yoon, J. H.; Jung, Y. Colon-targeted celecoxib ameliorates TNBS-induced rat colitis: A potential pharmacologic mechanism and therapeutic advantages. *European Journal of Pharmacology* **2014**, *726*, 49-56.

(11) Khor, B.; Gardet, A.; Xavier, R. J. Genetics and pathogenesis of inflammatory bowel disease. *Nature* **2011**, *474*, 307-317.

(12) Fell, J. M. E. Control of systemic and local inflammation with transforming growth factor β containing formulas. *Journal of Parenteral and Enteral Nutrition* **2005**, *29*, S126-S133.

(13) Braat, H.; Peppelenbosch, M. P.; Hommes, D. W. Immunology of Crohn's disease. *Annals of the New York Academy of Sciences* **2006**, *1072*, 135-154.

(14) Podolsky, D. K. Inflammatory bowel disease. *New England Journal of Medicine* **2002**, *347*, 417-429.

(15) Dubois, R. N.; Abramson, S. B.; Crofford, L.; Gupta, R. A.; Simon, L. S.; A. Van De Putte, L. B.; Lipsky, P. E. Cyclooxygenase in biology and disease. *The FASEB Journal* **1998**, *12*, 1063-1073.

(16) Vane, J. R.; Bakhle, Y. S.; Botting, R. M. Cyclooxygenases 1 and 2. *Annual Review of Pharmacology and Toxicology* **1998**, *38*, 97-120.

(17) Smith, W. L.; DeWitt, D. L.; Garavito, R. M. Cyclooxygenases: Structural, Cellular, and Molecular Biology. *Annual Review of Biochemistry* **2000**, *69*, 145-182.

(18) Wang, D.; DuBois, R. N. The role of COX-2 in intestinal inflammation and colorectal cancer. *Oncogene* **2010**, *29*, 781-788.

(19) Nakanishi, M.; Rosenberg, D. Multifaceted roles of PGE_2 in inflammation and cancer. *Semin Immunopathol* **2013**, *35*, 123-137.

(20) Cathcart, M. C.; Lysaght, J.; Pidgeon, G. Eicosanoid signalling pathways in the development and progression of colorectal cancer: novel approaches for prevention/intervention. *Cancer Metastasis Rev* **2011**, *30*, 363-385.

(21) Ferrer, I.; Thurman, E. M.; Barceló, D. Identification of ionic chloroacetanilide–herbicide metabolites in surface water and groundwater by HPLC/MS using negative ion spray. *Analytical Chemistry* **1997**, *69*, 4547-4553.

(22) Wollgast, J.; Pallaroni, L.; Agazzi, M. E.; Anklam, E. Analysis of procyanidins in chocolate by reversed-phase high-performance liquid chromatography with electrospray ionisation mass spectrometric and tandem mass spectrometric detection. *Journal of Chromatography A* **2001**, *926*, 211-220.

(23) Sánchez-Rabaneda, F.; Jáuregui, O.; Casals, I.; Andrés-Lacueva, C.; Izquierdo-Pulido, M.; Lamuela-Raventós, R. M. Liquid chromatographic/electrospray ionization tandem mass spectrometric study of the phenolic composition of cocoa (Theobroma cacao). *Journal of Mass Spectrometry* **2003**, *38*, 35-42.

(24) Wu, Z.; Gao, W.; Phelps, M. A.; Wu, D.; Miller, D. D.; Dalton, J. T. Favorable effects of weak acids on negative-ion electrospray ionization mass spectrometry. *Analytical Chemistry* **2004**, 76, 839-847.

(25) http://www.chemspider.com/

4 Effect of Cyclodextrins on Hydrophobic Analytes Recovery in Microdialysis

4.1 Cyclodextrin

4.1.1 Introduction

In the last chapter, we developed a LC-MS method to study 13 eicosanoids in rat colon microdialysates; however, there are some issues with from sample handling due to hydrophobicity of the eicosanoids, including bad reproducibility and high LODs and sample loss during serial dilution. In this chapter, we added cyclodextrin to the microdialysis perfusate to solve these issues.

Cyclodextrins (CD) are a class of cyclic oligosaccharides produced by starch enzyme digestion. Cyclodextrins consist of five or more (α-1,4)-linked α-D-glucopyranose units. The natural occurring cyclodextrins have six to eight glucose rings and are called α-, β-, γ-cyclodextrins, respectively. Cyclodextrins with less than five or more than eight glucose units do not exist in nature and are produced in very low yield when synthesized.[1,2]

Due to the conformation of the glucose units, CDs exhibit a hollow truncated cone shape. Figure 4.1 shows the chemical structure and 3D structure of a β-CD. The hydroxyl groups contribute to the hydrophilic outer layer. The central cavity has skeletal carbons and lone pairs of

ethereal oxygen atoms, which makes the central cavity lipophilic.[1,3]

Due to the hydroxyl groups on the hydrophilic outer layer, cyclodextrin is soluble in water. However, in the crystalline state, the hydroxyl groups also form strong intermolecular hydrogen bonds that render low solubility. The solubility of α-, β-, and γ-cyclodextrins in pure water at 25 °C are 145, 18.5 and 232 mg/mL, respectively.[4] In addition to the natural cyclodextrins discussed above, there are also several cyclodextrin derivatives, such as hydroxylpropyl β-, γ-cyclodextrin derivatives, methylated β-cyclodextrin derivatives and sulfobutylether β-synthesized cyclodextrin derivatives. These usually have better solubility than native cyclodextrin, because other groups substitute the hydrogen so there are no longer intermolecular hydrogen bonds. For example, 2-hydroxypropyl-β-cyclodextrin has a solubility of > 600 mg/mL in water at 25 °C.[4]

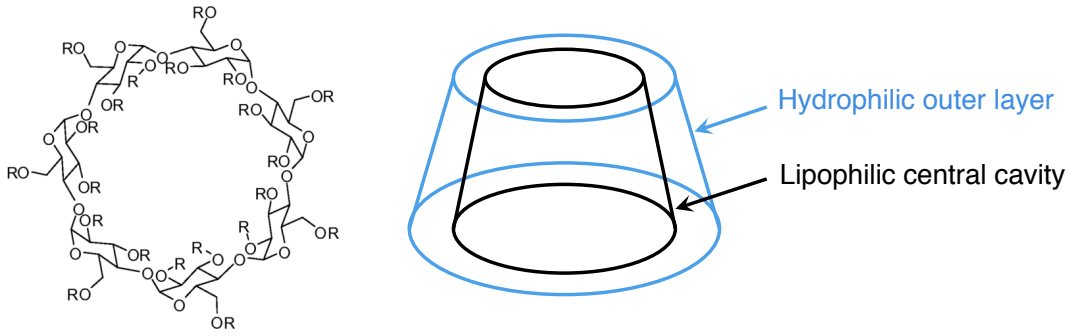

R=H in native cyclodextrin or R=substitute groups in cyclodextrin derivative

Figure 4.1 Structure of cyclodextrin. (Left) chemical structure of β-cyclodextrin and its derivatives. (Right) 3D cone shape structure of a cyclodextrin.

4.1.2 Inclusion Complex

Cyclodextrins have very important applications in the pharmaceutical industry and in separation science, because they can form inclusion complexes with other small molecules through hydrophobic interaction, hydrogen bonding, electrostatic interactions and van der Waals interactions. In an aqueous solution, one or more lipophilic small molecules, usually aromatic compounds, can go into the lipophilic cavity of cyclodextrin, forming a “host-guest” inclusion complex. Van der Waals forces and hydrogen bonding are the major forces involved in the inclusion process rather than covalent bonding.[2]

The inclusion complex has an extremely rapid equilibrium with host cyclodextrin and its small guest molecule or molecules.

cyclodextrin + guest molecule ↔ inclusion complex

The stoichiometry may vary with different size and properties of the cyclodextrin and guest molecules. The most common stoichiometry is 1:1 and 1:2 guest molecule/cyclodextrin. Moreover, the inclusion process is able to occur on different parts of the guest molecule based on structures of the molecule.[2,5,6]

4.1.3 Application

In the pharmaceutical industry, cyclodextrins have been used as a functional excipient to enhance solubility, bioavailability stability and flavor of drugs. More than 30 drugs on the market contain cyclodextrins. They are considered safe since hydrophilic cyclodextrins are not absorbed in the GI tract after an oral dose. However, the GI tract can absorb lipophilic cyclodextrins such as methylated cyclodextrins, so they are toxic and their pharmaceutical application is limited.[6] In separation science, cyclodextrins are used in liquid chromatography (LC) and capillary electrophoresis (CE), particularly for chiral separations.[3,7]

4.1.3.1 Pharmaceutical Application

Drugs delivery is easier if the administered drugs are soluble in aqueous solutions. On the other hand, most biological membranes are lipophilic. In order to achieve transcellular drug transport, drugs are preferred to be lipophilic. Therefore, the ideal drug molecule is both hydrophilic and lipophilic. However, not all the drugs possess both hydrophilic and lipophilic sites. There are several formulation strategies that can help solve this issue, and cyclodextrin addition is one of them.[6]

Higuchi and Connors proposed the classic phase-solubility classification.[8] They classified the complexes according to their substrate solubility into Type A and Type B. Type A are the ones whose solubility increases with more cyclodextrin, which usually occurs with the soluble

cyclodextrin derivatives. Type B are the ones whose solubility is still limited with more cyclodextrin, and at a certain point, cyclodextrin starts to precipitate out along with the drug. This is common with the less soluble natural cyclodextrins. In addition to Type A and B, Higuchi and Connors[8] also developed different subtypes, which include: A_L, A_P, A_N, B_I and B_S. The detailed phase-solubility profiles are described in Figure 4.2.[4,5,9]

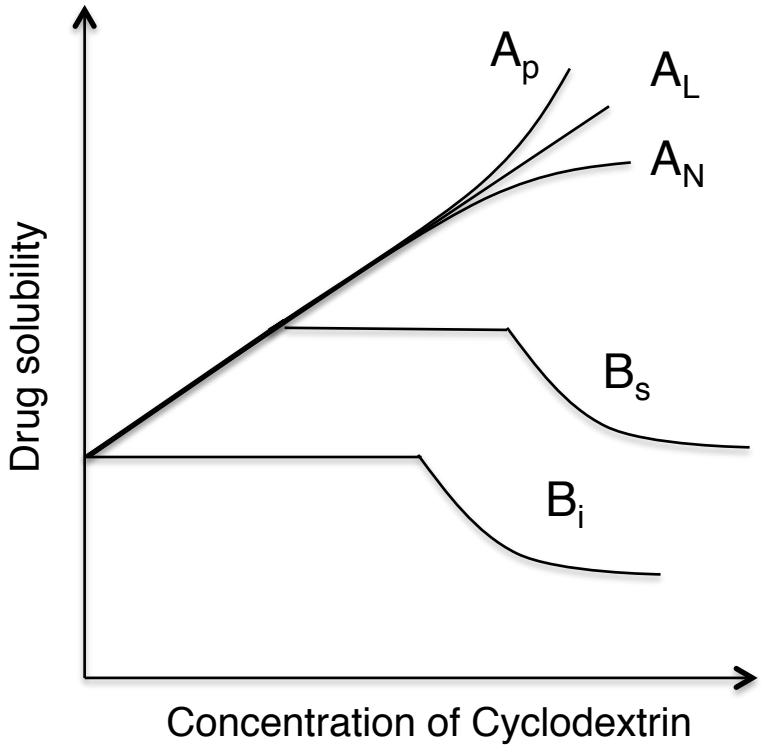

Figure 4.2 Phase-solubility classification, as previously described in reference 8.

4.1.3.2 Separation Application

Cyclodextrins exhibit chiral discrimination properties due to their large number of chiral centers. For example, α-, β- and γ-CD have 30, 35 and 40 chiral centers, respectively.[10] Cyclodextrins respond differently to different chiral guests and are used in LC and CE as chiral selectors.[7]

In LC, cyclodextrin is bonded to the stationary phase or added to the LC mobile phase. There are several commercially available chiral LC columns, such as Astec CYCLOBOND from Supelco Analytical, and ChiraDex from Agilent. Cyclodextrin chiral separations can be performed using normal phase, reverse phase, or hydrophilic interaction chromatography (HILIC).[11,12] In capillary electrophoresis, cyclodextrins are usually directly added to background electrolyte (BGE). β-cyclodextrin is the most commonly used cyclodextrin for CE chiral separations. It can be used in the simple capillary zone electrophoresis (CZE mode) to achieve affinity CE[13] or added along with sodium dodecyl sulfate (SDS) to be used in the CD-micellar electrokinetic chromatography (CD-MEKC) mode.[14] Besides adding natural cyclodextrins or neutral cyclodextrin derivatives, positively or negatively charged cyclodextrins are also widely applied for CE separations. Similarly when adding charged micelles in MECK, the charged CDs also migrate towards the outlet (or inlet) of a capillary and improve resolution.[3,15] In Chapter 2, we added CD to the BGE in capillary electrophoresis to enhance the separation of citrulline and ornithine in rat

brain microdialysate.

4.1.4 Objective of Applying Cyclodextrin in Colon Microdialysis

In Chapter 3, we developed a LC-MS method to study 13 eicosanoids for the analysis of rat colon microdialysate samples; however, it was not sufficient for the *in viv*o studies. First, the reproducibility and LODs were not optimal. In particular, because the eicosanoids exhibit low aqueous solubility, they precipitated out of the solution or attached to sample vial wall during sample preparation, especially in serial dilution. Also, the recovery of eicosanoids in the microdialysis experiment is relatively low. Therefore, most of the analytes in colon microdialysates relevant to these studies cannot be detected.

In order to solve these issues, cyclodextrin was added into the perfusate. It first improved the solubility of eicosanoids, so it stabilized their concentration in solution and improved reproducibility and sensitivity. Second, in the *in vivo* sampling process, it improved recovery by forming inclusion complexes with the small molecules.

4.2 Experimental

4.2.1 Chemicals and Solution Preparations

In addition to the reagents listed in chapter three, (2-hydroxypropyl)-β-cyclodextrin (HP-β-CD) was purchased from Sigma-Aldrich (St. Louis, MO, USA).

A standard solution (5 μM) of eicosanoids was prepared and stored

as described in Chapter 3. It was diluted to a concentration of 100 nM with Ringer's solution as the standard solution of an *in vitro* experiment. HP-β-CD was dissolved and diluted into 2, 4 and 6 mM with Ringer's solution as the perfusate of *in vitro* and *in vivo* experiments

4.2.2 Microdialysis Probe Fabrication

The linear microdialysis probe in this chapter was fabricated by threading two pieces of polyimide tubing into one piece of semipermeable membrane. Then the membrane was attached to the tubing by UV glue. The next two sections describe the fabrication of the two different linear probes that were evaluated in these studies.

4.2.2.1 PAN Membrane Probe Fabrication

The PAN membrane is transparent; hence, the fabrication is straightforward. Specifically, a 1.4 cm piece of PAN (340 μm o.d. and 240 μm i.d.) membrane was cut by a pair of sharp scissors and then two pieces of 10 cm polyimide tubing (163 μm o.d. and 122 μm i.d.) were inserted into the membrane 0.5 cm from both sides. In this way, the effective probe length was 0.5 cm. A microscope and ruler was used to ensure the exact positioning. A small droplet of UV glue was applied on the seam between the membrane and polyimide tubing. A small portion of the UV glue went into the tubing due to capillary action. Microscope observation was needed to ensure the UV glue did not go in too far thereby blocking the tubing or membrane. The PAN membrane with UV

glue on its seam was then put under a UV lamp for 30 seconds, or longer if necessary, until the UV glue was fully cured. Then same UV glue application procedure was repeated on the other side. Figure 4.3 shows the workflow of making a linear probe with PAN membrane.

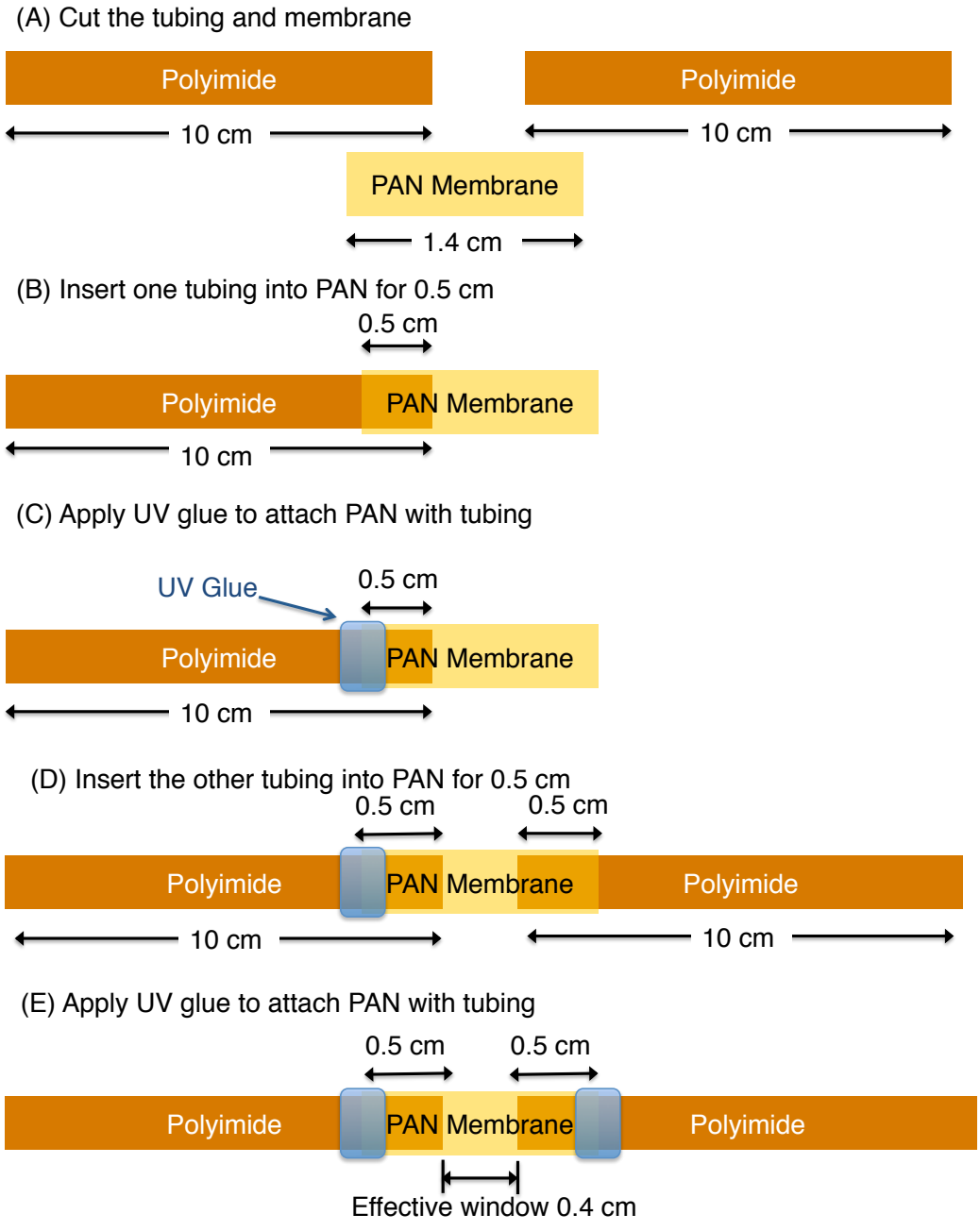

Figure 4.3 Procedure for fabricating a PAN membrane linear microdialysis probe.

4.2.2.2 PES Membrane Probe Fabrication

Most of the procedure for PES membrane probe fabrication was identical to that of PAN. The only difference was that a PES membrane is opaque, so the exact length had to be marked first. Specifically, 1.4 cm of PES (270 µm o.d. and 200 µm i.d.) membrane was cut by the sharp scissors and a Sharpie was used to mark the 0.5 cm positions on both polyimide tubing (163 µm o.d. and 122 µm i.d.). Then the polyimide tubing were inserted into the membrane to the exact marker position and glued by UV glue.

4.2.3 *In vitro* microdialysis recovery experiment

The *in vitro* experiment set up used in these experiments is illustrated in Figure 4.4. About 2 mL of a 100 nM standard solution dissolved in Ringer's solution containing the eicosanoids was prepared in a glass vial. The glass vial was placed on a magnetic stir hot plate to keep the solution at 37 ^{o}C and stirred continuously. The dialysis membrane was submerged in the standard solution. The probe inlet was connected to a 1 mL syringe pump that was used to introduce the perfusate through the probe at a flow rate of 1 µL/min. Glass autosampler vial inserts (silanized glass inserts preferred) were used to collect dialysate from the outlet every 15 min. Plastic vials were not used to prevent losing hydrophobic analytes to the walls.

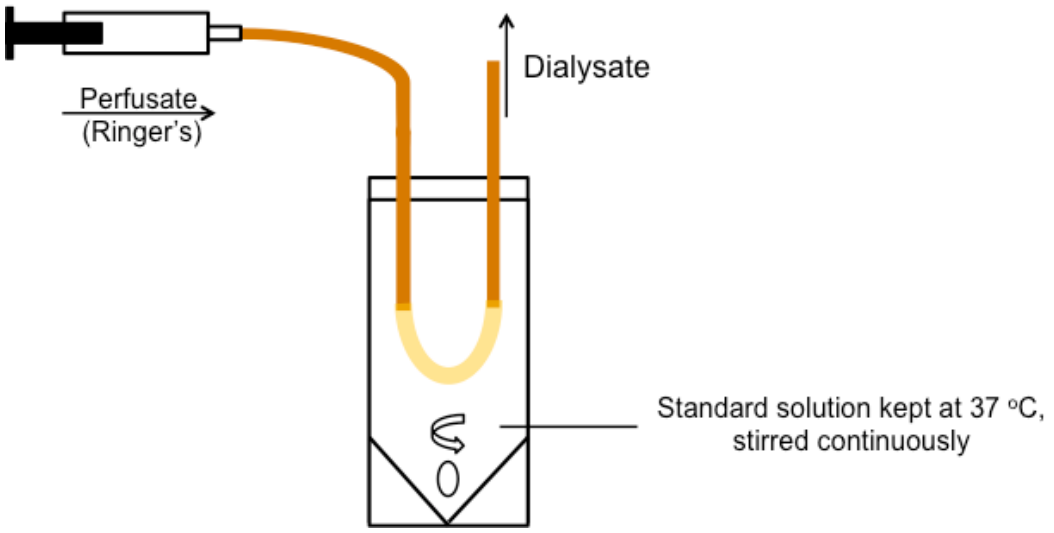

Figure 4.4 *In vitro* microdialysis experiment setup. The standard solution dissolved in Ringer's solution is kept at 37 °C and stirred continuously. A syringe pump is used to pump the perfusate (Ringer's solution) through the probe at a constant flow rate. The dialysate is collected and analyzed by a following analytical system.

4.2.4 Rat Surgery and *In Vivo* Microdialysis Sample Collection

All animal experiments were performed in accordance with the local Institutional Animal Care and Use Committee. The soft tissue linear microdialysis probes were fabricated in our lab as described in the previous section. All animal experiments were performed on female Sprague-Dawley rats weighing from 150-350 g. Female rats were utilized because they have thicker mucosa layer of the colon.

Rats were anesthetized in an isoflurane chamber. Supplemental isoflurane was administered throughout the entire surgery and experiment via a vaporizer. The rat body temperature was regulated at 37 ºC by a PhysioSuite temperature probe and heating pad (Kent Scientific Corporation, Torrington, Connecticut, USA). The rat was shaved around the abdomen after it was fully anesthetized.

An incision was made along the abdomen midline. The colon was gently identified and exposed for a cannula implantation. The colon was flushed with the saline solution to remove fecal particles. A 25-gauge needle was used as the microdialysis probe cannula and inserted into mucosa layers or lumen of the colon. The microdialysis probe was threaded through the needle, and then the needle was removed from the tissue. Tissue glue was applied on the probe and colon to secure the probe to the implantation point during the whole experiment.

After implantation surgery, Ringer's solution was perfused by a

BASi syringe pump (Bioanalytical Systems Inc., West Lafayette, IN, USA) at a 1 μL/min flow rate. Dialysate was collected every 15 min manually, and analyzed by the LC-MS method described in chapter three, or stored at -80 ^{o}C in the freezer.

4.3 Results and Discussions

4.3.1 Solubility and Reproducibility Improvement of Microdialysis Recovery Using Cyclodextrin

Most of the eicosanoids studied in this project are hydrophobic; they were recommended for dissolution in ethanol or other organic solvents. When prepared as high concentration stock solutions, they were dissolved in ethanol. However, microdialysis perfusates, such as saline or Ringer's solution, are aqueous solutions. In Chapter 3, low concentration standard solutions were prepared by dissolving the analytes in Ringer's solution. When performing the serial dilution, a large amount of the hydrophobic analytes was lost during each dilution, so the limit of detection (LOD) was only 10 nM. The limits of detection and reproducibility were improved with the methods described below.

In order to prevent the loss of hydrophobic analytes during sample preparation, the solubility of the analytes needed to be improved. A straightforward way used to handle this has been to dissolve the compounds in organic solvents. However, this method could not be applied to the *in vivo* rat study, since most organic solvents are toxic. They

would diffuse into the tissue and caused tissue damage or inaccurate results. Another way to improve solubility of hydrophobic compounds is to add cyclodextrin, as mentioned in the introduction. Soluble cyclodextrin derivatives can improve the solubility of hydrophobic compounds.

We chose 2-hydropropy-β-cyclodextrin (HP-β-CD) as an additive to the perfusate. Three concentrations (2 mM, 4 mM and 6 mM) of HP-β-CD were studied. They were all prepared in Ringer's solution. The analytes were then serial diluted with this cyclodextrin containing Ringer's solution to prepare 1, 2, 5, 10, 25, 50, 100 nM standard solutions of the 13 eicosanoid analytes. They were analyzed with the LC-MS method developed in chapter 3 to build a calibration curve and to determine LOD. Each sample was injected three times.

R^2 values of each calibration curve are shown in Table 4.1 and the LODs are shown in Table 4.2. The percent relative standard deviation (% RSD) by injecting 10 nM of standard solution five times was also determined. (Table 4.3) These results show that the LOD, R^2 and %RSD were all improved by adding cyclodextrin. Higher concentrations of CD further improved the results, but the difference between each concentration interval was not as significant as without CD and 2 mM CD.

Table 4.1 R^2 values of the calibration curves determined in different sample matrixes.

	0 mM HP-beta-CD	2 mM HP-beta-CD	4 mM HP-beta-CD	6 mM HP-beta-CD
6-keto	0.9907	0.9999	0.9989	0.9999
TXB	0.9898	0.998	0.9989	1
PGF	0.9879	0.9996	0.9989	0.9998
8-IsoPGF	0.9921	0.9999	0.9984	0.9997
PGE	0.9896	0.9998	0.9982	0.9999
PGD	0.9962	0.9993	0.9965	0.9996
LTC	0.9946	0.9981	0.9995	0.9993
LTD	0.9963	0.9992	0.9998	0.9993
LTE	0.998	0.9984	0.9996	0.9993
LTB	0.9841	0.9995	0.9995	0.9996
5-HETE	0.9577	0.9981	0.9993	0.9983
12-HETE	0.992	0.999	0.9994	0.9994
15-HETE	0.9934	0.9961	0.9987	0.9973

Table 4.2 Limits of detection (nM) determined for different sample matrixes by LC-MS.

Analytes	Ringer's	2 mM HP-beta-CD	4 mM HP-beta-CD	6 mM HP-beta-CD
6-keto	2	1	1	1
TXB	10	2	5	2
PGF	1	1	1	1
8-IsoPGF	1	1	1	1
PGE	1	1	1	1
PGD	2	1	1	1
LTC	1	1	1	1
LTD	1	1	1	1
LTE	1	1	1	1
LTB	1	1	1	1
5-HETE	2	1	1	1
12-HETE	2	1	1	1
15-HETE	2	1	1	1

Table 4.3 Percent relative standard deviation of LC-MS response of a 10 nM standard solution. (N=5)

	0 mM HP-beta-CD	2 mM HP-beta-CD	4 mM HP-beta-CD	6 mM HP-beta-CD
6-keto	10	5	4	5
TXB	8	9	6	10
PGF	3	6	5	3
8-IsoPGF	5	3	8	2
PGE	11	2	4	3
PGD	9	12	4	6
LTC	13	5	2	6
LTD	12	4	6	5
LTE	10	9	4	3
LTB	15	9	6	3
5-HETE	16	5	9	5
12-HETE	11	2	2	9
15-HETE	6	5	10	3
AVG	**10**	**6**	**6**	**5**

4.3.2 Microdialysis Membrane Optimization to Improve Relative Recovery

In addition to improving solubility, cyclodextrin has an even more important function in this project: improve microdialysis recovery. As noted in Chapter 1, relative recovery (RR) is defined as

$$RR = \frac{C_d}{C_s} \qquad \text{(equation 1.2)}$$

C_d is the concentration in the dialysate and C_s is the concentration in the extracellular fluid.

Relative recovery is also defined as:

$$RR = 1 - \exp\left[-\frac{1}{Q_d(R_d+R_m+R_e)}\right] \qquad \text{(equation 1.3)}$$

where Q_d is the flow rate of the perfusate, R_d is the mass transport resistance of dialysate, R_m is the mass transport resistance of the membrane, and R_e is the mass transport resistance of extracellular space.

Therefore, membrane material is one of the parameters that can change the microdialysis recovery. Common semipermeable membranes in microdialysis include polyacrylonitrile (PAN) polyethersulfone (PES), polyarylethersulfone (PAES), cuprophan (CUP), and cellulose acetate. PAN is the first choice of linear probe membranes in our lab, because it has a thicker wall and is more rigid (340 µm o.d. and 240 µm i.d.). It makes the linear probe easier to handle during probe implantation surgery,

and it lasts longer in the *in vivo* experiments, especially for long-term awake animal studies. Moreover, PAN membrane is transparent, so the fabrication is easier and the accuracy of length is better.

First, we investigated PAN as the probe membrane. We used the *in vitro* experiment setup illustrated in Figure 4.4 to study the microdialysis relative recovery. The collected dialysates were analyzed by the LC-MS method developed in Chapter 3. Although PAN has many advantages with regards to probe fabrication and *in vivo* studies, the recovery obtained with the PAN membrane probe was very low. This is because PAN is negatively charged[16] and repels that analytes from the membrane wall. Also, Yeping Zhao et al have also indicated that the thicker membrane wall decreased the microdialysis recovery.[16] As can be seen in Figure 4.6, the relative recoveries of PGs and TXB were between 20 and 30% and LTs were between 10 and 25%. The HETEs had the lowest recovery rate of less than 10%.

Due to the low recovery exhibited by the PAN membranes and PES membranes (270 µm o.d. and 200 µm i.d.) were investigated next. The *in vitro* experiment results showed Figure 4.6, PES membrane successfully improved the recovery of the hydrophobic LTs and HETEs. (Figure 4.5) On average, PES had ~80% improvement compared to PAN.D

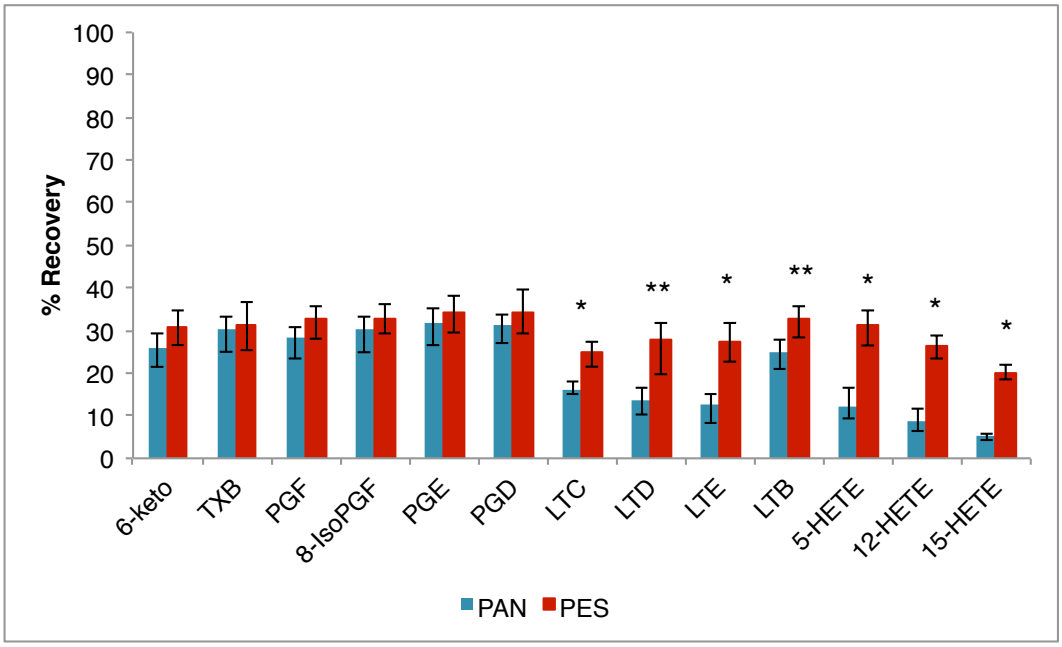

Figure 4.5 Relative recoveries achieved with PAN and PES membranes. * shows the result is significant in student t-test at p=0.05. ** shows the result is significant in student t-test at p=0.1

4.3.3 Microdialysis Relative Recovery Improvement by Cyclodextrin

Another approach to improve microdialysis recovery is to add affinity agents to the perfusate. Julie Stenken's group has performed extensive research on this. They added cyclodextrins, antibodies, and antibody linked flow cytometry beads into the perfusate to improve the recovery of small molecules, peptides and proteins.[17-21] This is because the trapping agents were able to interact with the corresponding analytes, so the concentration of the target analytes near the inner wall of the semipermeable membrane was reduced leading to a steeper concentration gradient. Microdialysis is a concentration gradient driven diffusion process. When the concentration gradient is increased, the relative recovery is also increased.[16] Trapping agents were chosen based on the structure of the target analytes. Cyclodextrins form inclusion complexes with small molecules that contain a hydrophobic and hydrophilic part and preferably an aromatic ring.[19] Antibodies were utilized to improve the recovery of corresponding peptide and proteins.[17,18,20]

According to Stenken's research, a higher concentration of affinity reagent does not directly relate to a higher recovery rate[19]; therefore, an optimum CD concentration needed to be determined. In order to investigate this, 2, 4, and 6 mM HP-beta-CD samples were dissolved in Ringer's solution and perfused through the probe. The concentrations were calculated based on corresponding calibration curve of the different

perfusates.

In vitro study results are shown in Figure 4.6. It can be seen that the relative recovery rates were greatly improved by adding cyclodextrin. By increasing the CD concentration from 0 to 4 mM, the relative recoveries also increased. When we continued adding CD at concentrations above 4 mM, the relative recovery decreased. This was consistent with Julie Stenken group's study.[19] They investigated ibuprofen's recovery improvement by adding CD, and observed that with higher concentrations of CD, the recovery decreased. However, there is no clear explanation on why this happens. It might be due to the CD's interaction with the membrane, or the inclusion complex's conjugation with each other.[19]

Another thing that needs to be noted is that if the CD goes into ESI ion source, it can result in ion suppression and reduce the sensitivity of the analytical method. Therefore, we employed a divert valve to guide the eluent for the first several minutes into a waste reservoir to reduce the amount of CD going into the mass spectrometer. However, the efficiency of this process still needs to be studied further. Therefore, the effect of sample matrix on the ESI-MS response was also evaluated. In this case, standard solutions containing 10 nM of 13 eicosanoid analytes were prepared in Ringer's solution and 2 mM, 4 mM, and 6 mM HP-beta-CD were in Ringer's solution. They were analyzed by the LC-MS system. The results in Figure 4.7 show that CD did not significantly reduce the signal

when divert valve was used. In contrast, low concentrations (2 mM) of CD improved the MS signal of hydrophobic LTs and HETEs. This might be because CD can improve eicosanoids solubility and reduce the amount of eicosanoids precipitated or attached to autosampler vial walls. After considering all results, 3 mM of CD in Ringer's solution was chosen as the optimized microdialysis perfusate for the *in vivo* experiment.

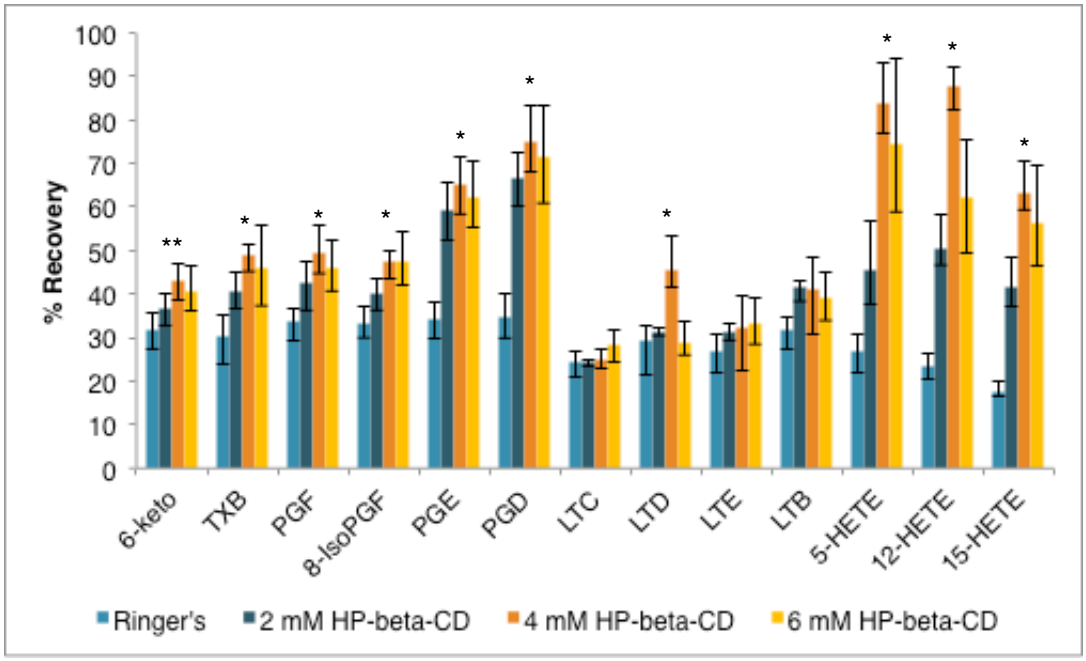

Figure 4.6 Relative recovery results for different concentrations of HP-beta-CD dissolved in perfusate. The recovery was measured with 100 nM analytes in the perfusate. * shows the result is significant in ANOVA F test at alpha=0.05. ** shows the result is significant in ANOVA F test at alpha=0.1

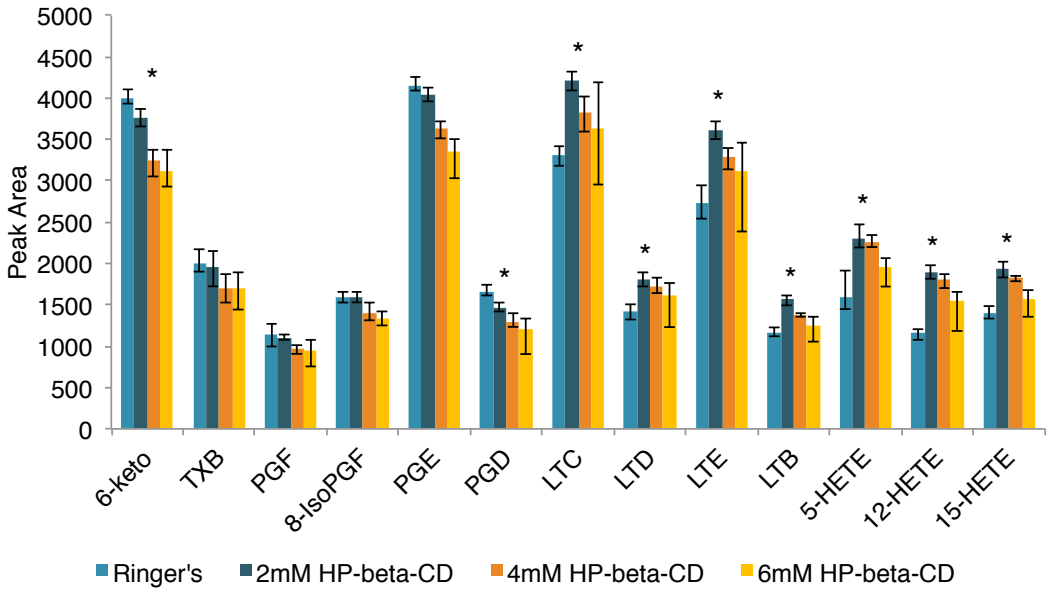

Figure 4.7 Sample matrix effect study results. 10 nM standard solutions were prepared in 0, 2, 4, 6 mM of HP-beta-CD containing Ringer's solution. ANOVA test was performed, the results of all analytes are significant in ANOVA F test at alpha=0.05. Student t-test was performed between Ringer's and 2 mM HP-beta-CD groups. * shows the data was statistical significant at p=0.05.

4.3.4 *In vivo* Colon Microdialysate Analysis

One *in vivo* study was performed to test this method. The microdialysis probe was implanted into a mucosa layer of a rat colon and 3 mM HP-beta-CD was perfused through the probe at a flow rate of 1 µL/min. The dialysate was injected into LC-MS and analyzed by the previously described method. The chromatograms are shown in Figure 4.8. Six out of 13 analytes were detected. Although not all the analytes were above the LOD, this sample was from a healthy rat without any induced inflammation. The target analytes are inflammation biomarkers and we expected to see low or no response of them. In the future studies, after inducing inflammatory bowel disease in the rats, the concentrations are expected to be higher and hopefully above the LOQ.

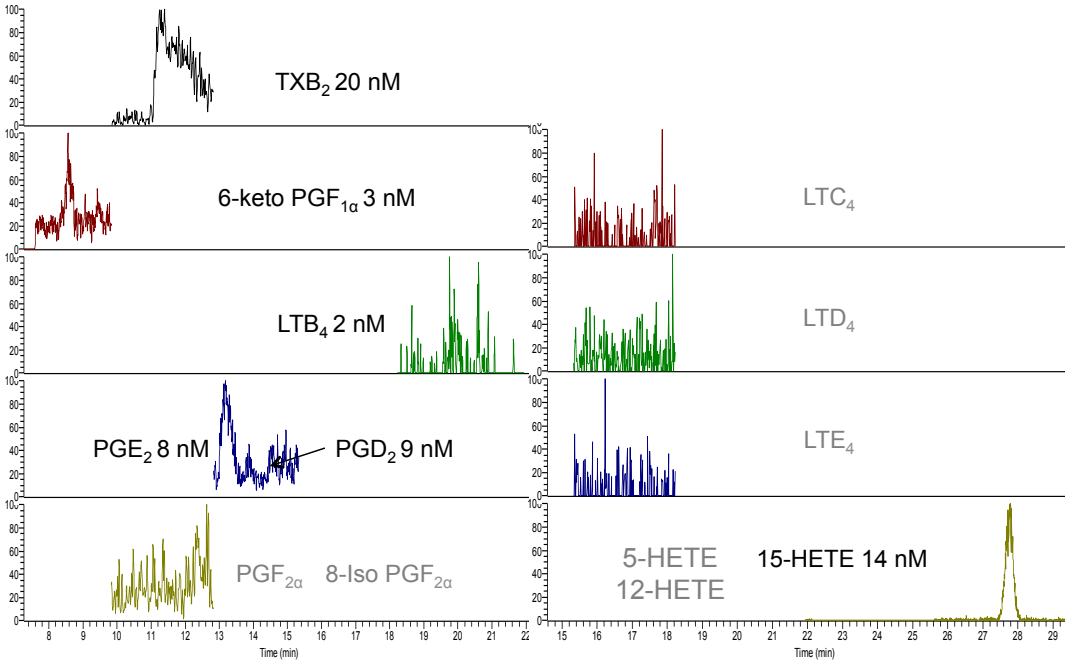

Figure 4.8 LC-MS Chromatograms of basal rat colon microdialysate.

4.4 Conclusion

This chapter describes the continued optimization of the method to study eicosanoids in rat colon microdialysates. We added cyclodextrin, which not only improved microdialysis recovery, but also improved the solubility of eicosanoids to reduce sample loss. We also changed the membrane material from PAN to PES. With these efforts, the microdialysis recovery was successfully improved from 5–30% to 40–85% and some of the compounds could be detected in basal colon microdialysates.

4.5 References

(1) Miranda, J. C. d.; Martins, T. E. A.; Veiga, F.; Ferraz, H. G. Cyclodextrins and ternary complexes: technology to improve solubility of poorly soluble drugs. *Brazilian Journal of Pharmaceutical Sciences* **2011**, *47*, 665-681.

(2) Davis, M. E.; Brewster, M. E. Cyclodextrin-based pharmaceutics: past, present and future. *Nature Reviews Drug Discovery* **2004**, *3*, 1023-1035.

(3) Tang, W.; Ng, S. C. Monosubstituted positively charged cyclodextrins: Synthesis and applications in chiral separation. *Journal of Separation Science* **2008**, *31*, 3246-3256.

(4) Loftsson, T.; Brewster, M. E. Cyclodextrins as functional excipients: Methods to enhance complexation efficiency. *Journal of Pharmaceutical Sciences* **2012**, *101*, 3019-3032.

(5) Del Valle, E. M. M. Cyclodextrins and their uses: a review. *Process Biochemistry* **2004**, *39*, 1033-1046.

(6) Loftsson, T.; Jarho, P.; Másson, M.; Järvinen, T. Cyclodextrins in drug delivery. *Expert Opinion on Drug Delivery* **2005**, *2*, 335-351.

(7) Schneiderman, E.; Stalcup, A. M. Cyclodextrins: a versatile tool in separation science. *Journal of Chromatography B: Biomedical Sciences and Applications* **2000**, *745*, 83-102.

(8) Higuchi T, C. K. Phase solubility techniques. *Advances in Analytical Chemistry and Instrumentation* **1965**, *4*, 117-212.

(9) Brewster, M. E.; Loftsson, T. Cyclodextrins as pharmaceutical solubilizers. *Advanced Drug Delivery Reviews* **2007**, *59*,

645-666.

(10) Lu, H.; Chen, G. Recent advances of enantioseparations in capillary electrophoresis and capillary electrochromatography. *Analytical Methods* **2011**, *3*, 488-508.

(11) Jandera, P. Stationary and mobile phases in hydrophilic interaction chromatography: a review. *Analytica Chimica Acta* **2011**, *692*, 1-25.

(12) Ward, T. J.; Ward, K. D. Chiral separations: A review of current topics and trends. *Analytical Chemistry* **2012**, *84*, 626-635.

(13) Berzas Nevado, J. J.; Castañeda Peñalvo, G.; Jiménez Sánchez, J. C.; Mochón, M. C.; Rodríguez Dorado, R. M.; Villar Navarro, M. Optimisation and validation of a new CE method for the determination of lansoprazole enantiomers in pharmaceuticals. *Electrophoresis* **2009**, *30*, 2940-2946.

(14) Giuffrida, A.; Tabera, L.; González, R.; Cucinotta, V.; Cifuentes, A. Chiral analysis of amino acids from conventional and transgenic yeasts. *Journal of Chromatography B* **2008**, *875*, 243-247.

(15) Tsioupi, D. A.; Stefan-vanStaden, R.-I.; Kapnissi-Christodoulou, C. P. Chiral selectors in CE: Recent developments and applications. *Electrophoresis* **2013**, *34*, 178-204.

(16) Zhao, Y.; Liang, X.; Lunte, C. Comparison of recovery and delivery in vitro for calibration of microdialysis probes *Analytica Chimica Acta* **1995**, *316* 403-410.

(17) Duo, J.; Fletcher, H.; Stenken, J. A. Natural and synthetic affinity agents as microdialysis sampling mass transport enhancers: Current progress and future perspectives. *Biosensors and Bioelectronics* **2006**, *22*, 449-457.

(18) Fletcher, H. J.; Stenken, J. A. An *in vitro* comparison of microdialysis relative recovery of Met- and Leu-enkephalin using cyclodextrins and antibodies as affinity agents. *Analytica Chimica Acta* **2008**, *620*, 170-175.

(19) Khramov, A. N.; Stenken, J. A. Enhanced microdialysis extraction efficiency of ibuprofen *in vitro* by facilitated transport with β-cyclodextrin. *Analytical Chemistry* **1999**, *71*, 1257-1264.

(20) Ao, X.; Sellati, T. J.; Stenken, J. A. Enhanced microdialysis relative recovery of inflammatory cytokines using antibody-coated microspheres analyzed by flow cytometry. *Analytical Chemistry* **2004**, *76*, 3777-3784.

(21) Wang, Y.; Stenken, J. A. Affinity-based microdialysis sampling using heparin for *in vitro* collection of human cytokines. *Analytica Chimica Acta* **2009**, *651*, 105-111.

5 Enzyme Facilitated Deconjugation to Study Stability of Antibody Drug Conjugates

5.1 Introduction

5.1.1 Antibody Drug Conjugates

5.1.1.1 Cancer and Cancer Therapy

Cancer represents one of the leading causes of death in the world. The American Cancer Society's annual report, Cancer Facts and Figures 2015, states that in the US alone, there will be "1,658,370 new cancer cases diagnosed and 589,430 cancer deaths."[1] Cancer treatment has become a major focus in academic world and pharmaceutical industry. Common cancer treatments include surgery, radiation therapy, chemotherapy, and precision medicine.

Most cytotoxic anticancer drugs are nonspecific, which means they not only target the fast growing cancer cells but also healthy tissues. Side effects often include hair loss, fatigue, infection, memory or concentration problems, nausea, and vomiting. They also have a narrow therapeutic window, and they are usually dosed near their maximum tolerated dose (MTD). This limits their efficacy and can lead to multidrug resistance.[2,3]

Monoclonal antibodies (mAb) are a type of cancer therapy that has high specificity and can reduce the side effects of chemotherapy. mAbs are a class of large proteins with molecular weights of approximately 150

kDa. The antibodies bind to specific antigens on the surface of the tumor. There are several commercially available mAb therapies, including Avastin®, Rituxan®, and Herceptin®. Although mAbs exhibit high specificity and lower side effects than cytotoxic anticancer drugs, it also has the disadvantage that its potency is limited.[4,5]

5.1.1.2 Antibody Drug Conjugates

To improve the cytotoxic drug's specificity while maintaining its potency, antibody drug conjugates (ADCs), have drawn a lot of attention in recent years. The basic idea behind ADCs is to bind a nonspecific high potency drug with a site-specific monoclonal antibody, so it can be directly delivered to the tumor site. There are three major compartments of ADC: monoclonal antibody, cytotoxic drug, and a linker that combines them.

The first generation ADC was gemtuzumab ozogamicin (Mylotarg®), which was designed to treat acute myeloid leukemia. The US Food and Drug Administration (FDA) approved Mylotarg® in 2000.[6] However, it was withdrawn from the market later because its linker was not stable, so the ADC was not did not survive systematic circulation and the cytotoxic drug was released too fast.[7] The second generation of ADCs featured improved stability through more stable linkers. The FDA approved second generation ADC drug includes ADCETRIS® (brentuximab vedotin) by Seattle Genetics[8] and KADCYLA® (ado-trastuzumab emtansine) by Genentech.[9]

5.1.2 Anatomy of an ADC

The three major components of the ADC are shown in Figure 5.1.

5.1.2.1 Antibody

The most critical requirement of the antibody component of ADC is high specificity. The antibody must specifically bind to the tumor antigen on the surface of the cancer cell. After binding, the ADC is internalized into the cancer cell and the cytotoxic drug is released in the lysosomal compartment. If the antibody does not exhibit (or show) high specificity, it can also bind to normal tissue and result in toxicity to healthy tissue.[2,10]

5.1.2.2 Linker

The linker connects cytotoxic drug with the monoclonal antibody (mAb). The linker has to be stable during systemic circulation until the ADC reaches the tumor site. There are currently two types of linkers: cleavable linkers and non-cleavable linkers.

Cleavable linkers are the most common. These include chemically labile linkers (acid labile linkers and disulfide linkers) and enzyme labile linkers (protease cleavable linkers). The pH of blood is between 7.3–7.5, while endosomes and lysomes exist in an acidic pH of 4.5–6.5. The acid labile linkers are stable at neutral pH and therefore do not degrade in systemic circulation. However, following internalization into tumor cells, the linker is cleaved and the cytotoxic drug is released. The disulfide linkers have similar cleaving mechanism to the acid labile linker. Cytoplasms of

tumor cells contain a much higher concentration of glutathione than that of blood, so the disulfide linkers are stable in blood circulation. After the ADCs are internalized by the tumor cells, the disulfide linkers are reduced and cleaved from mAb by the high concentration of glutathione. Enzyme labile linkers are more stable than chemically labile linkers in systemic blood circulation. They are engineered to be cleavable by lysosomal proteases. The linker of the model ADC in this project is a protease labile linker. Each model ADC has two valine-citrulline linkers that can be cleaved with cathepsin B, a cysteine protease.

The non-cleavable linkers are those that are still connected to toxin after internalization. They are very stable in blood circulation; however, the drawback is that cytotoxic drugs cannot diffuse into neighboring tumor cells. Therefore, the ADCs with non-cleavable linkers usually show less potency.[3,10]

5.1.2.3 Cytotoxic Drug

The cytotoxic drug part on an ADC must exhibit high potency. It must have a good free drug half-maximal inhibitory concentration (IC_{50}) that is usually in the sub-nano molar range. Also, in order to be successfully connected to the antibody, it needs to have suitable functional groups for connection, and it must remain stable in circulation until ADC reaches the tumor sites. The mechanism of drug action varies depending on the cancer being treated. The most common mechanisms include: DNA

double-strand strand scission (monomethyl auristatin E (MMAE)), and tubulin polymerisation inhibition (calicheamicins).[2,10]

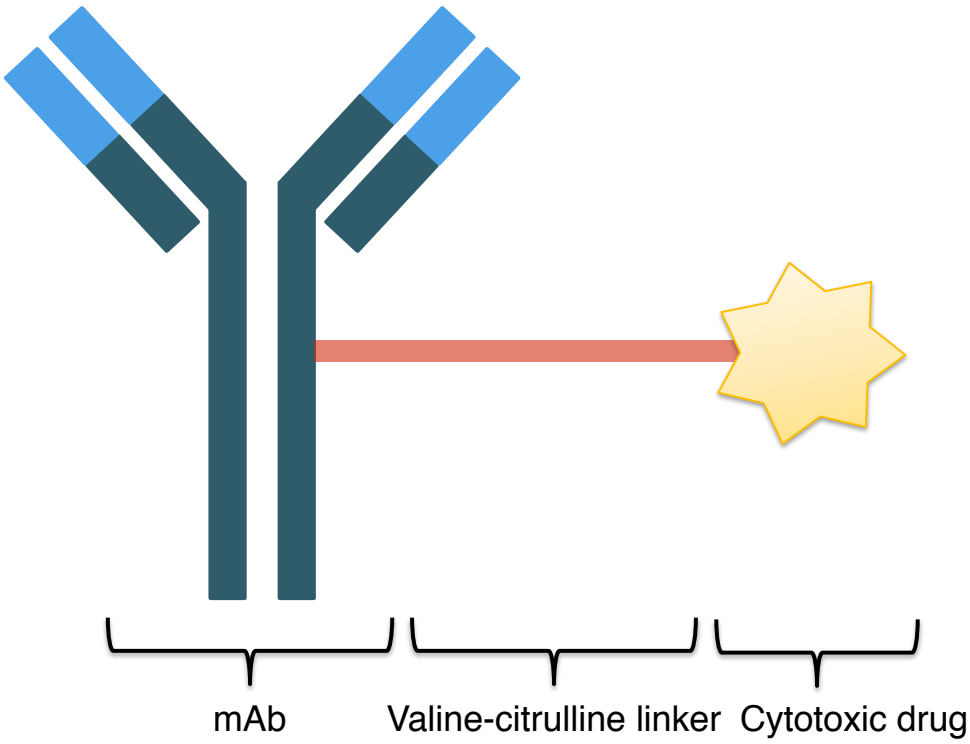

Figure 5.1 Three major compartments of antibody drug conjugates: monoclonal antibody, linker and small molecule cytotoxic drug.

5.1.3 Analysis of ADC

Since ADC is a combination of the three components introduced above, the complexity of the drug is greatly increased compared to either mAb or small molecule cytotoxic drug alone. The linkage site and the chemical properties of different mAbs and cytotoxic drugs will greatly affect the physicochemical properties of ADCs as well as the applicable analytical methods. The analytical methods that are applicable for the native parent mAb cannot be directly applied to the ADC. And for each different ADC, new analytical methods are needed. Information critical to clinical efficacy such as drug potency, drug and linker stability, drug to antibody ratio (DAR), drug distribution, size variant needs to be determined with analytical/bioanalytical methods.[11,12] The following is a brief summary of the current analytical methods that are applicable to ADC:

The simplest ADC analysis method is LC-UV. The mAb has A_{max} at ~280 nm and the cytotoxic drugs their own A_{max} based on the structure.[11] LC-UV analyses are performed to determine drug stability and DAR.[13] In order to determine size variation, size exclusion chromatography (SEC)[14] and sodium dodecyl sulfate polyacrylamide gel electrophoresis (SDS-PAGE)[15] are commonly used. The drug distribution term here refers to the fragments of antibody that contain different numbers of cytotoxic drug. Mass spectrometry such as matrix-assisted laser desorption and

ionization (MALDI), electrospray ionization (ESI), or time-of-flight (TOF) is used to determine drug distribution.[16-18]

In this project, we focused on the analysis of the small molecule cytotoxic drug attached to the antibody. The challenge is that the molecular weight (MW) of the small molecule drug (1.5 kDa) is quite different from that of the antibody (150 kDa). It is therefore hard to accurately determine the degradation on the small molecule after it is linked to a large protein using separation methods that are based on size such as SDS PAGE or SEC.

5.1.4 Objective

In this project, we used enzyme deconjugation to cleave off the small molecule cytotoxic drug from ADC prior to analysis. We were able to directly investigate the degradation of small molecule toxins with the LC-UV method. One application of this method is to study the stability of the model ADC under different conditions. There are two types of conditions that were studied: (1) degradation in the presence of conjugation reagents left over and (2) the effect of formulation excipients.

5.2 Experiment

5.2.1 Reagents and Materials

Acetonitrile (ACN, HPLC grade) was purchased from J. T. Baker (Phillipsburg, NJ, USA). Trifluoroacetic acid (TFA) and histidine acetate were purchased from Sigma-Aldrich (St. Louis, MO, USA). Deionized

water was obtained from an in-house Milli-Q system (Millpore, Billerica, CA, USA). Cathepsin B (human liver) was received from EMD Millipore (Billerica, MA, USA). Cathepsin L (human liver) was purchased from Sigma-Aldrich (St. Louis, MO, USA). Bromelain was received from Fisher Scientific (Pittsburgh, PA, USA). Pepsin from porcine gastric mucosa was purchased from Sigma-Aldrich (St. Louis, MO, USA). Trypsin (MS grade) was purchased from Thermo Scientific (Waltham, MA, USA). Cathespin D (human liver) and α-chymotrypsin (bovine pancreases) were purchased from Alfa Aesar (Ward Hill, MA, USA).

Sodium acetate, sodium citrate monobasic, D-(+)-trehalose dehydrate, N,N-dimethylacetamide (DMA), N,N-dimethylformamide (DMF), dimethyl sulfoxide (DMSO), hydrogen peroxide solution 30 % (w/w) in H2O, L-methionine sulfoximine (MSX), DL-dithiothreitol (DTT), (L)-dehydroascorbic acid (DHA), N-acetyl-L-cysteine (NAC), and ethylenediaminetetraacetic acid tetrasodium salt dihydrate (EDTA) were purchased from Sigma-Aldrich (St. Louis, MO, USA). Sodium phosphate monobasic monohydrate was purchased from Fisher Scientific (Pittsburgh, PA, USA). Sodium chloride (NaCl) and lactose monohydrate were purchased from EMD Millipore (Billerica, MA, USA). Sucrose and polysorbate 20 were purchased from Spectrum Chemical Manufacturing Corp (Gardena, CA, USA). Tris(2-carboxyethyl)phosphine hydrochloride (TCEP) and sodium succinate hexahydrate were purchased from Alfa

Aesar (Ward Hill, MA, USA). Sodium tartrate dehydrate was purchased from GFS Chemicals, Inc. (Powell, OH 43065) L-arginine, free base was purchased from Amresco (Solon, OH, USA). 50% sodium hydroxide solution (NaOH), hydrochloric acid (HCl 36.5%-38.0%), and benzyl alcohol were purchased from Avantor Performance Materials (Center Valley, PA, USA).

ADC samples and the active free drug standards in this study were provided by Genentech (South San Francisco, CA, USA).

5.2.2 Compatibility Study Procedure

The model ADC sample was dissolved in 20 mM histidine acetate buffer (pH 6) at 50 mg/mL. The conjugation reagents and/or formulation excipients were dissolved in deionized water and pH adjusted with hydrochloric acid and/or sodium hydroxide. 25 μL of the conjugation reagent or excipient was added to 25 μL model ADC sample. The vial was put in a 40 ^{o}C, 75% humidity oven to incubate for either one or seven days.

5.2.3 Enzyme Digestion Procedure

The ADC samples were digested by aliquoting 50 μL of the ADC solution and 25 μL of bromelain (1.0 mg/mL in water) in a vial and incubating for 8 hours at 40 °C. Following incubation, the protein was precipitated by adding 150 μL ACN. The precipitated samples were then centrifuged at 13,000 rpm for 10 minutes, and then the supernatant was transferred to a vial for HPLC analysis. Standard solutions of the free drug

were prepared in ACN:water (1:1) diluent at a concentration of 0.1 mg/mL.

5.2.4 LC-UV Conditions

LC analyses were performed using Agilent 1200 system (Agilent, Santa Clara, CA) equipped with quaternary pump, vacuum degasser, auto-sampler, column thermostat, and a diode array detector. Empower (Waters, Milford, MA) was used to collect and process the data. The sample was analyzed by using a Poroshell SB-Aq column (150 × 3.0 mm, 2.7 μm, Agilent, Sunnyvale, CA, USA). Initial conditions were set at 80% solvent A (0.05% TFA in water) and 20% solvent B (ACN). Solvent B was increased to 50% in 20 minutes using a linear gradient and then to 90% in 10 minutes. Solvent B was held at 90% for 5 min followed by a reequilibration step at 20% B for 5 min. The flow rate was maintained at 0.5 mL/min, the column temperature at 25 ^{o}C, and the injection volume was 10 μL. UV detection wavelength measured at 225 nm with a 4 nm bandwidth.

5.3 Results and Discussion

5.3.1 Enzyme Screening

The model ADC used in this project was engineered to be sensitive to lysosomal proteases. It has two valine-citrulline linkers that can be cleaved with cathepsin B. However, cathepsin B was not 100% effective and it is very expensive. Therefore, we performed screening assay to determine if there are any better enzyme candidates. We screened eight

enzymes including: cathepsin B (extracted from human liver), cathepsin B (extracted from bovine spleen), bromelain, pepsin, cathepsin D, trypsin and chymotrypsin. We determined the amount of free drug that was cleaved from ADC within 24 hours to evaluate the efficiency of the enzyme. The results are shown in Figure 5.2. The four cysteine proteases, including cathepsin B (human liver), cathepsin B (bovine spleen), cathepsin D and bromelain, can cleave off free drug from ADC. However, the other four enzymes, which are aspartate and serine proteases, showed very low efficiency of cleavage. Among the four effective cysteine proteases, bromelain achieved the best cleavage efficiency. Therefore, we chose bromelain as our enzyme instead of the originally designed cathepsin B. Another significant advantage of bromelain is that its cost is only 1/100000 that of cathepsin B, since bromelain is extracted from pineapple stem.

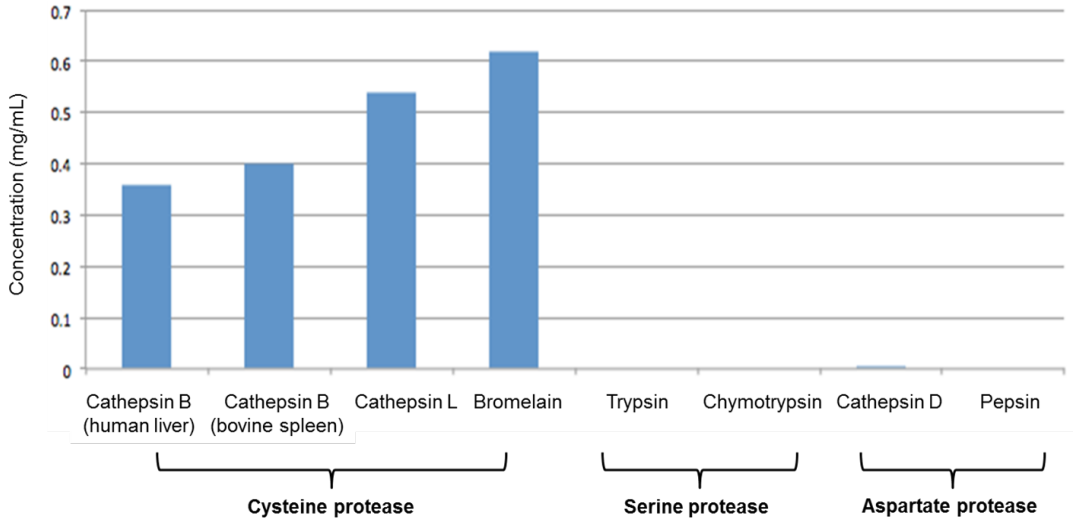

Figure 5.2 Comparison of the release of the free drug from the model ADC by different enzymes.

5.3.2 Method Validation

Figure 5.3 shows pictures of solutions of ADC treated with cathepsin B (Figure 5.3B) and bromelain (Figure 5.3C). The first picture (Figure 5.3A) shows a picture of the control group without any enzyme treatment. The model ADC produced a blue precipitant after being treated with acetonitrile and centrifuged. Figure 5.3B is the ADC deconjugated with cathepsin B. In this case, some free drug was cleaved and released into solution so the solution turned to blue and the blue color of ADC precipitant became lighter. However, when the ADC was treated with bromelain (Figure 5.3C), all of the drug was cleaved and released into the solution, so the antibody precipitant became white and the solution became dark blue. This straightforwardly proved that bromelain could completely cleave off free drug from ADC.

Other quantification validations were also performed, including precision, limits of quantification, calibration curve, and spike recovery. The precision was determined with 100 μg/mL ADC. The system precision was evaluated by injecting the same sample five times, while the method precision was evaluated by performing the entire enzyme deconjugation and LC-UV analysis five times. The system precision %RSD and method precision %RSD are 0.2% and 1.4%, respectively. The spike recovery was determined by spiking 100 μg/mL of the free drug standard into the bare mAb sample. The spike recovery is 104.1%, which proved no sample loss

of with this method. The detailed results are shown in Table 5.1. This method exhibited great reproducibility, linearity and recovery.

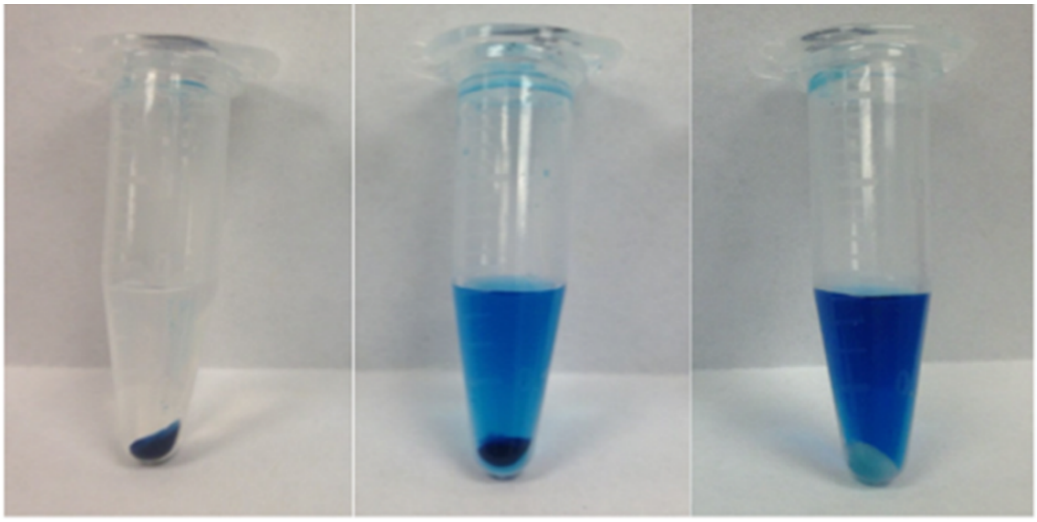

(A) Control: ADC (B) ADC and Cathepsin B (C) ADC and Bromelain

Figure 5.3 Pictures of the ADC samples treated with cathepsin B and bromelain as compared to the control ADC sample without enzyme.

Table 5.1 A summary of method validation data.

Criteria	Results
System precision (n=5)	%RSD = 0.2%
Method precision (n=5)	%RSD = 1.4%
LOQ in ADC sample	1 μg/mL
Calibration curve	y=73937x-48032 (r^2=0.9999) range: 0.5-500μg/mL
Spike recovery (n=3)	104.1%

5.4 Application

We studied the stability of ADC in the presence of two types of reagents. The first type was the conjugation reagent. During the ADC conjugation process, many reagents are used, for example N,N-dimethylacetamide (DMA), N,N-dimethylformamide (DMF), dimethyl sulfoxide (DMSO), polyglycol (PG), hydrogen peroxide, L-methionine sulfoximine (MSX), DL-dithiothreitol (DTT), (L)-dehydroascorbic acid (DHA), N-acetyl-L-cysteine (NAC) and Tris(2-carboxyethyl)phosphine hydrochloride (TCEP) and arginine. If the amounts of these conjugation reagents are not well controlled, they might still be present in the ADC sample after conjugation process and affect the stability of ADC. The second type is formulation excipients, which are mixed with ADC to form dosage form, for example sodium acetate, sodium phosphate, sodium citrate, sodium tartrate, EDTA, NaCl, lactose, sucrose, trehalose, PS 20. We also want to investigate if they will affect the stability of ADC.

To perform the study, the ADC sample was first mixed with one of reagents of interest listed above and vortexed. The vial was stored in a 40 ^{o}C and 75% humidity in an oven. There were three time points used: day 1, day 7, and another sample without incubation as day 0. Then they were deconjugated by bromelain and analyzed by the LC-UV method described in this chapter.

Figure 5.4 uses L-methionine sulfoximine (MSX) as an example to

illustrate the analysis of each reagent. Three different concentrations of MSX were studied (1, 10, 100 mM). MSX was mixed with the ADC sample and stored at 40 ^{o}C and at 75% humidity for 0 day, 1 day and 7 days. Another ADC sample was mixed with water only without any MSX to serve as control. On the chromatogram shown in Figure 5.4, the peak at ~ 27 min is the free drug peak, whose peak area change is used to evaluate drug degradation. The model ADC was compatible with low concentrations (1 mM) MSX from day 0-7. However, with higher concentrations (10 and 100 mM), the ADC is only stable within the first 24 hours and the free drug peak decreased and degradation peaks started to form at day 7.

Figure 5.5 and 5.6 show a summary of all the compatibility study results. The color of each block on the table indicates the free drug peak area loss compared to control. The darker blue color means the reagents are less compatible with our ADC sample. The following section discusses each reagent individually.

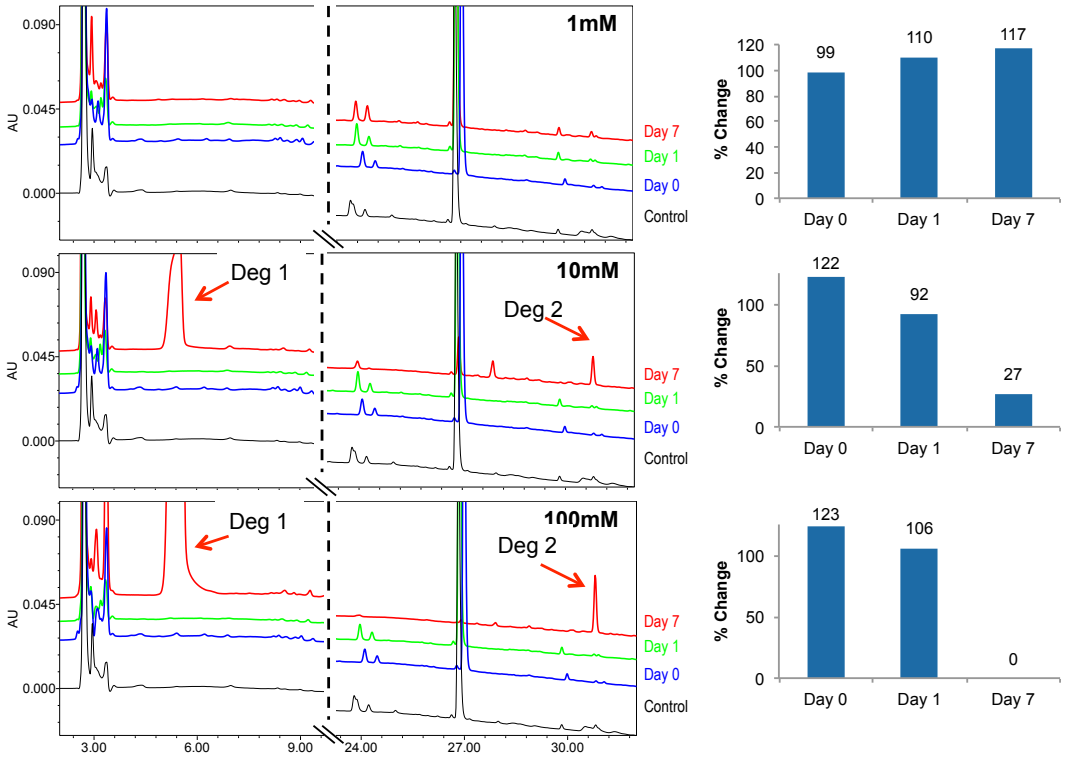

Figure 5.4 Compatibility study results of MSX. LC-UV chromatograms are shown on the left. Quantification comparisons of free drug peak are shown on the right.

5.4.1 Conjugation Reagents

5.4.1.1 Organic Solvents

PG, DMA, DMF, and DMSO are typically used to dissolve hydrophobic small molecules during the conjugation process. They improve the solubility of small molecules as well as conjugation efficiencies. DMA, DMF, and DMSO were diluted in deionized water to 20% pH adjusted to 5, 7 and 9 with HCl and NaOH. PG was diluted to 10%, 25% and 50% pH adjusted to 5, 7 and 9. No obvious changes in free drug were observed.

5.4.1.2 H_2O_2

H_2O_2 is used to clean the labware, so there might be trace amounts left in the drug sample. In these experiments, concentrations of 0.01, 0.05 and 0.1% (v/v) of H_2O_2 were studied. Sine H_2O_2 is a strong oxidant; even the lowest concentration of H_2O_2 resulted in 80% of free drug peak loss within 24 hours.

5.4.1.3 Methionine Sulfoximine

MSX is an irreversible inhibitor of glutamine synthetase. It is commonly added in cell cultures to inhibit growth of unwanted bacteria and fungus. MSX concentrations of 1mM, 10mM and 100mM MSX were studied. The results show that in the presence of 1mM MSX, the free drug was stable for 7 days. As the MSX concentration increased, degradation started to show up on day 4, while it remained compatible within 24 hours.

5.4.1.4 N-acetyl-L-cysteine

NAC is used to clear out linker drug residue in the conjugation process by reacting with unreacted maleimide functional groups. The result showed that it was incompatible with the small molecule drug on ADC even with low concentrations. We analyzed the degradation with TOF LC-MS; the result showed that the NAC added to the cytotoxic drug moiety.

5.4.1.5 Dithiothreitol and Tris(carboxyethyl)phosphinehydrochloride

DTT and TCEP are two commonly used reductants in the antibody conjugation process. They are used to reduce the disulfide bond and open the interchain of antibody, so the linker or cytotoxic drug can be engineered to the antibody. In the presence of 1 mM TCEP, the small molecule drug was stable for seven days. Since TCEP has strong reducing capability at high concentrations, TCEP became incompatible with the model ADC at 10 mM and 100 mM. DTT also has strong reducing capability, the ADC was unstable under any conditions in the presences of DTT.

5.4.1.6 Dehydroascorbic acid

DHA is an oxidant. It has a function opposite to that of DTT and TCEP. DHA is used to reoxidize the opened interchain disulfide bond. Similarly to TCEP, ADC was compatible with low concentrations of DHA. As the DHA concentration increased, the free drug peak was gone and

two degradation peaks were formed.

5.4.1.7 Arginine

Arginine was added to improve the solubility and inhibit protein aggregation during the conjugation reaction. An obvious decrease in the free drug peak was observed; however, no obvious degradation peak appeared with the 225 nm UV spectrum. This might because the new degradation products that were produced absorbed at another wavelength, .

5.4.2 Formulation Excipients

5.4.2.1 Buffer

Acetate, phosphate, citrate and tartrate are the four commonly used buffers in the formulation of ADCs. Studies have shown that they might have the drug stability issues in formulation. Therefore buffers at 1, 10, 100 mM and pH 5, 7, 9 for each sample were tested. The results showed higher concentrations and pH values of phosphate and citrate buffer caused stability issues. The reason could be that phosphate is a nucleophile and attacks electrophilic centers. Citrate buffers are normally used between pH 3.0-6.2. In this case, the instability could be due to the high pH conditions used where the buffer capacity is low.

5.4.2.2 Chelating reagents

EDTA and citrate were added to the ADC formulation as chelating reagents. They can react with metal centers in the protein. New ADC

degradation peaks were observed, this suggested EDTA under went degradation.

5.4.2.3 Sugar and Other Reagents

Lactose, sucrose and trehalose are sugars used as bulking agents and lyoprotectants that protect freeze-dried drug in the formulation. NaCl is a tonicity adjusting agent and PS 20 is a commonly used surfactant in ADC synthesizing process. They are relatively stable and compatible with our ADC.

Day 1 vs Control

Reagent	Condition		
PG	5% pH=5	5% pH=7	5% pH=9
	12.5% pH=5	12.5% pH=7	12.5% pH=9
	25% pH=5	25% pH=7	25% pH=9
DMA	10% pH=5	10% pH=7	10% pH=9
DMF	10% pH=5	10% pH=7	10% pH=9
DMSO	10% pH=5	10% pH=7	10% pH=9
H_2O_2	0.01%	0.05%	0.10%
MSX	1 mM	10 mM	100 mM
DTT	1 mM	10 mM	100 mM
TCEP	1 mM	10 mM	100 mM
DHA	1 mM	10 mM	100 mM
NAC	1 mM	10 mM	100 mM
Arginine	1 mM	10 mM	100 mM

Day 7 vs Control

Reagent	Condition		
PG	5% pH=5	5% pH=7	5% pH=9
	12.5% pH=5	12.5% pH=7	12.5% pH=9
	25% pH=5	25% pH=7	25% pH=9
DMA	10% pH=5	10% pH=7	10% pH=9
DMF	10% pH=5	10% pH=7	10% pH=9
DMSO	10% pH=5	10% pH=7	10% pH=9
H2O2	0.01%	0.05%	0.10%
MSX	1 mM	10 mM	100 mM
DTT	1 mM	10 mM	100 mM
TCEP	1 mM	10 mM	100 mM
DHA	1 mM	10 mM	100 mM
NAC	1 mM	10 mM	100 mM
Arginine	1 mM	10 mM	100 mM

vs control
90-100%
70-90%
50-70%
30-50%
10-30%
<10%

Figure 5.5 Compatibility study results summary of the conjugation reagents left over with ADC

Day 1 vs Control

Excipient	Condition		
Sodium Acetate	1 mM pH=5	1 mM pH=7	1 mM pH=9
	10 mM pH=5	10 mM pH=7	10 mM pH=9
	100 mM pH=5	100 mM pH=7	100 mM pH=9
Sodium Phosphate	1 mM pH=5	1 mM pH=7	1 mM pH=9
	10 mM pH=5	10 mM pH=7	10 mM pH=9
	100 mM pH=5	100 mM pH=7	100 mM pH=9
Sodium Citrtrate	1 mM pH=5	1 mM pH=7	1 mM pH=9
	10 mM pH=5	10 mM pH=7	10 mM pH=9
	100 mM pH=5	100 mM pH=7	100 mM pH=9
Sodium Tartrate	1 mM pH=5	1 mM pH=7	1 mM pH=9
	10 mM pH=5	10 mM pH=7	10 mM pH=9
	100 mM pH=5	100 mM pH=7	100 mM pH=9
EDTA	1 mM pH=5	1 mM pH=7	1 mM pH=9
	10 mM pH=5	10 mM pH=7	10 mM pH=9
	100 mM pH=5	100 mM pH=7	100 mM pH=9
NaCl	1 mM pH=5	1 mM pH=7	1 mM pH=9
	10 mM pH=5	10 mM pH=7	10 mM pH=9
	100 mM pH=5	100 mM pH=7	100 mM pH=9
Lactose	1 mM pH=5	1 mM pH=7	1 mM pH=9
	10 mM pH=5	10 mM pH=7	10 mM pH=9
	100 mM pH=5	100 mM pH=7	100 mM pH=9
Sucrose	1 mM pH=5	1 mM pH=7	1 mM pH=9
	10 mM pH=5	10 mM pH=7	10 mM pH=9
	100 mM pH=5	100 mM pH=7	100 mM pH=9
Trehalose	1 mM pH=5	1 mM pH=7	1 mM pH=9
	10 mM pH=5	10 mM pH=7	10 mM pH=9
	100 mM pH=5	100 mM pH=7	100 mM pH=9
PS 20	0.05%	0.10%	0.20%

Day 7 vs Control

Excipient	Condition		
Sodium Acetate	1 mM pH=5	1 mM pH=7	1 mM pH=9
	10 mM pH=5	10 mM pH=7	10 mM pH=9
	100 mM pH=5	100 mM pH=7	100 mM pH=9
Sodium Phosphate	1 mM pH=5	1 mM pH=7	1 mM pH=9
	10 mM pH=5	10 mM pH=7	10 mM pH=9
	100 mM pH=5	100 mM pH=7	100 mM pH=9
Sodium Citrtrate	1 mM pH=5	1 mM pH=7	1 mM pH=9
	10 mM pH=5	10 mM pH=7	10 mM pH=9
	100 mM pH=5	100 mM pH=7	100 mM pH=9
Sodium Tartrate	1 mM pH=5	1 mM pH=7	1 mM pH=9
	10 mM pH=5	10 mM pH=7	10 mM pH=9
	100 mM pH=5	100 mM pH=7	100 mM pH=9
EDTA	1 mM pH=5	1 mM pH=7	1 mM pH=9
	10 mM pH=5	10 mM pH=7	10 mM pH=9
	100 mM pH=5	100 mM pH=7	100 mM pH=9
NaCl	1 mM pH=5	1 mM pH=7	1 mM pH=9
	10 mM pH=5	10 mM pH=7	10 mM pH=9
	100 mM pH=5	100 mM pH=7	100 mM pH=9
Lactose	1 mM pH=5	1 mM pH=7	1 mM pH=9
	10 mM pH=5	10 mM pH=7	10 mM pH=9
	100 mM pH=5	100 mM pH=7	100 mM pH=9
Sucrose	1 mM pH=5	1 mM pH=7	1 mM pH=9
	10 mM pH=5	10 mM pH=7	10 mM pH=9
	100 mM pH=5	100 mM pH=7	100 mM pH=9
Trehalose	1 mM pH=5	1 mM pH=7	1 mM pH=9
	10 mM pH=5	10 mM pH=7	10 mM pH=9
	100 mM pH=5	100 mM pH=7	100 mM pH=9
PS 20	0.05%	0.10%	0.20%

vs control
90-100%
70-90%
50-70%
30-50%
10-30%
<10%

Figure 5.6 Compatibility study results summary of the formulation excipients with ADC.

5.5 Conclusion

An enzymatic deconjugation method was successfully developed and validated for the analysis of small molecule drugs in ADCs. A systematic compatibility investigation of conjugation reagents and formulation excipients with ADC was carried out. The future ADC engineer researchers can refer to the compatibility study results to improve the stability of ADC formulations.

5.6 References

(1) http://www.cancer.gov/about-cancer/what-is-cancer/statistics.

(2) Chari, R. V. J. Targeted cancer therapy: Conferring specificity to cytotoxic drugs. *Accounts of Chemical Research* **2008**, *41*, 98-107.

(3) Ducry, L.; Stump, B. Antibody–drug conjugates: Linking cytotoxic payloads to monoclonal antibodies. *Bioconjugate Chemistry* **2010**, *21*, 5-13.

(4) Reichert, J. M.; Rosensweig, C. J.; Faden, L. B.; Dewitz, M. C. Monoclonal antibody successes in the clinic. *Nature Biotechnology* **2005**, *23*, 1073-1078.

(5) Shuptrine, C. W.; Surana, R.; Weiner, L. M. Monoclonal antibodies for the treatment of cancer. *Seminars in Cancer Biology* **2012**, *22*, 3-13.

(6) Sievers, E. L.; Linenberger, M. Mylotarg: antibody-targeted chemotherapy comes of age. *Current Opinion in Oncology* **2001**, *13*, 522-527.

(7) Ravandi, F. Gemtuzumab ozogamicin: One size does not fit all—the case for personalized therapy. *Journal of Clinical Oncology* **2011**, *29*, 349-351.

(8) Senter, P. D.; Sievers, E. L. The discovery and development of brentuximab vedotin for use in relapsed Hodgkin lymphoma and systemic anaplastic large cell lymphoma. *Nature Biotechnology* **2012**, *30*, 631-637.

(9) Lewis Phillips, G. D.; Li, G.; Dugger, D. L.; Crocker, L. M.;

Parsons, K. L.; Mai, E.; Blättler, W. A.; Lambert, J. M.; Chari, R. V. J.; Lutz, R. J.; Wong, W. L. T.; Jacobson, F. S.; Koeppen, H.; Schwall, R. H.; Kenkare-Mitra, S. R.; Spencer, S. D.; Sliwkowski, M. X. Targeting HER2-positive breast cancer with Trastuzumab-DM1, an antibody–cytotoxic drug conjugate. *Cancer Research* **2008**, *68*, 9280-9290.

(10) Panowksi, S.; Bhakta, S.; Raab, H.; Polakis, P.; Junutula, J. R. Site-specific antibody drug conjugates for cancer therapy. *mAbs* **2014**, *6*, 34-45.

(11) Alley, S. C.; Zhang, X.; Okeley, N. M.; Anderson, M.; Law, C.-L.; Senter, P. D.; Benjamin, D. R. The pharmacologic basis for antibody-auristatin conjugate activity. *Journal of Pharmacology and Experimental Therapeutics* **2009**, *330*, 932-938.

(12) Wakankar, A.; Chen, Y.; Gokarn, Y.; Jacobson, F. S. Analytical methods for physicochemical characterization of antibody drug conjugates. *mAbs* **2011**, *3*, 161-172.

(13) Hamblett, K. J.; Senter, P. D.; Chace, D. F.; Sun, M. M. C.; Lenox, J.; Cerveny, C. G.; Kissler, K. M.; Bernhardt, S. X.; Kopcha, A. K.; Zabinski, R. F.; Meyer, D. L.; Francisco, J. A. Effects of drug loading on the antitumor activity of a monoclonal antibody drug conjugate. *Clinical Cancer Research* **2004**, *10*, 7063-7070.

(14) Doronina, S. O.; Toki, B. E.; Torgov, M. Y.; Mendelsohn, B. A.; Cerveny, C. G.; Chace, D. F.; DeBlanc, R. L.; Gearing, R. P.; Bovee, T. D.; Siegall, C. B.; Francisco, J. A.; Wahl, A. F.; Meyer, D. L.; Senter, P. D. Development of potent monoclonal antibody auristatin conjugates for cancer therapy. *Nature Biotechnology* **2003**, *21*, 778-784.

(15) Stan, A. C.; Radu, D. L.; Casares, S.; Bona, C. A.; Brumeanu, T.-D. Antineoplastic efficacy of Doxorubicin enzymatically

assembled on galactose residues of a monoclonal antibody specific for the carcinoembryonic antigen. *Cancer Research* **1999**, *59*, 115-121.

(16) Siegel, M. M.; Tabei, K.; Kunz, A.; Hollander, I. J.; Hamann, P. R.; Bell, D. H.; Berkenkamp, S.; Hillenkamp, F. Calicheamicin Derivatives conjugated to monoclonal antibodies: Determination of loading values and distributions by infrared and UV matrix-assisted laser desorption/ionization mass spectrometry and electrospray ionization mass spectrometry. *Analytical Chemistry* **1997**, *69*, 2716-2726.

(17) Lazar, A. C.; Wang, L.; Blättler, W. A.; Amphlett, G.; Lambert, J. M.; Zhang, W. Analysis of the composition of immunoconjugates using size-exclusion chromatography coupled to mass spectrometry. *Rapid Communications in Mass Spectrometry* **2005**, *19*, 1806-1814.

(18) Wang, L.; Amphlett, G.; Blättler, W. A.; Lambert, J. M.; Zhang, W. Structural characterization of the maytansinoid–monoclonal antibody immunoconjugate, huN901–DM1, by mass spectrometry. *Protein Science* **2005**, *14*, 2436-2446.

6 Conclusions and Future Directions

6.1 CE-LIF Method Development for the Determination of Amino Acids in Rat Brain Microdialysates to Study Epileptic Seizure

6.1.1 Conclusions

Oxidative stress is an important secondary effect of epileptic seizure. Nitric oxide is one of the reactive nitrogen species in the brain.[1,2] In this project, ornithine and citrulline were chosen as stable indicators of nitric oxide production in rat brain during epileptic seizures.

We first developed a capillary electrophoresis with laser induced fluorescence (CE-LIF) method to detect ornithine and citrulline in rat brain microdialysis samples. Ornithine and citrulline were derivatized with 4-(N,N-dimethylaminosulfonyl)-7-fluoro-2,1,3-benzoxadiazole (DBD-F)[3], and then they were separated by cyclodextrin assisted capillary electrophoresis. 2-hydroxypropy-beta-cyclodextrin and ethanol were added into background electrolytes to improve resolutions. The limit of detection (LODs) for ornithine and citrulline were 23 nM and 9 nM respectively.

This method was employed in an *in vivo* awake rat microdialysis study. The microdialysis probe was implanted into rat brain hippocampus region. Ten millimolar 3-mercaptopropionic acid (3-MPA) was perfused

through the probe as convulsant to induce focal seizure.[4,5] The results showed, after 3-MPA dosing, the concentration of citrulline increased by ~50% and the concentration of ornithine increase by ~100%. Citrulline and ornithine both stayed relatively leveled for ~3 hours. This confirmed the NO production during epileptic seizure.

6.1.2 Future Directions

The DBD-F derivatization and cyclodextrin modified CE separation not only can be applied to ornithine and citrulline in rat brain microdialysis samples, but also for the determination of other amino acids in microdialysis samples.

The change in ornithine and citrulline concentration as a function of time can be compared with other studies in the future to get a better picture of the role of oxidative stress in epileptic seizure. It also can be correlated with other biomarkers to determine the oxidative damage due to oxidative stress in epileptic seizure. Furthermore, it also can be correlated with the study of how antioxidants modulate oxidative damage.

6.2 LC-MS Method Development of Eicosanoids in Rat Colon Microdialysate to Study Inflammatory Bowel Disease

6.2.1 Conclusions

Cyclooxygenase (COX) and lipoxygenase (LOX) are two enzymatic pathways in inflammatory bowel disease (IBD). We chose 13 eicosanoids as the biomarkers for COX and LOX pathways to study the exact

enzymatic mechanisms of IBD.[6,7] In this project, we focused on the development of a LC-MS/MS method to study the biomarkers in rat colon microdialysate.

We first successfully developed an LC-MS/MS method to separate and detect the 13 eicosanoids. The separation was obtained on a reverse phase LC column. Gradient elution with A: water and 60 mM acetic acid B: acetonitrile with 60 mM acetic acid was used to separate 13 eicosanoids. MS conditions were optimized to achieve the best LODs.

2-Hydroxypropy-beta-cyclodextrin was added in the microdialysis perfusate to improve the recovery of hydrophobic analytes from 5–30% to 40–85%. The cyclodextrin also managed to improve the solubility of hydrophobic analytes, which prevented the analytes from precipitating out of the solution or attaching to the vial walls. The LODs were further improved to ~2 nM.

6.2.2 Future Directions

In the future, this LC-MS method will be used in the analysis of *in vivo* rat colon microdialysis study of IBD. 2,4,6-trinitrobenzene sulfonic acid (TNBS) will be perfused into rat colon to induce IBD[8], and the concentration change of the eicosanoids will be monitored to investigate the enzymatic mechanism of IBD. Furthermore, rats will also be dosed with several IBD medications on the market, and the enzyme activities can be further correlated with these treatment performances.

6.3 Enzymatic Deconjugation to Study Stability of Antibody Drug Conjugates

Antibody drug conjugates (ADCs) are a new class of anticancer drugs that improve the cytotoxic drug's specificity while maintaining its potency.[9] In this project, we chose bromelain as an enzyme to fully cleave off the small molecule cytotoxic drug from the ADC prior to the analysis. With this enzymatic deconjugation method, we were able to directly investigate the degradation of small molecule toxins with the LC-UV method. One application of this method is to study the stability of the model ADC under different conditions. There are two types of conditions studied: in the presence of left over conjugation reagents and with formulation excipients. Two tables were generated to summarize the ADC stability under different conditions. ADC engineer researchers can refer to the compatibility study results to improve the stability of ADC formulations in the future.

6.4 References

(1) Li, J.; O, W.; Li, W.; Jiang, Z.; Ghanbari, H. A. Oxidative stress and neurodegenerative disorders. *International Journal of Molecular Sciences* **2013**, *14*, 24438-24475.

(2) Iadecola, C.; Zhang, F.; Xu, S.; Casey, R.; Elizabeth Ross, M. Inducible nitric oxide synthase gene expression in brain following cerebral ischemia. *J Cereb Blood Flow Metab* **1995**, *15*, 378-384.

(3) Sugiura, K.; Min, J. Z.; Toyo'oka, T.; Inagaki, S. Rapid, sensitive and simultaneous determination of fluorescence-labeled polyamines in human hair by high-pressure liquid chromatography coupled with electrospray-ionization time-of-flight mass spectrometry. *Journal of Chromatography A* **2008**, *1205*, 94-102.

(4) Crick, E. W.; Osorio, I.; Frei, M.; Mayer, A. P.; Lunte, C. E. Correlation of 3-mercaptopropionic acid induced seizures and changes in striatal neurotransmitters monitored by microdialysis. *European Journal of Pharmaceutical Sciences* **2014**, *57*, 25-33.

(5) Mayer, A. P.; Osorio, I.; Lunte, C. E. Microperfusion of 3-MPA into the brain augments GABA. *Epilepsy & behavior : E&B* **2013**, *29*, 478-484.

(6) Wang, D.; DuBois, R. N. The role of COX-2 in intestinal inflammation and colorectal cancer. *Oncogene* **2010**, *29*, 781-788.

(7) Cathcart, M.-C.; Lysaght, J.; Pidgeon, G. Eicosanoid signalling pathways in the development and progression of colorectal cancer: novel approaches for prevention/intervention. *Cancer Metastasis Review* **2011**, *30*, 363-385.

(8) Scheiffele, F.; Fuss, I. J.: Induction of TNBS colitis in mice. In *Current Protocols in Immunology*; John Wiley & Sons, Inc., 2001.

(9) Ducry, L.; Stump, B. Antibody–drug conjugates: Linking cytotoxic payloads to monoclonal antibodies. *Bioconjugate Chemistry* **2010**, *21*, 5-13.